Mechanisms of priming and elongation during ubiquitin chain formation

Dissertation

zur Erlangung des akademischen Grades

doctor rerum naturalium

(Dr. rer. nat.)

im Fach Biologie

eingereicht an der

Lebenswissenschaftlichen Fakultät der Humboldt-Universität zu Berlin

von

M.Sc. Christian Lips

Präsidentin der Humboldt-Universität zu Berlin

Prof. Dr.-Ing. Dr. Sabine Kunst

Dekan der Lebenswissenschaftlichen Fakultät

Prof. Dr. Bernhard Grimm

Gutachter:

1. Prof. Dr. Thomas Sommer
2. Prof. Dr. Andreas Herrmann
3. Prof. Dr. Thorsten Hoppe

Tag der mündlichen Prüfung: 06.12.2019

Abstract

The interaction of RING-finger ubiquitin (Ub) ligases (E3 enzymes) with Ub conjugating enzymes (E2 enzymes) dictates how fast a Ub modification is synthesized on a client protein. This thesis addresses the catalytic stimulation of the E2 enzymes Ubc6 and Ubc7 by their cognate E3 enzymes Hrd1 and Doa10. Results show that Ubc6~Ub conjugates adopt closed conformations more readily than Ubc7~Ub conjugates, indicative for an inherently higher propensity to transfer Ub. The catalytic activity of Ubc7 can be stimulated by a RING domain which relies on so-called linchpin allostery. This drives Ubc7~Ub intermediates into a closed conformation. In addition, specific contacts of the RING-finger domain and the Ub moiety in an E2~Ub conjugate were identified which further restrict the flexibility of the conjugate and thereby increase the reactivity of the E2~Ub intermediate. This seems to represent a common mechanism for the stimulation of E2 enzymes because similar contacts of RING-finger proteins with Ub have been observed for other Ub ligases.

Poly-Ub signals on proteins are generated in successive steps. The first reaction, called “priming”, comprises the attachment of an initial Ub moiety to the target. This requires high flexibility of the involved enzymes to modify acceptor sites in a versatile environment. The second step is the sequential addition of Ub to previously attached Ub molecules in a process termed elongation. In contrast to priming, the formation of uniform Ub chains relies on the repeated and robust conjugation of Ub moieties in a mostly invariant setting. Ub ligases employ different strategies to meet the divergent requirements of these reactions. Doa10 uses separate E2 enzymes for priming and elongation. This thesis shows that Hrd1 efficiently stimulates a single E2 enzyme for the catalysis of both steps via linchpin allostery.

Furthermore, a nuclear Ub ligase, termed the Asi complex, is analyzed. This complex harbors two RING-finger proteins which both are required for the poly-ubiquitination of client proteins. However, due to technical restraints, their individual contribution to the poly-Ub reaction could not be determined.

Key words: PQC, ERAD, E3-mediated E2 stimulation, linchpin allostery, priming, elongation

Zusammenfassung

Die Interaktion von RING-finger-Ubiquitin (Ub)-Ligasen (E3-Enzyme) mit Ub-konjugierenden Enzymen (E2-Enzyme) bestimmt wie schnell ein Zielprotein mit einer Ub-Modifikation versehen wird. In dieser Arbeit wird die Stimulation der E2-Enzyme Ubc6 und Ubc7 durch die E3-Enzyme Hrd1 und Doa10 untersucht. Es wird gezeigt, dass Ubc6~Ub-Konjugate bereitwilliger sogenannte *closed conformations* annehmen als Ubc7~Ub-Konjugate, was wiederum die Tendenz, Ub zu übertragen, steigert. Die katalytische Aktivität von Ubc7 kann durch RING-Domänen stimuliert werden. Durch einen allosterischen Mechanismus, der *linchpin allostery*, werden Ubc7~Ub-Intermediate in *closed conformations* gedrängt. Zusätzlich werden spezifische Kontakte zwischen RING-finger-Domänen und der Ub-Einheit in einem E2~Ub-Konjugat identifiziert. Diese schränken die Flexibilität des Konjugates weiter ein und begünstigen dadurch die Reaktivität des E2~Ub-Intermediates. Dieser Mechanismus scheint weit verbreitet zu sein und wurde schon bei anderen Ub-Ligasen beobachtet.

Poly-Ub-Signale werden in mehreren Schritten generiert. In einer *Priming* genannten Reaktion wird die erste Ub-Einheit auf das Zielprotein übertragen. Dieser Vorgang erfordert sehr flexible Enzyme, die in diversem Umfeld Akzeptorstellen finden und mit Ub modifizieren. Die zweite Reaktion, die *elongation*, umfasst das schrittweise Anheften weiterer Ub-Moleküle an die erste Einheit. Im Gegensatz zum *Priming*, beruht die Bildung einheitlicher Ketten auf der wiederholten und robusten Konjugation von Ub-Molekülen in gleichbleibendem Milieu. Ub-Ligasen verwenden verschiedene Strategien, um die unterschiedlichen Herausforderungen dieser Reaktionen zu bewältigen. Während Doa10 je ein E2-Enzym pro Reaktion nutzt, kann Hrd1 ein einzelnes E2-Enzym durch *linchpin allostery* ausreichend stimulieren, um beide Prozesse durchzuführen, wie diese Arbeit zeigt.

Darüber hinaus wird ein Ub-Ligase-Komplex des Zellkerns, der Asi-Komplex, untersucht. Diese Ligase umfasst zwei RING-finger-Proteine, die für die Poly-Ubiquitinierung von Substraten benötigt werden. Unglücklicherweise konnte der Beitrag der jeweiligen Untereinheiten an der Substratmarkierung, aufgrund technischer Probleme, nicht im Detail bestimmt werden.

Schlagwörter: PQC, ERAD, E3-vermittelte E2-Stimulation, *linchpin allostery*, *priming*, *elongation*

Contributions

Work in this thesis regarding the stimulation of Ubc6 and Ubc7 by their cognate E3 ligases Hrd1 and Doa10 as well as experiments conducted to analyze the versatility of ERAD ligases in yeast cells (sections 2.1 and 2.2) are subject of a collaborative effort between the groups of Prof. Dr. Thomas Sommer and Prof. Dr. Rachel Klevit.

This work was inspired by a hypothesis that myself and Dr. Annika Weber set forth to analyze. After I conducted the first preliminary experiments, we teamed up with Dr. Tobias Ritterhoff and Prof. Dr. Rachel Klevit who supported us with detailed investigations with respect to the mechanisms underlying E3-mediated stimulation of E2 enzymes. To this end, Dr. Tobias Ritterhoff performed the herein presented discharge assays and NMR measurements. I performed *in vitro* chain elongation and substrate ubiquitination experiments as well as degradation assays in yeast cells.

Results presented in this work are currently prepared for publication.

Lips, C *et al.* “Diversity in E2/E3 pairing and activation mechanisms ensures functional flexibility.”

The results presented in section 2.3 address the analysis of the Asi complex, a second project that was single-handedly designed and driven by my ideas.

Table of Contents

1. Introduction

Around 40 years ago, Aaron Ciechanover, Avram Hershko and Irwin Rose characterized a small polypeptide, later identified as ubiquitin (Ub)[1], to be a post-translational modifier involved in protein breakdown[2–4]. By now it has been established that ubiquitination of proteins controls virtually every process in eukaryotic cells. Accordingly, defects in the ubiquitination machinery have been associated with the onset of several malignancies, including neurodegenerative diseases, cancer and inflammation, to name a few[5,6]. Consequently, Ub-associated enzymes represent attractive targets for the treatment of these diseases and the detailed study of their function is a prerequisite for the development of therapeutic strategies.

1.1 Ubiquitin and the ubiquitination cascade

The 76 amino acid peptide ubiquitin is conserved in all eukaryotes. As a post-translational modification Ub is conjugated to proteins and thereby changes the fate of the target regarding its stability, sub-cellular localization or activity. Next to its well-established role in directing proteins to proteasomal breakdown, Ub is involved in non-proteolytic processes such as DNA repair, chromatin remodeling and membrane trafficking[7]. These different functions rely on highly specialized cellular pathways for the generation of individual Ub signals and their decoding. The versatility of this system is even further expanded by other small proteins, among those the “Small ubiquitin-like modifier” (SUMO), “Neural precursor cell expressed, developmentally down-regulated 8” (NEDD8), “Interferon-stimulated gene product 15” (ISG15) and “Autophagy-related protein 8” (Atg8), which are conjugated to polypeptides via enzymatic machineries highly reminiscent of the ubiquitin system[8].

Ubiquitin is attached to target proteins via its carboxy-terminal glycine residue using a three-step enzymatic cascade (Fig. 1-1). First, the carboxy-terminus of Ub is adenylated upon hydrolysis of ATP by a ubiquitin activating E1 enzyme and covalently attached to a cysteine residue in the enzyme via a thioester bond. The yeast *S. cerevisiae* contains one of such enzymes whereas humans harbor two closely related variants[9,10].

Next, Ub is transferred to a cysteine residue in the catalytic site of a ubiquitin conjugating E2 enzyme, by a transesterification reaction. While 12 of such E2 enzymes have been identified in yeast, there are approximately 60 known in human cells. Of note, each E2 enzyme displays slightly distinct enzymatic properties, which contribute to the type of generated Ub signal.

In the last step, Ub is covalently attached to an appropriate acceptor side, typically the ε-amino group of a lysine residue, within a target protein. This reaction involves ubiquitin ligases, also known as E3 enzymes, which determine the specificity of ubiquitination by binding to the substrates. Importantly, each E3 enzyme only works with an appointed set of E2 enzymes, which defines the layout of the Ub signal on its client proteins. Since essentially any protein can become a substrate of the Ub system and the Ub ligases must specifically interact with all these clients to promote ubiquitination, the E3 enzymes form the largest group within the Ub system. There are three major types of E3 ligases that differ in their reaction mechanism.

Ub ligases of the “Really Interesting New Gene” (RING)-type harbor a cysteine-rich region termed the RING-finger domain which attains its characteristic fold by complexing zinc ions. Via their RING-finger, these ligases bind E2 enzymes and bring them into spatial proximity to the target. At the same time, the association with the RING-finger stimulates the catalytic activity of the E2 enzymes for the direct transfer of Ub to client proteins. RING finger-related proteins like “Ubiquitin-box” (U-box), “Plant homeodomain” (PHD) and “Leukemia-associated protein” (LAP) ligases also contain an E2 binding region and display a similar reaction mechanism[11]. Around 95 % of all known E3s belong to the group of RING-finger and RING finger-like proteins, with about 100 members in yeast and over 500 in humans[9,10].

Ligases of the “Homologous to the E6AP Carboxyl Terminus” (HECT)-type contain a cysteine residue in their catalytic center. For this class of ligases, an E2 enzyme first transfers Ub to the cysteine in the HECT domain via transesterification and then the Ub moiety is conjugated to the bound substrate. Therefore, HECT ligases not only select the target for ubiquitination, but also determine the character of the generated Ub signal. Six HECT-type ligases have been identified in yeast and approximately 28 are known in human cells[9–11].

The third class of E3 enzymes is termed “RING-in-between-RING” (RBR) ligases. Such enzymes contain three different domains: RING domain 1 binds and activates the E2 enzymes, the “in-between-RING” (IBR) domain mediates protein-protein interactions and the catalytic RING domain 2 harbors an active site cysteine. RBR ligases employ a RING/HECT-hybrid mechanism, in which the charged E2 bound by RING1 transfers Ub to the catalytic cysteine residue in RING2. The Ub is then conjugated to the client. RBR ligases comprise the smallest class of E3 enzymes respresented by two species in yeast and around 14 in humans[12–14].

Ub can itself serve as acceptor for Ub modifications and thereby give rise to Ub chains. Depending on the catalytic properties of the involved E2 enzymes, the HECT and RBR ligases, substrates can be mono-ubiquitinated or decorated with poly-Ub molecules. This is referred to as the ubiquitin code, which will be explained in more detail in the following section.

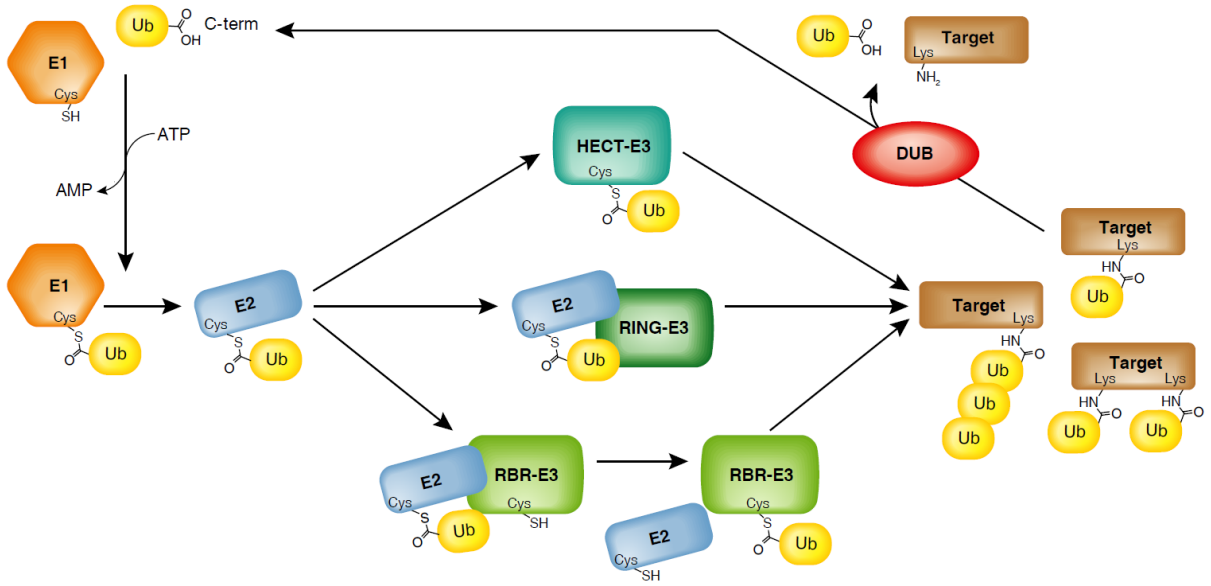

Figure 1-1: The ubiquitination cascade. Ubiquitination is achieved in the course of a three-step reaction cascade involving E1, E2, and E3 enzymes. As a result target molecules are decorated with distinct Ub signals. Ubiquitination is counteracted by the function of deubiquitinating enzymes (DUBs). Adopted from Smit & Sixma[15].

Ub modifications are dynamic and can be edited by proteases, called “deubiquitinating enzymes” (DUBs). Individual DUBs are highly specific for the Ub signals they act on. Some DUBs completely detach all Ub molecules from a protein, while others remove single Ub moieties from the tip of an appointed Ub chain or cleave inside a poly-Ub molecule and thereby dismount several Ub moieties at once. A well-characterized function of DUBs is associated with the activity of the 26S proteasome. Here, several DUBs cooperate to hydrolyze Ub chains from client

proteins, which allows their passage into the catalytic core of the proteasome and recycling of Ub. It is still a matter of intense studies how the relatively small number of DUBs, with 17 putative enzymes in yeast and around 100 in humans, can specifically modulate the highly diverse Ub signals in a cell[16–18].

1.2 The ubiquitin code

Ubiquitination is a highly versatile modification that comes in many different flavors (Fig. 1-2). The simplest signal is the addition of a single Ub moiety to a target, also referred to as mono-ubiquitination. While ubiquitination preferentially occurs on lysine residues in the client (canonical ubiquitination), also serines, threonines, cysteines or amino-terminal methionines can serve as acceptor sites (atypical ubiquitination)[19–22]. Modification of several residues in a target results in a different signal, called multiple mono-ubiquitination.

Ub itself harbors seven lysine residues and an amino-terminal methionine, which each can serve as acceptors for additional Ub moieties. The attachment of Ub to another Ub molecule that is already conjugated to a target causes the formation of a Ub chain. Depending on the acceptor site used within Ub, these chains comprise different linkage types. For example, poly-Ub molecules connected via lysine 48 in Ub are referred to as K48-linked Ub chains. In addition to homotypic chains, which exclusively contain entities attached to the same acceptor site, heterotypic or branched chains can be formed. Importantly, poly-Ub molecules connected via different linkages display distinct topological and structural properties, which are recognized by downstream acting factors.

Ub itself was shown to be subjected to other post-translational modifications, such as phosphorylation, acetylation, or even SUMOylation. An important role for Ub phosphorylated on serine 65 has been found in PARKIN-mediated mitophagy[23]. Acetylation of Ub is readily detected in cells and was shown to inhibit the formation of Ub chains. Ub acetylation seems to contribute to the stabilization of mono-ubiquitinated histone H2B, but the detailed role of this modification in this process still remains elusive[24]. Moreover, SUMOylated Ub species at lysine residues K6, K11, K27, K48 and K63 have been detected in cells, but again their biological function is unclear[25].

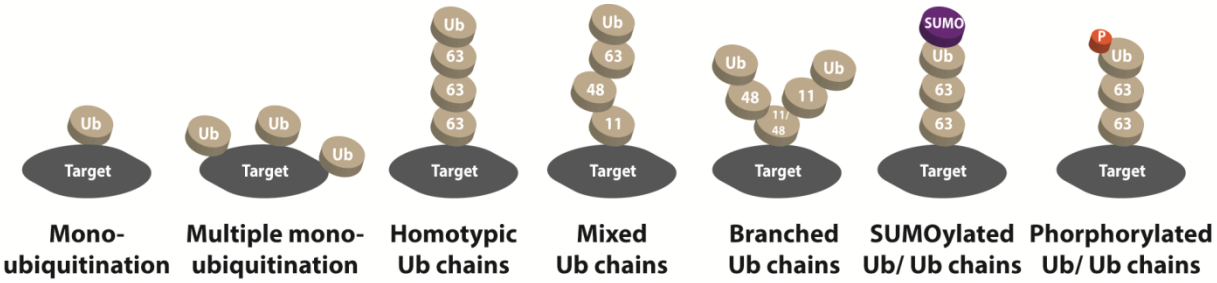

Figure 1-2: The ubiquitin code. Various signals can be formed by ubiquitination of targets that in turn activate a great amount of distinct signaling pathways. Numbers in Ub spheres represent the modified lysine inside the Ub molecule.

This large diversity of Ub modifications routes client proteins into very different cellular pathways. Table 1-1 summarizes our knowledge on how distinct Ub signals modulate specific cellular activities[26–28].

Proteins encompassing so-called “ubiquitin binding domains” (UBDs) decode individual Ub signals. Each UBD can specifically interact with a defined Ub structure and route the attached client into a selected pathway. UBDs encompass domains of different folds which determine the specificity in signal recognition. Examples are zinc fingers, “Ubiquitin-associated” (UBA) domains and “Plekstrin Homology” (PH) folds[29]. Most mono-Ub binding UBDs directly bind the hydrophobic patch of Ub by a ubiquitin-interacting motif (UIM) or ubiquitin-binding zinc fingers (UBZ). Other UBD-carrying proteins can detect Ub chains by displaying a distinct interaction motif for a specific Ub linkage type. The recognition of long and complex chains is often mediated by effector proteins harboring several UBDs that allow multivalent interactions with Ub. Thus, multifaceted Ub interactors have evolved that specifically decode the diverse signals displayed by this post-translational modification.

Table 1-1: Specific Ub modification activate distinct signaling pathways[26–28]

Ub modification	Signaling outcome
Mono-Ub	Regulation of protein-protein interactions, cellular localization, lysosomal degradation
Multiple Mono-Ub	Cellular localization, proteasomal degradation
M1-linked (linear) chains	Inflammation and immunity
K6-linked chains	DNA damage response, mitophagy
K11-linked chains	Implicated in non-canonical NF-κB signaling, T-cell activation and EGF receptor trafficking, yeast ERAD
K27-linked chains	Protein recruitment, DNA repair, autoimmunity
K29-linked chains	Proteasomal degradation, proteasome regulation, epigenetics
K33-linked chains	*trans*-Golgi network trafficking
K48-linked chains	Proteasomal degradation
K63-linked chains	DNA repair, innate immune response, mitophagy, protein sorting, protein translation, autophagy
Mixed chains	K29/K48-mixed chains → ubiquitin-fusion degradation pathway (UFD), DNA repair M1/K63-mixed chains → NF-κB signaling
Branched chains	K48/K11-branched chains → cell cycle control K48/K63-branched chains → NF-κB signaling
SUMOylated Ub	Indications in heat shock response and protein homestasis
Phosphorylated Ub	Ser65-phosphorylated Ub → mitophagy
Acetylated Ub	Possible stabilization of mono-ubiquitinated histone H2B

1.3 Ub in Endoplasmic reticulum-associated protein degradation

Protein maturation is a complex process which is compromised by environmental stress or by mutations in the coding genes. Misfolded polypeptides that arise from unsuccessful folding attempts are typically dysfunctional and pose a threat for the maintenance of cellular homeostasis. Therefore, cells harbor potent quality control systems that detect unproductively folded protein species, facilitate their refolding and eliminate terminally misfolded molecules. Such quality control systems are found in every cellular compartment where they make an essential contribution for the function of the corresponding organelle. One of the main functions of the Ub system is the removal of defective proteins from the cell and Ub ligases constitute the central components of most quality control systems. The ligases label their clients with Ub signals that either target them for proteasomal hydrolysis or route them to autophagosomes for degradation.

Proteins of the secretory pathway have to enter the endoplasmic reticulum (ER) in an unfolded state through a narrow pore, termed the translocon. In the ER, they attain their native structure before they are released to downstream acting compartments. Even though protein maturation is assisted and tightly regulated by folding enzymes, this process is error-prone and can eventually result in the formation of terminally malfolded polypeptides[30]. Such aberrant species may form proteotoxic aggregates, which have been linked to the onset of several neurodegenerative diseases and type II diabetes[31]. “Endoplasmic reticulum-associated protein degradation” (ERAD) eliminates misfolded proteins by routing them into the cytoplasm where they are decorated with poly-Ub and degraded by proteasomes. Additionally, the ERAD pathway also regulates the amount of metabolic enzymes in the sterol biosynthesis pathway[32].

1.4 Ub ligases involved in ERAD

The yeast *S. cerevisiae* harbors ERAD Ub ligases which each target a specific subset of client proteins[33]. Membrane-bound polypeptides with structural defects in their cytosolic parts are termed ERAD-C substrates and are processed by the Doa10 ligase. Integral membrane proteins exposing lesions inside their transmembrane segments are classified as ERAD-M substrates and are degraded in a Hrd1-

dependent manner. Finally, misfolded polypeptides residing inside the ER lumen belong to the ERAD-L class which is also targeted by the Hrd1 ligase. Importantly, ERAD-L substrates have to be first extracted from the ER before they can be assessed by the Ub system and the proteasome in the cytoplasm.

The Hrd1 and Doa10 RING-finger proteins are the central components of large and highly conserved multi-subunit protein complexes (Fig. 1-3). The integral membrane protein Hrd1 contains a RING-finger in its cytoplasmic domain at the carboxy-terminus and serves as a Ub ligase. Hrd1 tightly binds to Hrd3 which exposes several so-called “Suppressor enhancer of Lin12-like” (SEL1L) repeats into the ER lumen. Together with the associated protein Yos9, a glycan-binding lectin in the ER lumen, Hrd3 is thought to constitute the substrate receptor of the Hrd1 Ub ligase complex[34]. In the ER membrane, Hrd1 is in close contact with the membrane proteins Usa1 and Der1. While Usa1 is a scaffolding protein that controls the assembly and oligomerization of the complex, Der1 was shown to participate in the dislocation of ERAD-L substrates from the ER lumen[35,36].

The modification of Hrd1 client proteins with K48-linked poly-Ub chains mainly involves the E2 enzyme Ubc7. Ubc7 is recruited to the ligase by binding to the membrane protein Cue1[37,38]. In absence of Cue1, Ubc7 becomes short-lived, while the association with Cue1 causes a structural rearrangement in the E2, which stimulates its catalytic activity[38–40]. Moreover, Cue1 contains a UBD termed CUE domain which positions Ubc7 at K48-linked poly-Ub and thereby facilitates the elongation of Ub chains[41,42]. Hrd1 also binds to the membrane protein Ubx2 which recruits a cytoplasmic protein complex containing the “ATPase associated with diverse cellular activities” (AAA-ATPase) Cdc48, Npl4 and Ufd1 to the ligase[43]. This Cdc48 complex is a Ub-dependent chaperone that binds poly-ubiquitinated proteins and possibly extracts them from the ER to allow their processing by 26S proteasomes[44–46].

The Doa10 Ub ligase is integrated into the membranes of the ER and the inner nucleus by 14 transmembrane segments[47]. This protein exposes a short soluble region at its amino-terminus into the cyto- and nucleoplasm that harbors the RING-finger domain. For substrate processing, Doa10 teams up with the E2 enzymes Ubc6, which itself contains a membrane-spanning region, and the Ubc7/Cue1 complex[48]. The Doa10 Ub ligase also encompasses Ubx2 and the Cdc48 complex[33].

While the mechanisms of substrate selection at the Doa10 ligase are still elusive, the ubiquitination of client proteins by Ubc6 and Ubc7 was studied in more detail. Doa10 employs Ubc6 for the initial conjugation of single Ub moieties on a protein that are then elongated to K48-linked Ub chains by Ubc7[20]. Hence, in contrast to Hrd1, the processing of Doa10 clients requires separate E2 enzymes for the priming with Ub and the generation of a poly-Ub signal. Importantly, Ubc6 attaches Ub not only to lysines, but also to the non-canonical acceptor sites serine and threonine via an oxyester bond[20]. This unusual activity is thought to broaden the substrate range of the Doa10 quality control Ub ligase.

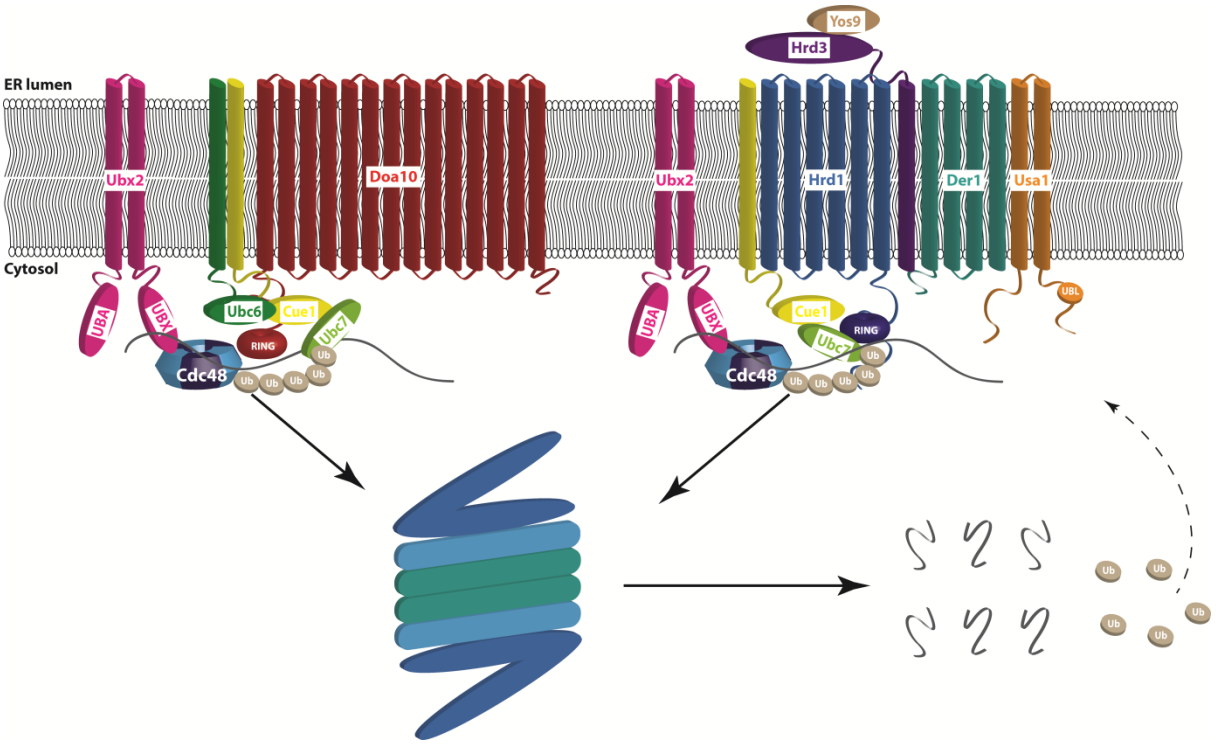

Figure 1-3: Schematic presentation of the Doa10 and Hrd1 ligase complexes. The multi-subunit complexes recognize and modify substrates with Ub signals. Targets are then extracted by the AAA-ATPase Cdc48 and handed over for proteasomal disposal.

1.5 Inner nuclear membrane-associated protein degradation

A pathway recently described as “Inner nuclear membrane-associated protein degradation” (INMAD) contributes to protein quality control in the inner nuclear membrane and the nucleus[49]. A membrane-bound ubiquitin ligase, termed the Asi complex, is the major player of INMAD. The components of the Asi complex were initially identified in a genetic screen for suppressors of mislocalized Stp1 and Stp2[50,51]. Stp1 and Stp2 are transcription factors that control the expression of amino

acid permeases in response to external stimuli[52,53]. In the presence of amino acids, the precursor forms of Stp1 and Stp2, which reside in the cytoplasm, are cleaved by a subunit of the so-called SPS sensor. Processed Stp1 and Stp2 are then imported into the nucleus where they induce the expression of target genes[54]. Unprocessed Stp1 and Stp2, which eventually leak into the nucleus in absence of amino acids, are ubiquitinated by the Asi complex and degraded by proteasomes. This prevents unsolicited gene expression[50,51,55]. Intriguingly, the Asi complex also targets specific membrane-bound proteins involved in later steps of sterol biosynthesis similar to the ERAD ligases Hrd1 and Doa10[56].

The Asi complex contains two highly homologous membrane proteins, Asi1 and Asi3, which each expose a RING-finger domain at their carboxy-terminus into the nucleoplasm (Fig. 1-4). Both proteins constitute *bona fide* ubiquitin ligases. The Asi complex also harbors another membrane-embedded subunit termed Asi2, but the function of this protein is unknown. For ubiquitination of its client proteins, the Asi complex employs the E2 enzyme Ubc7. Two other Ub conjugating enzymes, Ubc4 and Ubc6, were also associated with the function of the Asi complex. However, their role at this ligase is unclear[56,57].

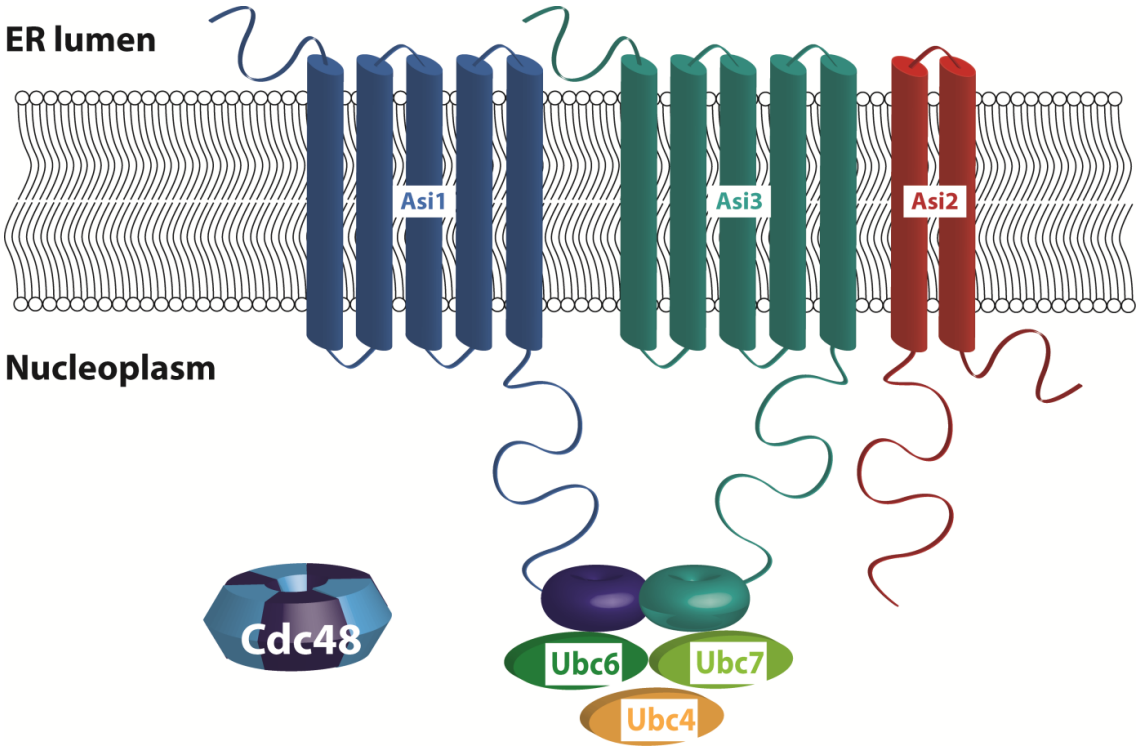

Figure 1-4: Schematic presentation of the Asi complex. The Asi complex is composed of two RING-finger domain-containing ubiquitin ligases. Both act in conjunction with the *bona fide* accessory factor Asi2. The ubiquitin conjugating enzymes Ubc4, Ubc6 and Ubc7 are implicated to take part in Asi-dependent substrate processing. Extraction of substrates from the inner nuclear membrane is facilitated by the AAA-ATPase Cdc48.

1.6 Stimulation of E2 enzymes by RING-type E3 ubiquitin ligases

The vast majority of all E3 enzymes are RING-type Ub ligases. This class of proteins is characterized by a RING-finger domain where a conserved cysteine motif coordinates two zinc ions in a cross-braced arrangement. The RING scaffold serves to bind E2 enzymes[58].

RING-type ligases adopt different topological architectures. Some are found to be monomeric including the CBL family of RING E3 ligases (c-CBL, CBL-B, CBL-C)[59]. Others function as homodimers as BIRC7 or several members of the TRIM family[60,61]. Then again, RING-type ligases are found to form heterodimers as the famous example of the BRCA1/BARD1 complex shows[62]. Moreover, RING domain-containing proteins can assemble into large complexes mediated by a Cullin protein scaffold, so-called Cullin-type RING ligases (CRLs). The cell cycle-regulating CRLs SCF (Skp1-Cul1-F-box protein) and APC (anaphase promoting complex) are just two amongst many other examples[63].

E2 enzymes are characterized by their catalytic core domain, the ubiquitin-conjugating (UBC) domain. This domain is formed by an α/β fold, typically with four α-helices and a four-stranded β-sheet[64]. It also harbors the catalytic cysteine which forms a transient thioester with Ub during the ubiquitination reaction. Different E2s encompass distinct catalytic behaviors ranging from the efficient mono-ubiquitination of targets to the processive formation of Ub chains of a specific linkage type.

RING/E2 interactions are governed by a shallow groove which is formed by the zinc-coordinating loops and the central α-helix of the RING domain (Fig. 1-5). The UBC domain of an E2 is bound on the backside rather than in close proximity to the catalytic center. Noteworthy, the interaction surface of the E2, which is bound to the RING, overlaps with the surface that is utilized for E1/E2 interaction. Thus, it was proposed that E2 enzymes need to dissociate from their cognate RING domains after Ub transfer in order to enter a new charging cycle[65]. An exception has been discussed in regard to the APC. Here, distinct interactions between RING and E2, remote from the previously defined surfaces, could allow recharging of the E3-bound E2 to support rapid Ub chain synthesis[66]. Generally, E2/E3 interactions are characterized by low affinities[58]. Accordingly, co-immunoprecipitation experiments of E2s and E3s are rarely successful causing the need for biophysical measurements

like NMR or X-ray crystallography to analyze physical interactions. In recent years, a powerful tool for the characterization of functional interactions between Ub ligases and their cognate ubiquitin conjugating enzymes was established. So-called discharge assays involving small molecules provide the means to analyze the inherent activities of E2 enzymes and their stimulation by E3 catalytic domains[67].

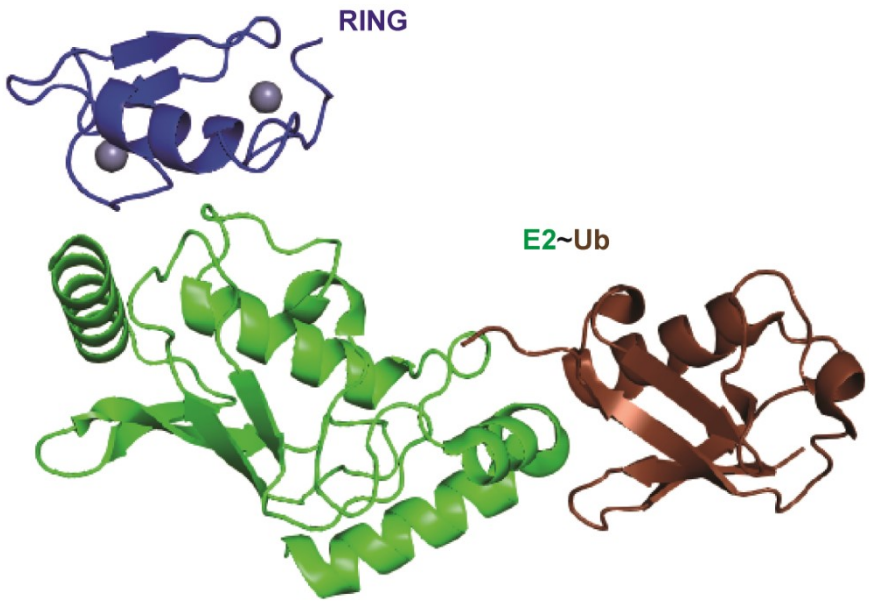

Figure 1-5: Exemplary interaction of a RING domain with an E2~Ub conjugate. Crystal structure of the RNF165 RING domain in complex with a UbcH5b~Ub conjugate. The figure is based on PDB file 5ULH.

RING E3 ligases do not only bring substrate and E2 enzyme into close proximity to allow efficient transfer of Ub, they also stimulate the intrinsic activity of E2s. RING domains bind to a region remote from the active site of the E2[58]. Thus, RING-mediated stimulation of a cognate E2 enzyme must be facilitated by an allosteric mechanism. Conjugates formed by E2 enzymes and Ub assume a variety of different “open” and “closed” states[68]. By now it has been established that E2~Ub conjugates need to adopt a closed conformation as a prerequisite for Ub transfer to client molecules. A recent study provided much needed inside in how a RING domain pushes an E2~Ub conjugate into such an arrangement by an allosteric mechanism (Fig. 1-6)[69]. This involves the residue at the so-called linchpin position of a RING domain which is situated directly downstream of the last zinc-coordinating cysteine pair. This linchpin allostery involves positively charged residues, like arginine or lysine that expose long side chains into the backbone of the E2 where they form a hydrogen bond. The conformational space of an E2~Ub conjugate (Fig. 1-6, green sphere) is therefore restricted upon interaction with a RING domain which exerts

linchpin allostery (Fig. 1-6, blue sphere). Thus, RING domains harboring conserved arginines or lysines at the linchpin position comprise the activity to directly stimulate the transfer of Ub from E2 enzymes enabling a spatiotemporal regulation of substrate ubiquitination.

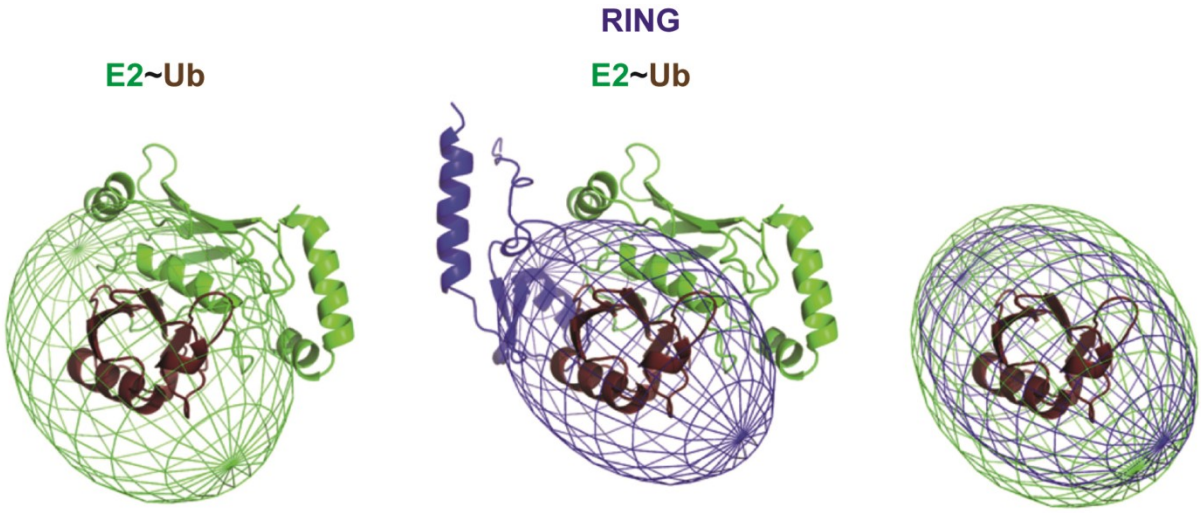

Figure 1-6: The conformational space of an E2~Ub conjugate can be restricted by interaction with a RING-finger domain. The formation of a covalent hydrogen bond between the residue at the linchpin position of a RING-finger domain and the backbone of the E2 pushes the conjugate into a closed conformation. Spheres represent the conformational space that the E2~Ub conjugate can adopt. Modified from Pruneda *et al.*[69]

1.7 Aims of this study

Protein quality control is important to protect cells from proteotoxic stress. It is unknown why there is more than one PQC ubiquitin ligase in cells. To understand the requirement for those multiple protein degradation pathways, their function needs to be elicited and their mechanisms of substrate processing need to be unraveled in molecular detail. Therefore, the requirements of different E3 ligases for distinct E2 enzymes and the specific stimulation of E2s need to be investigated.

To shed light on the differential requirements of the Hrd1 and Doa10 ligases regarding their cognate E2 enzymes, the E3-mediated stimulation of Ubc6 and Ubc7 was to be analyzed in reconstituted *in vitro* systems. Special focus was set on the differential effects of RING domain-facilitated linchpin allostery during the sequential steps of substrate priming and Ub chain elongation.

Simultaneously, distinct alterations abrogating priming and elongation in cells were to be introduced using yeast as a model system. This approach should elucidate how priming and Ub chain elongation are facilitated at the ERAD E3 ligases in the context of the ER membrane and which factors contribute to either process.

Finally, the third ER membrane-bound yeast Ub ligase, the Asi complex, was to be analyzed. To this end, the involvement of single subunits in complex function was addressed with special regard to the distinct contribution of the Asi1 and Asi3 RING domains. Moreover, complex organization and the requirement for distinct E2 enzymes at the complex were to be analyzed in molecular detail. Furthermore, an *in vitro* assay should be established to monitor Asi complex-mediated ubiquitination of client proteins in a reconstituted system.

2. Results

2.1 Hrd1 and Doa10 RING domains stimulate Ubc6 and Ubc7 activity by different mechanisms

2.1.1 Doa10 harbors a non-canonical residue at its linchpin position

The Doa10 and Hrd1 ubiquitin ligases display different requirements regarding the E2 enzymes they cooperate with. While the degradation of Doa10 client proteins relies on the sequential action of Ubc6 and Ubc7, Ubc7 alone suffices for the processing of Hrd1 substrates. To explore such mechanistic differences of both E3 ligases in the ubiquitinating reaction, a sequence alignment of their RING finger domains was conducted (Fig. 2-1).

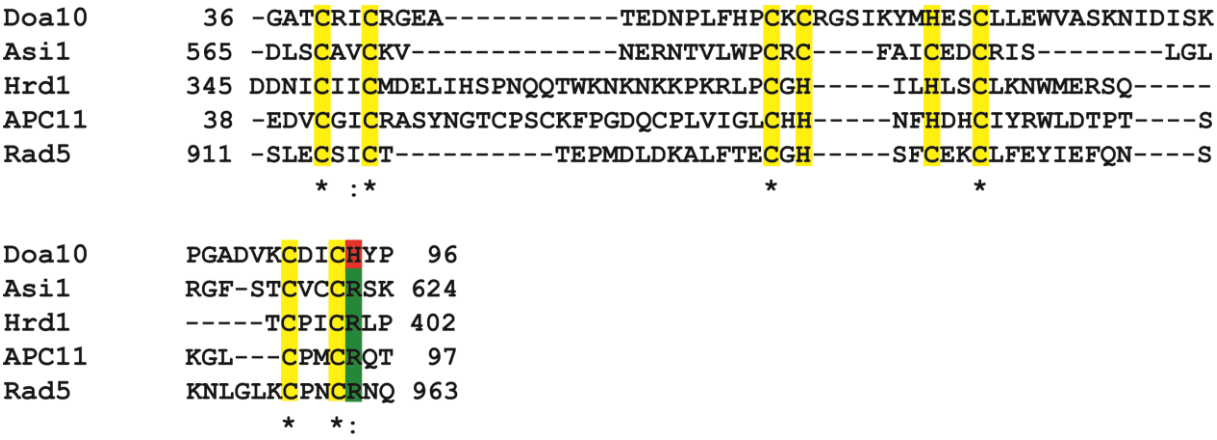

Figure 2-1: Sequence alignment of yeast E3 ligase RING domains. Sequence alignment was conducted with Clustal Omega. Conserved zinc-coordinating residues are highlighted in yellow. Residues at the linchpin-position are colored in red/green. Asterisks mark conserved residues. Colons mark chemically similar residues.

Most canonical RING domains harbor an arginine or a lysine residue at their so-called linchpin position which is located immediately downstream of the most carboxy-terminal zinc-coordinating pair of cysteines. These positively charged residues expose long side chains into the backbone of the interacting E2~Ub conjugate. The formation of a hydrogen bond restricts the conformational space of the conjugate and pushes it into a “closed conformation”. This is a prerequisite for the transfer of Ub to target proteins[69]. In contrast to the Hrd1 RING domain, which contains such an arginine at the linchpin position, Doa10 harbors a histidine at the corresponding site. While histidine can serve as a donor for hydrogen bond formation in an appropriate chemical environment, its side chain is much shorter and probably

does not extend far enough into the E2 backbone. Therefore, the non-canonical linchpin residue of Doa10 can be expected to be less efficient in E2 stimulation.

2.1.2 E3 RING-finger ligases stimulate Ubc6 and Ubc7 activity by different mechanisms

Detailed analyses of Doa10's and Hrd1's linchpin residues were conducted to evaluate differences in the interaction with their cognate E2 enzymes and resulting effects in E2 behavior. To this end, a series of Doa10 and Hrd1 RING domain variants were generated and studied in reconstituted *in vitro* ubiquitination assays containing purified components (Fig. 2-2).

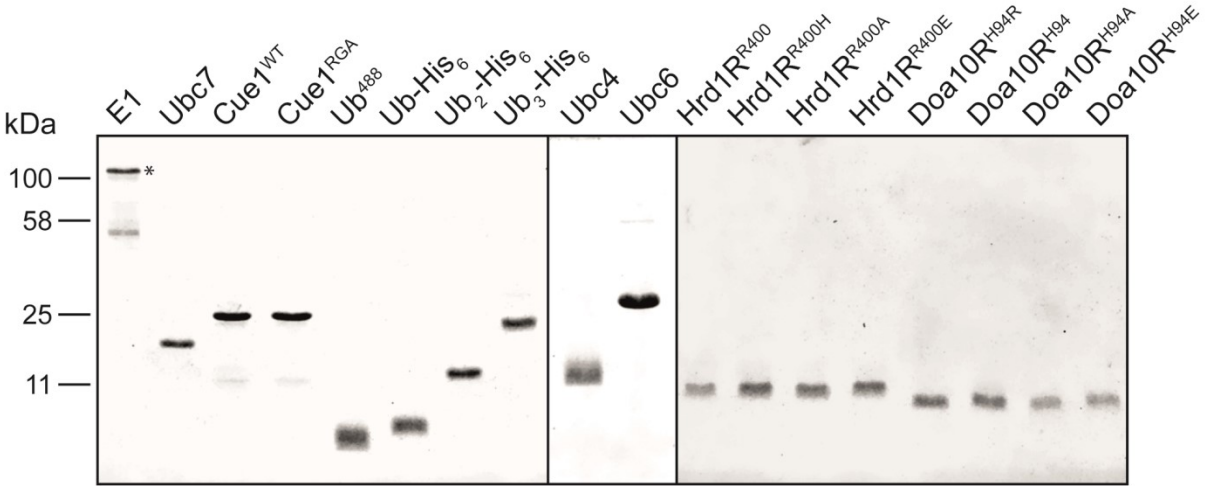

Figure 2-2: Purified components for *in vitro* ubiquitination assays. Coomassie-stained SDS-PAGE gels showing purified components heterologously expressed in *E. coli*. Architecture of depicted constructs is listed in table 4-2. Hrd1R or Doa10R correspond to constructs comprising the RING domains of each enzyme. Asterisk marks the respective signal for the E1 enzyme.

The linchpin residue in each RING domain was substituted with the corresponding basic residue of the other RING domain, the polar residue alanine, or the acidic amino acid glutamate. The last two variants cannot form hydrogen bonds and thereby should not be able to stimulate the transfer of Ub from the interacting E2s via linchpin allostery. In order to reconstitute ubiquitination *in vitro*, other purified components of the Ub cascade were added, such as E1 enzyme, E2s, e.g. Ubc4, Ubc6 or Ubc7, the cytosolic part of the Ubc7 cofactor Cue1 and either monomeric Ub or preformed Ub chains of different lengths. With this toolset in hand, *in vitro* Ub chain formation was monitored in step-by-step reactions to determine the contribution of the involved enzymes.

2.1.3 Stimulation of Ubc7 activity relies on a particular linchpin residue

The first step in forming a Ub chain is the transfer of a Ub moiety to a nucleophilic side chain of a target protein. This primes the substrate for the addition of further Ub moieties. In most cases, Ub is attached to the ε-amino group of lysine residues but some specialized E2s, like Ubc6, may also facilitate Ub transfer to hydroxyl groups of serines or threonines. This initial ubiquitination event can be studied in Ub discharge assays onto small molecules. Therefore, E2 enzymes were charged with Ub in a first reaction and subsequently incubated with appropriate acceptors for Ub attachment. To compare the reactivity of Ubc6 and Ubc7, discharge reactions were performed on ethanolamine (Fig. 2-3 A). Ethanolamine harbors a hydroxyl and an amino group and thereby meets possible preferences of Ubc6 and Ubc7 for lysines or hydroxylated amino acids as acceptor sites of Ub. Any decline in the amount of Ub-charged E2 (Ubc7~Ub) over time was visualized on Coomassie-stained gels (Fig. 2-3 B, C) and quantified (Fig. 2-3 D, E). Single exponential fits of these data were used to calculate turnover rates (Fig. 2-3 F, G).

All reactions contained the Ubc7-binding region (U7BR) of Cue1 which induces conformational changes and thereby activates Ubc7[40,70]. Discharge assays with Doa10 RING variants were incubated at 37 °C while the Hrd1 reactions were conducted at room temperature due to general differences of the Doa10 and Hrd1 constructs to stimulate this E2 enzyme. Assays without RING domains demonstrated an intrinsic propensity of Ubc7 to transfer Ub onto targets. Depending on the residue at the linchpin position, this reaction was accelerated at different rates upon addition of the Doa10 or Hrd1 RING domains. Hrd1 and Doa10 constructs containing an arginine at this site facilitated Ub transfer most efficiently. A Doa10 variant harboring the endogenous histidine stimulated catalysis of Ubc7~Ub nearly as good suggesting that in the context of the Doa10 RING, histidine can serve as a hydrogen bond donor for linchpin allostery. Conversely, Hrd1 featuring a histidine at the linchpin position was significantly impaired in supporting Ubc7~Ub discharge comparable to the effect of an alanine substitution. This implies that the Hrd1 RING does not provide the chemical environment needed for histidine-mediated linchpin allostery. Alanine-substituted RINGs promoted moderate activation of Ubc7, which hints to another yet unknown linchpin-independent mechanism as discussed in section 2.1.2.3. RING variants harboring a glutamate at the linchpin position were completely inert for Ubc7

stimulation despite their ability to bind E2 enzymes, as seen later for Ubc6 (compare Fig. 2-4).

Taken together, these results show that RING-mediated stimulation of the canonical E2 Ubc7 clearly depends on the nature of the position residue.

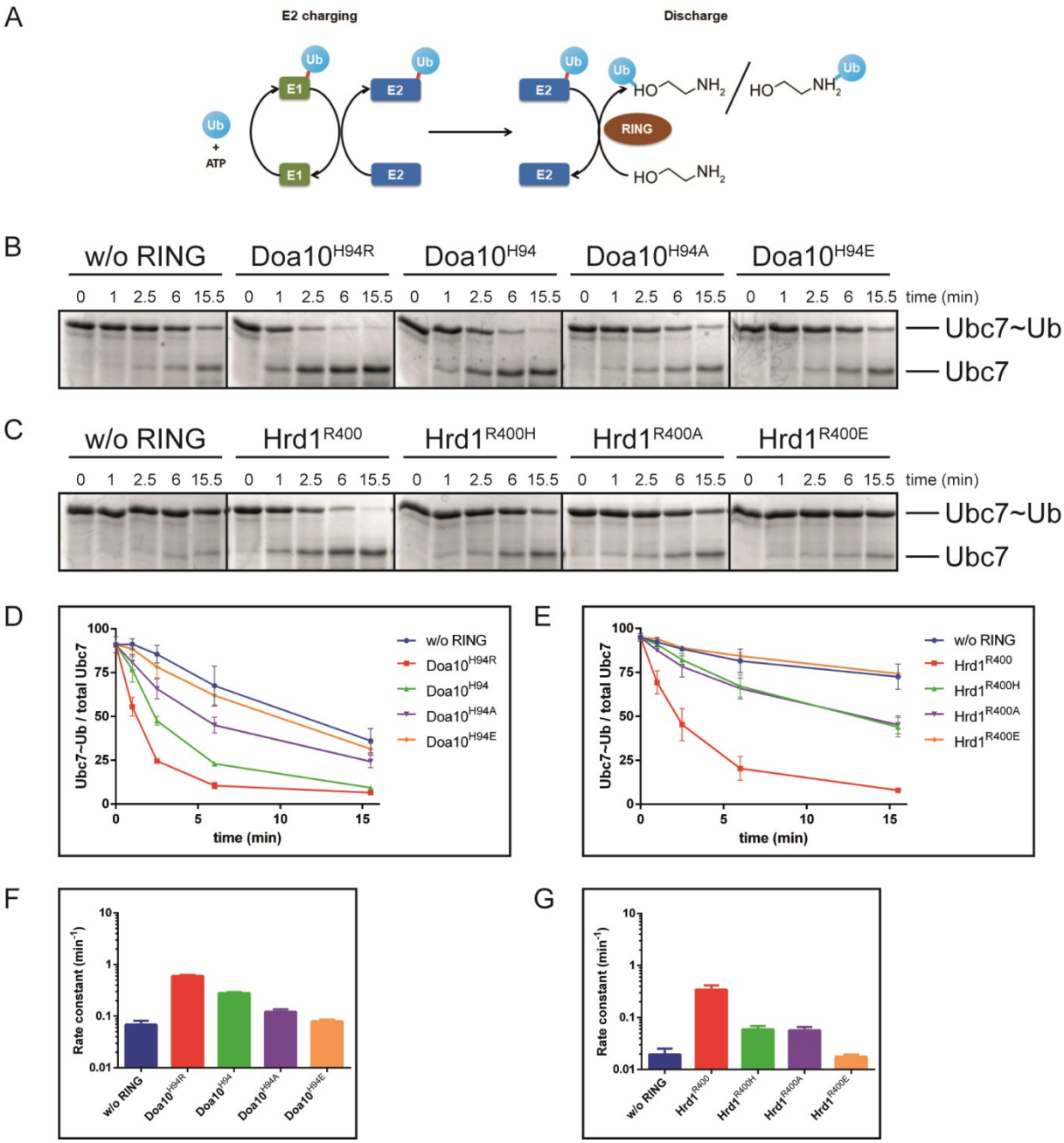

Figure 2-3: Ubc7 is stimulated in a linchpin-dependent manner. (A) Scheme of discharge reactions modified from von Delbrück *et al.*[42] (B, C) Representative Coomassie-stained SDS-PAGE gels showing the decrease in the Ubc7~Ub conjugate and the increase in free Ubc7 over time dependent on different (B) Doa10 and (C) Hrd1 RING domain variants. Reactions with Doa10 and Hrd1 variants were incubated at 37 °C and room temperature, respectively. (D, E) Quantifcations of Ubc7~Ub conjugates as seen in (B) and (C). (F, G) Kinetic rate constants extracted from single exponential fits of the data in (D) and (E). Error bars represent the standard deviation of mean of at least three independent experiments. Assays were performed by Dr. Tobias Ritterhoff.

2.1.4 Ubc6 activity is stimulated by a linchpin-independent mechanism

To compare the reactivity of Ubc6 and Ubc7, discharge assays containing Ubc6 were performed. These reactions were incubated at room temperature. In contrast to Ubc7, Ub transfer by Ubc6 was stimulated by the Doa10 and Hrd1 RING domains irrespective of the identity of the linchpin residue. Consequently, while Ubc7 discharge assays gave a characteristic pattern depending on the introduced substitutions, reactions containing Ubc6 showed clustering of the recorded graphs (Fig. 2-4).

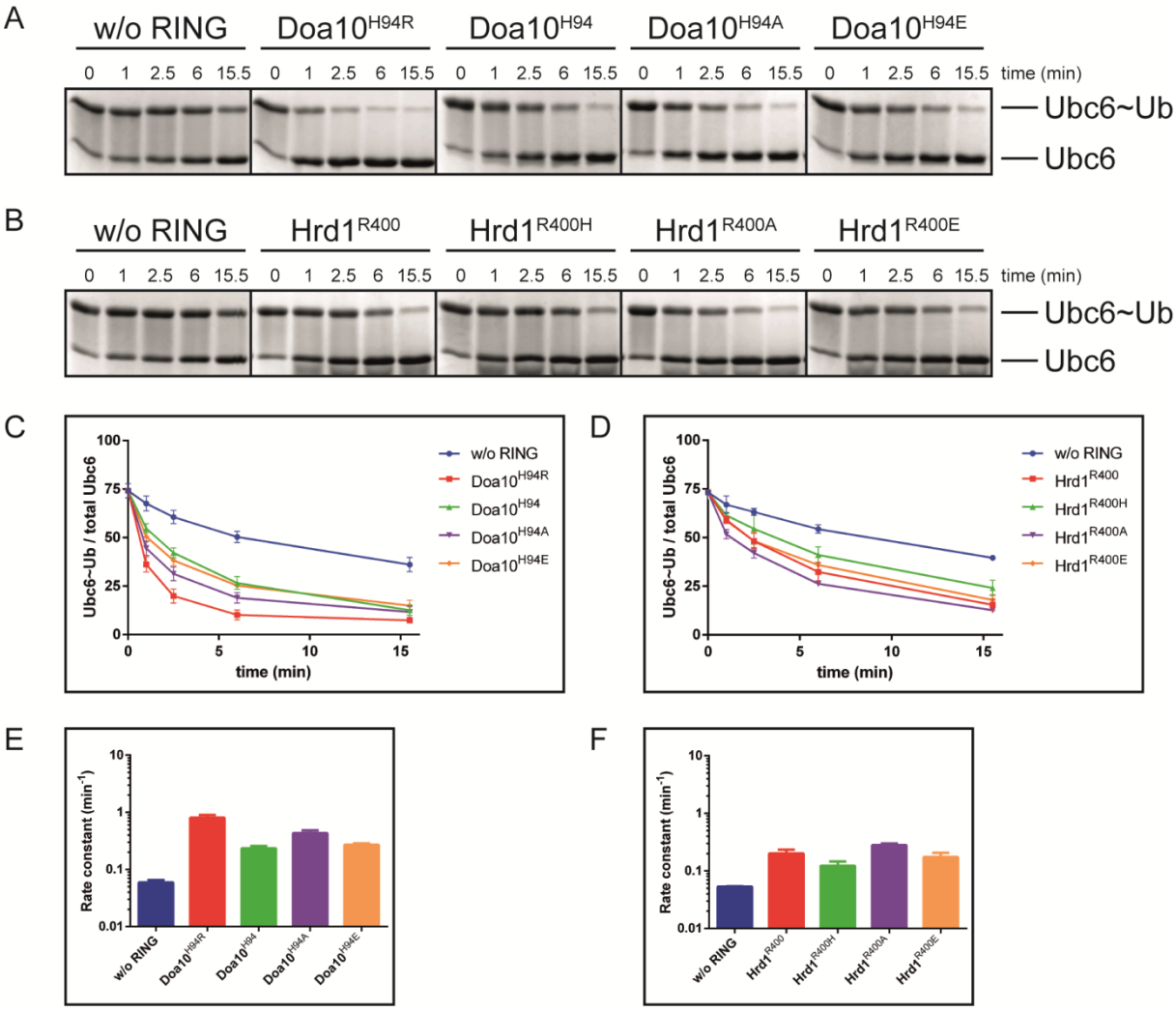

Figure 2-4: Ubc6 is stimulated via a linchpin-independent mechanism. (A, B) Representative Coomassie-stained SDS-PAGE gels showing the decrease in the Ubc6~Ub conjugate and the increase in free Ubc6 over time dependent on different (A) Doa10 and (A) Hrd1 RING domain variants. All reactions were performed at room temperature. (C, D) Quantifcations of Ubc6~Ub conjugates as seen in (A) and (B). (E, F) Kinetic rate constants extracted from single exponential fits of the data in (C) and (D). Error bars represent the standard deviation of mean of at least three independent experiments. Assays were performed by Dr. Tobias Ritterhoff.

Overall, Ub discharge from Ubc6 was substantially faster than that from Ubc7 implying that this E2 enzyme transfers Ub more readily to targets. Addition of different RING domain variants led to an efficient stimulation of Ubc6's inherent activity albeit the linchpin variants revealed no significant differences in reaction rates. It is noteworthy that Doa10 RING variants generally enhanced Ub discharge from Ubc6 to a greater extent than Hrd1 variants indicating a tight and probably more conserved functional interaction of this E2/E3 pair. Importantly, glutamate-substituted RINGs promoted Ubc6 activity to a similar degree as the other variants pointing out that they were still able to bind the E2 enzymes while they did not induce linchpin-mediated conformational changes.

The presented data indicate that Ubc6 activity is stimulated by a RING-dependent mechanism that does not involve the linchpin position.

2.1.5 Ubc6 adopts a closed conformation more readily than Ubc7

To gain a deeper understanding of the E2/E3 interactions and thereby the E3-mediated stimulation of E2 enzyme activity, NMR titration experiments were performed. In the first setup, Ub was labeled with deuterium (^{2}H) and heavy nitrogen isotopes (^{15}N) and stably conjugated to the designated E2s via a disulfide bridge. For that purpose, a Ub variant with a C-terminal cysteine was used (Ub^{G76C}) and conjugated to the active site cysteine of the E2 enzymes. Chemical shift perturbations (CSPs) in comparison to free Ub were recorded and mapped over the amino acid sequence of the protein (Fig. 2-5).

When an E2~Ub conjugate adopts the closed conformation, subtle structural changes can be observed in the hydrophobic patch of Ub. Indeed, prominent shifts at distinct sites within this region were detected when Ub was conjugated to the E2s. Presumably, Ubc6~Ub and Ubc7~Ub adopt closed conformations as a prerequisite for Ub transfer. Interestingly, the CSP pattern of Ubc6~Ub and Ubc7~Ub displayed different profiles. Overall, CSPs and especially changes in the hydrophobic patch of Ub were more pronounced in the Ubc6~Ub conjugate suggesting that it adopts a catalytic active conformation more readily than Ubc7.

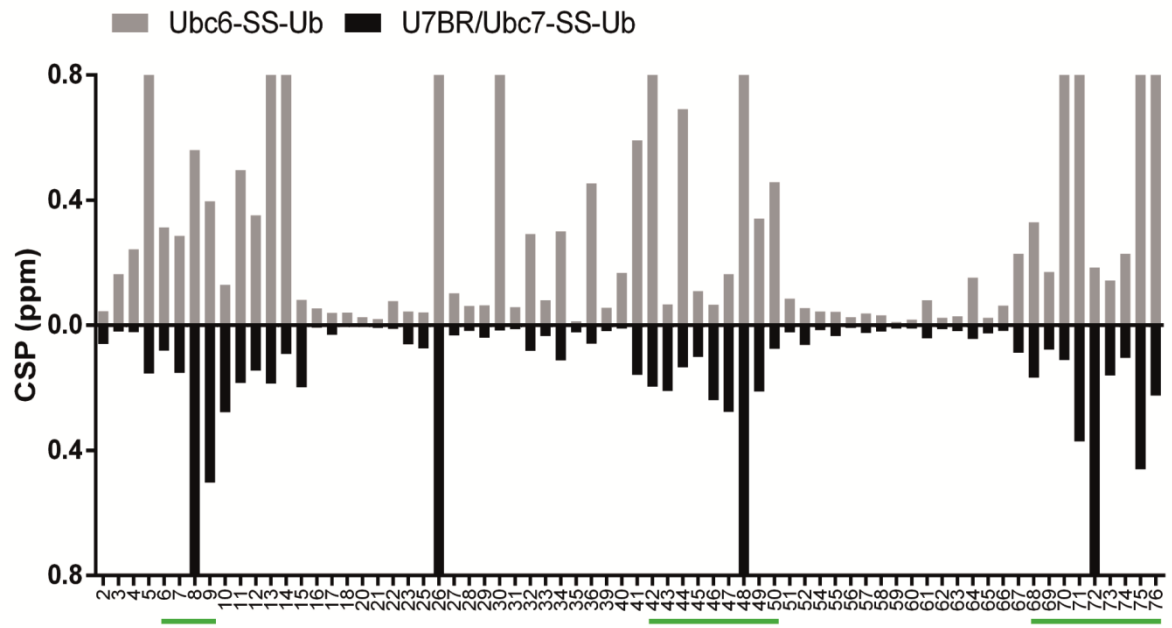

Figure 2-5: The Ubc6~Ub conjugate is predisposed to form the closed conformation. Shown are chemical shift perturbations from HSQC-TROSY experiments of stably conjugated ($^{2}H/^{15}N$) Ub^{G76S} to either Ubc6 (top) or Ubc7 (bottom) in relation to free Ub mapped over its sequence. Unassignable residues are shown as off-scale. Residues of the hydrophobic patch (closed conformation interaction interface) are underlined in green. Measurements were performed by Dr. Tobias Ritterhoff.

Canonical E2's interact with three distinct regions within the RING domains of E3 enzymes, the first and last Zinc binding CXXC motifs and a conserved α-helix of the RING fold[64]. To address the interaction of Ubc6/Ubc7 with the RINGs, NMR titration experiments employing $^{2}H/^{15}N$-labeled Doa10 RING variants and unlabeled E2~Ub conjugates were conducted. Recorded specific intensity losses for each residue per equivalent of conjugate were mapped onto the sequence of the employed Doa10 construct (Fig. 2-6). This calculated value was used since experiments in the slow exchange regime (e.g. E2/E3 titrations) usually give weak CSP signals that are difficult to detect.

In these experiments, we noted significant differences at the Doa10 linchpin position (Fig. 2-6 A). Ubc7~Ub induced a prominent doubling of the peak that corresponds to histidine 94 indicative for a physical interaction with this residue. In contrast, this amino acid was unaffected upon titration of Ubc6~Ub. When mutated to an alanine, neither Ubc6~Ub nor Ubc7~Ub caused a shift at this site. This result supports the idea that histidine facilitates linchpin allostery in the context of the Doa10 RING domain. Moreover, it confirms the notion that the activation of Ubc7 by RING domains depends on the nature of the linchpin residue, while stimulation of Ubc6 does not involve this site.

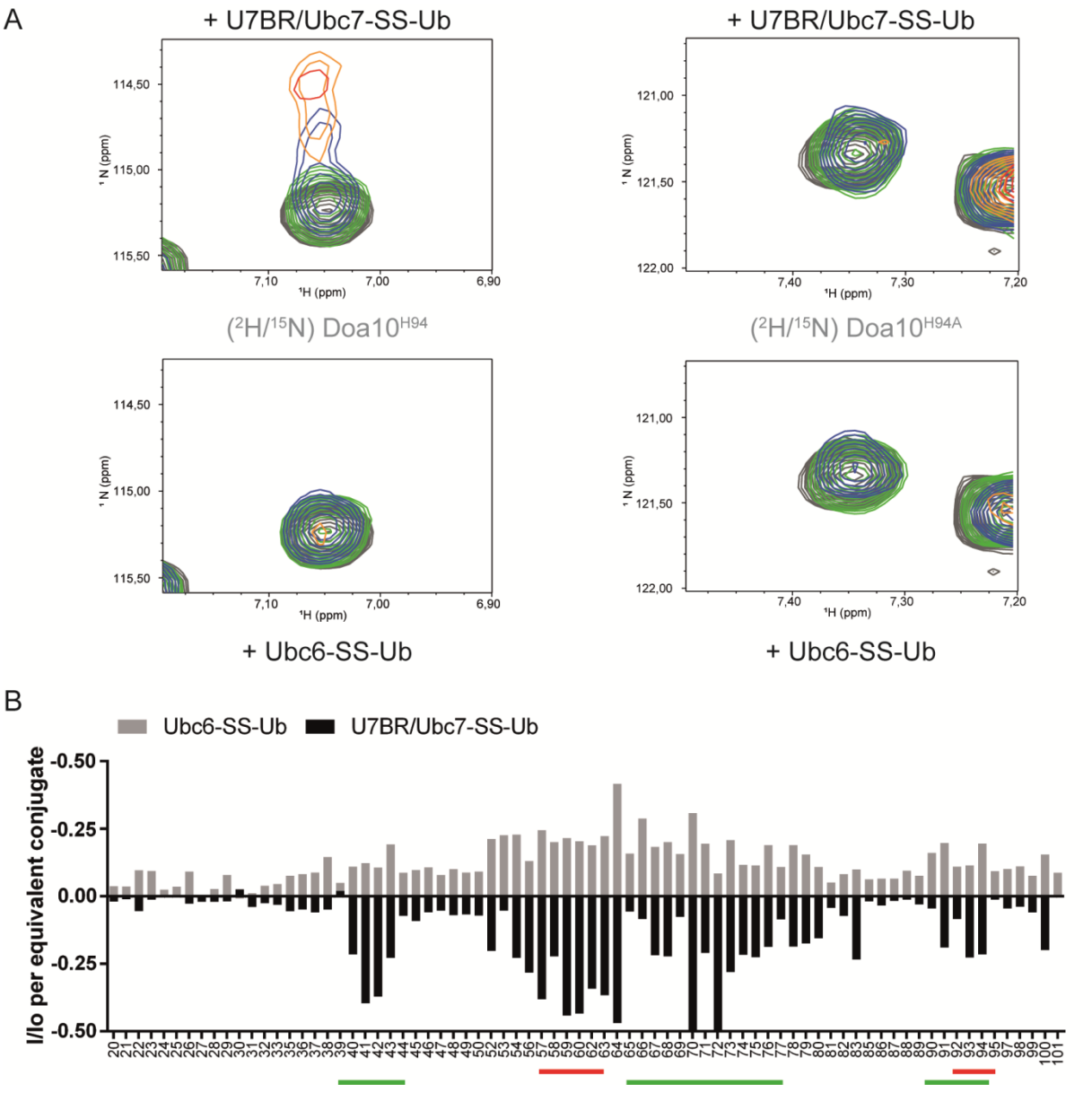

Figure 2-6: Canonical binding of E2~Ub to Doa10. (A) Representative spectra from HSQC-TROSY experiments showing peak doublings induced by titration of Ubc7~Ub (top) or Ubc6~Ub (bottom) on the linchpin position of the Doa10 RING domain containing either histidine (left) or alanine (right). Peak colors are as follows: gray: ($^{2}H/^{15}N$) Doa10, green: equimolar amount of E2~Ub, blue: 2 x E2~Ub, orange: 4x E2~Ub, red: 8x E2~Ub. (B) Specific intensity losses per equivalent of conjugate induced by Ubc6~Ub (top) or Ubc7~Ub (bottom) plotted over the sequence of the Doa10 RING construct. Regions where canonical E2 binding takes place are underlined in green. Presumed Ub contacts are underlined in red. Unassignable residues are shown as off-scale. Measurements were performed by Dr. Tobias Ritterhoff.

Overall, titration of the E2~Ub conjugates induced specific intensity losses at the canonical residues involved in E2 binding (Fig. 2-6 B). Interestingly, titration of Ubc6~Ub generally resulted in less pronounced effects on the Doa10 RING than Ubc7~Ub, even though the binding affinities of the RING for either E2 as determined by NMR were comparable. Doa10/Ub contacts were relatively more pronounced in the Ubc6~Ub conjugate, suggesting that RING/Ub interaction plays a role in E2

stimulation. Upon titration of the Ubc7~Ub conjugate, clear shifts were visible at the E2 binding sites indicating a canonical interaction between Doa10 and Ubc7. Also with this conjugate, changes were detected at residues involved in Ub binding, supporting the recent idea that RING/Ub contacts are important for ubiquitination reactions[71].

Following these results, direct contacts of the E2-conjugated Ub to the RING domains were investigated. Again, ($^{2}H/^{15}N$)-labeled Ub was stably conjugated to either Ubc6 or Ubc7 and subsequently titrated with unlabeled Doa10^{H94} (Fig. 2-7) or Hrd1^{R400} (Fig. 2-8) RING domains. Observed intensity losses in comparison to the above presented conjugates (compare Fig. 2-5) were mapped onto the sequence of Ub.

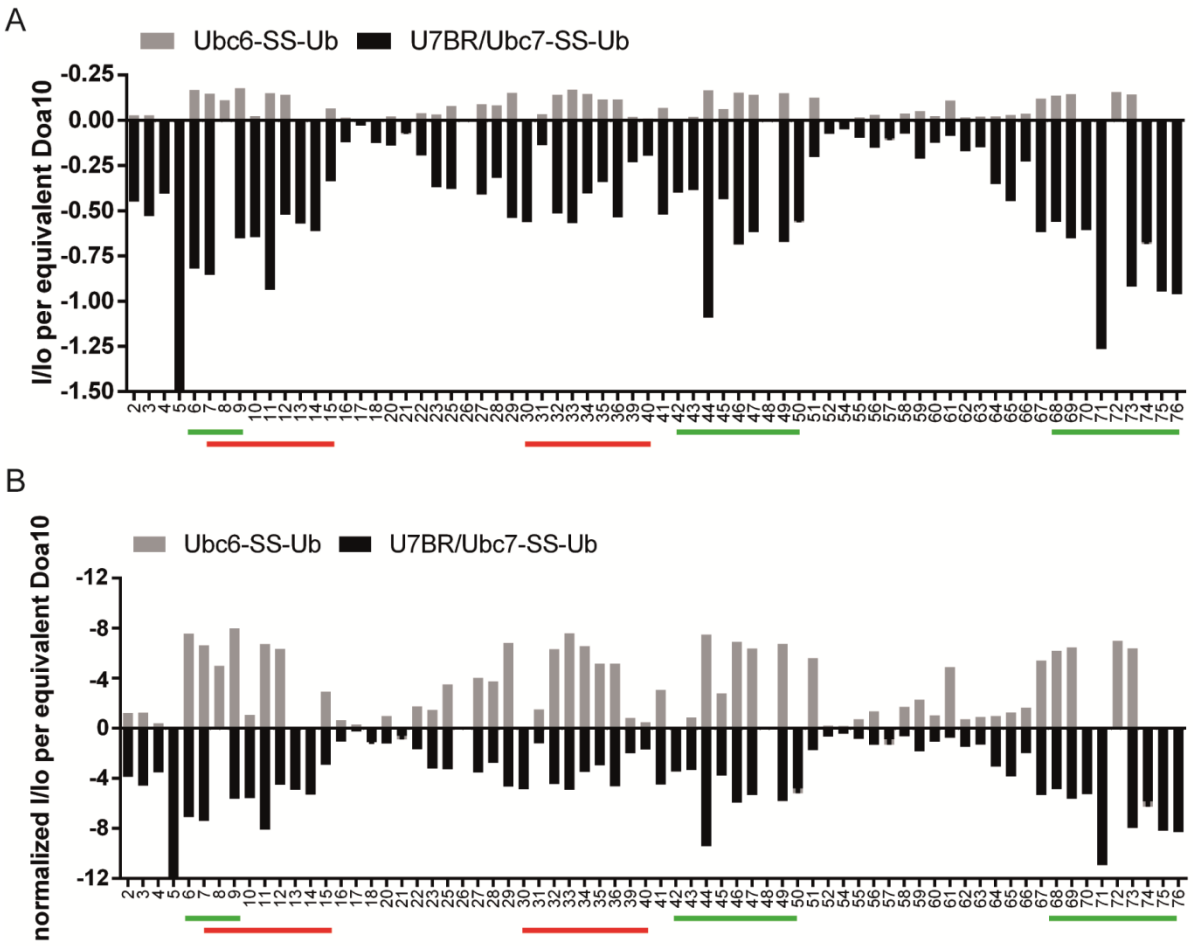

Figure 2-7: The Doa10 RING contacts Ub in E2~Ub conjugates. (A) Specific intensity losses of Ub residues per equivalent of Doa10 were plotted over the sequence Ub which was either conjugated to Ubc6 (top) or Ubc7 (bottom). (B) Intensity losses were normalized in relation to the average intensity loss of residues 16-22 and 52-63 of Ub. Residues of the hydrophobic patch are underlined in green. Presumed Doa10 contacts are underlined in red. Unassignable residues are shown as off-scale. Measurements were performed by Dr. Tobias Ritterhoff.

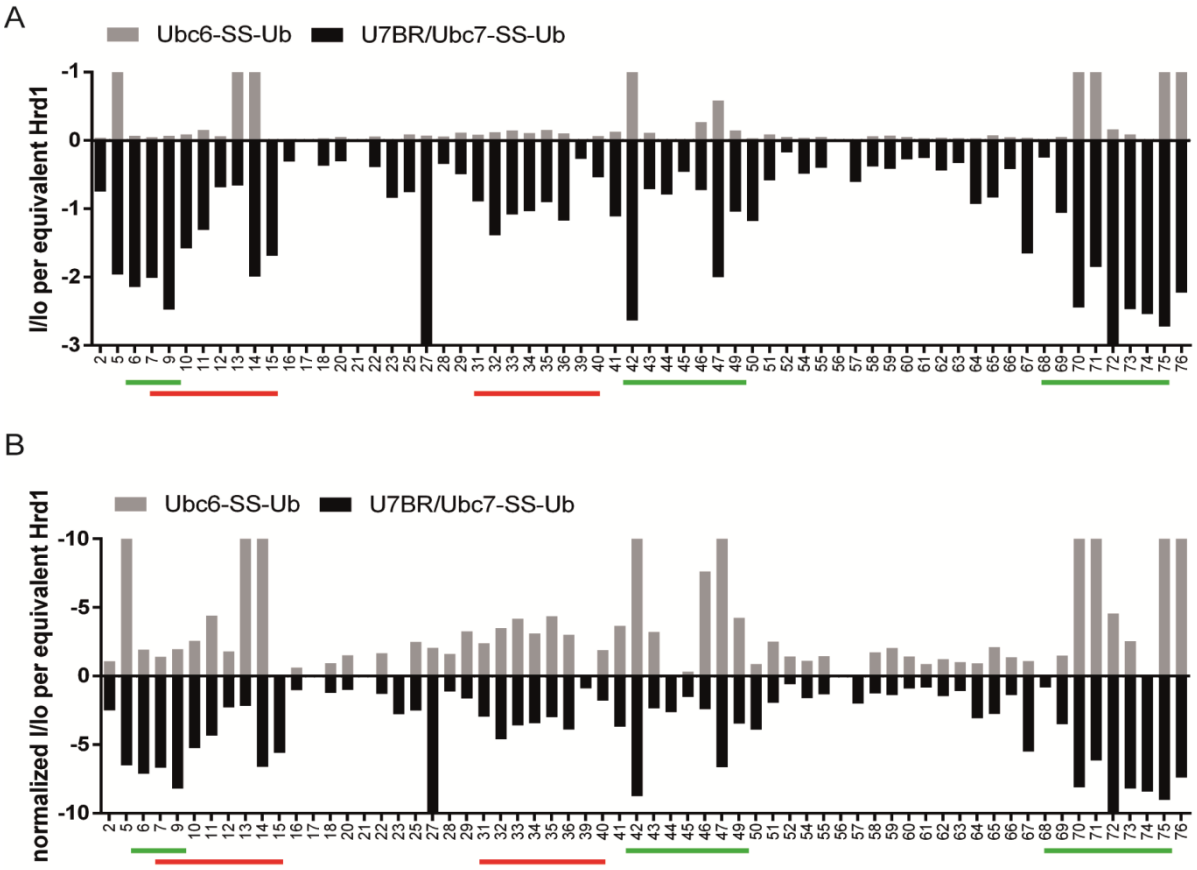

Figure 2-8: The Hrd1 RING contacts Ub in E2~Ub conjugates. (A) Specific intensity losses of Ub residues per equivalent of Hrd1 were plotted over the sequence Ub which was either conjugated to Ubc6 (top) or Ubc7 (bottom). (B) Intensity losses were normalized in relation to the average intensity loss of residues 16-22 and 52-63 of Ub. Residues of the hydrophobic patch are underlined in green. Presumed Hrd1 contacts are underlined in red. Unassignable residues are shown as off-scale. Measurements were performed by Dr. Tobias Ritterhoff.

It is readily visible that the effects of the RING titrations on Ubc6~Ub are drastically less pronounced than on Ubc7~Ub, especially at the closed conformation interface (Fig. 2-7 A, Fig. 2-8 A). The strong responses that RINGs elicit on the Ubc7~Ub conjugate imply that, upon interaction, the conjugate is heavily pushed into a closed conformation thereby being activated. Those responses are likely due to linchpin-mediated allostery, explaining the robust stimulation of Ubc7 in the discharge assays (Fig. 2-3). Ubc6, on the other hand, only shows minor responses to RING titrations. For means of visualization, the effects of the RING titrations were normalized in relation to the average intensity loss of ubiquitins residues 16-22 and 52-63 which are not involved in any reported interactions (Fig. 2-7 B, Fig. 2-8 B). The RING domains made clear contacts with Ub in the Ubc6~Ub conjugate without showing more pronounced shifts in the hydrophobic patch.

In summary, the results suggest that Ubc6 is inherently more biased towards a closed conformation than Ubc7. Contacts between RING domains and Ub are sufficient to stabilize this conformation and thereby allow a RING-dependent stimulation of the Ub transfer. At the same time, this means that Ubc6 is mostly independent of linchpin-mediated activation, while stimulation of Ubc7 heavily relies on this allostery. Contacts between RING domains and Ub in the Ubc7~Ub conjugate indicate that RING/Ub interaction is a general mechanism in stabilizing closed conformations and thereby enhances the ability of E2s to transfer Ub to targets.

2.1.6 K48-linked Ub chain formation by Ubc7 only partially relies on stimulation by the RING domain

Substrates labeled with poly-Ub linked via lysine 48 (K48) are in most cases degraded by the 26 S proteasome[72]. The E2 enzyme Ubc7 with its cofactor Cue1 is a very efficient K48-chain builder and can therefore generate such a degradation signal[38]. So far in this thesis, the effect of RING domains on the first step in Ub chain formation, the general transfer of Ub from E2 enzymes, was analyzed. This did not address the involvement of the RINGs in Ub chain formation. Accordingly, *in vitro* studies to monitor the detailed contribution of E2s and E3s in the individual steps during Ub chain formation were performed. To this end, the same constructs from the discharge and NMR assays were used, except for the addition of the complete cytosolic part of Cue1 instead of the U7BR domain (compare purification Fig. 2-2).

To address the mechanism of chain elongation in molecular detail, an assay was adopted from von Delbrück *et al.*[42] Monomeric or polymeric, C-terminally His_6-tagged Ub species (Ub-His_6, Ub_2-His_6, Ub_3-His_6) were added in high molecular excess and served as acceptors for additional Ub moieties during chain formation, thus resembling substrate-conjugated Ub. Conjugation of Alexa Fluor™ 488-labeled Ub (Ub^{488}) to these molecules by Ubc7 in single turnover experiments was then followed over time in presence of different RING domain variants (Fig. 2-9 A). Fluorescent signals of the products were visualized (Fig. 2-9 B, D), quantified in relation to whole-lane fluorescence and plotted over time (Fig. 2-9 C, E). Single exponential fits were then calculated to extract turnover rates (Fig. 2-9 F, G).

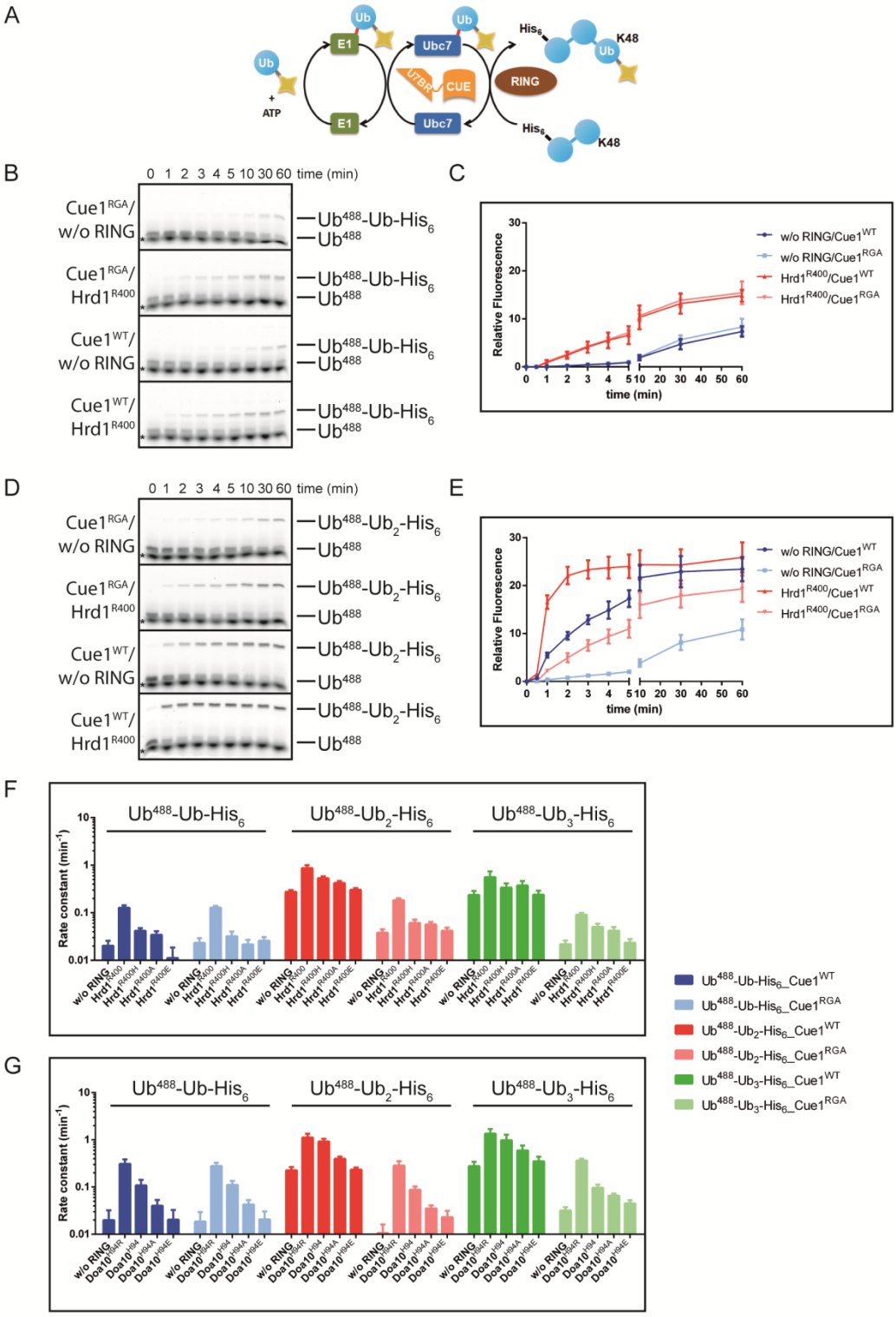

Figure 2-9: Chain elongation by Ubc7 is less dependent on RING stimulation. (A) Scheme of single turnover chain elongation reactions modified from von Delbrück *et al.*[42] (B-E) Representative fluorescence scans of elongation reactions from (B) mono- to diubiquitin and (D) di- to triubiquitin. Asterisks mark free fluorescent dye which could not be completely removed after labeling. Fluorescence signal of the respective reaction products in relation to whole-lane fluorescence was quantified and plotted as a function of time (C, E). (F, G) Kinetic rate constants for (F) Hrd1-dependent and (G) Doa10-dependent elongation reactions in cooperation with Cue1^{WT} (dark colored) or Cue1^{RGA} (light colored) were extracted from single exponential fits of resulting curves. Error bars represent the standard deviation of mean of at least three independent experiments.

In these experiments, not only the impact of the RING domains on Ub chain formation was investigated but also the contribution of the Ubc7 cofactor Cue1. Cue1 is embedded in the ER membrane where it recruits Ubc7 to ER-resident E3 ligases[37] and promotes Ubc7-mediated K48-linked Ub chain formation. Binding of Cue1 causes a steric activation of Ubc7[40,70]. Moreover, the CUE domain of Cue1 aligns growing Ub chains with Ubc7 and thereby facilitates chain elongation[41,42,73]. It has been shown that Cue1 preferentially associates with the penultimate Ub moiety in a K48-linked poly-Ub chain and that a change of residues 76-78 (LAP → RGA) in the CUE domain abrogates binding and impairs chain elongation. With this variant in hand, the effects of the RING and CUE domains on Ub chain elongation were analyzed.

Ubc7-mediated elongation of the priming Ub moiety (Ub-His_6) was readily stimulated by the wild type Hrd1 RING domain independently of the Cue1 variant in the assay (Fig. 2-9 B, C). Addition of different Hrd1 or Doa10 RING domain constructs resulted in a similar reaction pattern as observed in the discharge experiments on ethanolamine (Fig. 2-9 F, G, blue bars). This demonstrates an enzymatic activation of Ubc7 by linchpin-mediated allostery. All tested RING domain variants displayed comparable reaction kinetics in presence of $Cue1^{WT}$ or $Cue1^{RGA}$ suggesting that the first step in chain elongation is not stimulated by the alignment of Ubc7 to the acceptor Ub via Cue1.

When the elongation of chains containing two or three Ub molecules was followed, linchpin-substituted RING domains showed the same overall behavior as was observed in the discharge assays on smaller molecules (Fig. 2-9 F, G, red and green bars). However, in contrast to the elongation of the monomeric Ub, turnover of longer chains was significantly accelerated by $Cue1^{WT}$, but not by the Ub binding-deficient $Cue1^{RGA}$ variant (Fig. 2-9 D, E). This result confirms published information that binding of Cue1 requires at least two Ub moieties[42]. While supplementation of RING domains led to an additive stimulation in the first 10 minutes of the reaction, the kinetic curves converged at later timepoints (Fig. 2-9 E). Importantly, wild type Cue1 stimulated the intrinsic chain elongation capacity of Ubc7 stronger than the addition of a RING domain. The Ub binding deficient $Cue1^{RGA}$ variant accelerated Ub chain formation to a similar degree than the elongation of mono-Ub.

In general, early steps in Ub chain formation are stimulated by a mechanism involving the linchpin residue in the RING domain. The extension of longer chains is still accelerated by the RING domain, but the alignment of these substrates with Ubc7 via Cue1 now constitutes the dominant stimulating factor. This implies that during poly-Ub synthesis, the impact of the RING domain on the reaction decreases along with the length of the assembled Ub chain. The addition of Ub moieties is then primarily facilitated by the positioning of the Ubc7/Cue1 complex on the growing chain via the CUE domain.

2.1.7 *In vitro* ubiquitination of proteins by Ubc7 is stimulated by Hrd1

Ub discharge from E2 enzymes and Ubc7-mediated Ub chain elongation have been analyzed extensively in the previous sections. Still, it is unclear if the modification of protein substrates is affected by any of the reported interactions. To address this issue, an *in vitro* substrate ubiquitination assay based on an experimental setup by Bays *et al.*[74] was established. The authors fused a peptide stretch termed “S peptide”, which is derived from bovine RNase A and is commonly used in protein purification procedures, to the Hrd1 RING domain. The S peptide epitope displays a high affinity for binding the remaining part of the RNase A termed “S protein”, with which it forms the so-called RNase S[75] (Fig. 2-10 A). In the *in vitro* assay, the S peptide-RING fusions are recruited to the S protein which serves as an acceptor for ubiquitination.

Ubc7 predominantly generates unanchored Ub chains in *in vitro* experiments[41], and therefore any modifications on the S protein can only be visualized upon direct detection of the substrate. To increase the sensitivity of the assay, a technique for fluorescent labeling via the so-called Tub-tag labeling approach was implemented[76]. A construct comprising a short α-tubulin-derived recognition peptide fused to the C-terminus of the S protein was purified and modified with 3-Azido-L-tyrosine by the addition of tubulin tyrosine ligase. This allowed for site-specific strain-promoted azide-alkyne cycloaddition[77] (SPAAC) introducing dibenzocyclooctyne (DBCO)-strained Alexa Fluor™ 488 into the substrate. In the first step, experiments performed by Bays *et al.*[74] using the E2 enzyme Ubc4 were recapitulated and further extended by including appointed variants of the Hrd1 and Doa10 RING domains (Fig. 2-10 B).

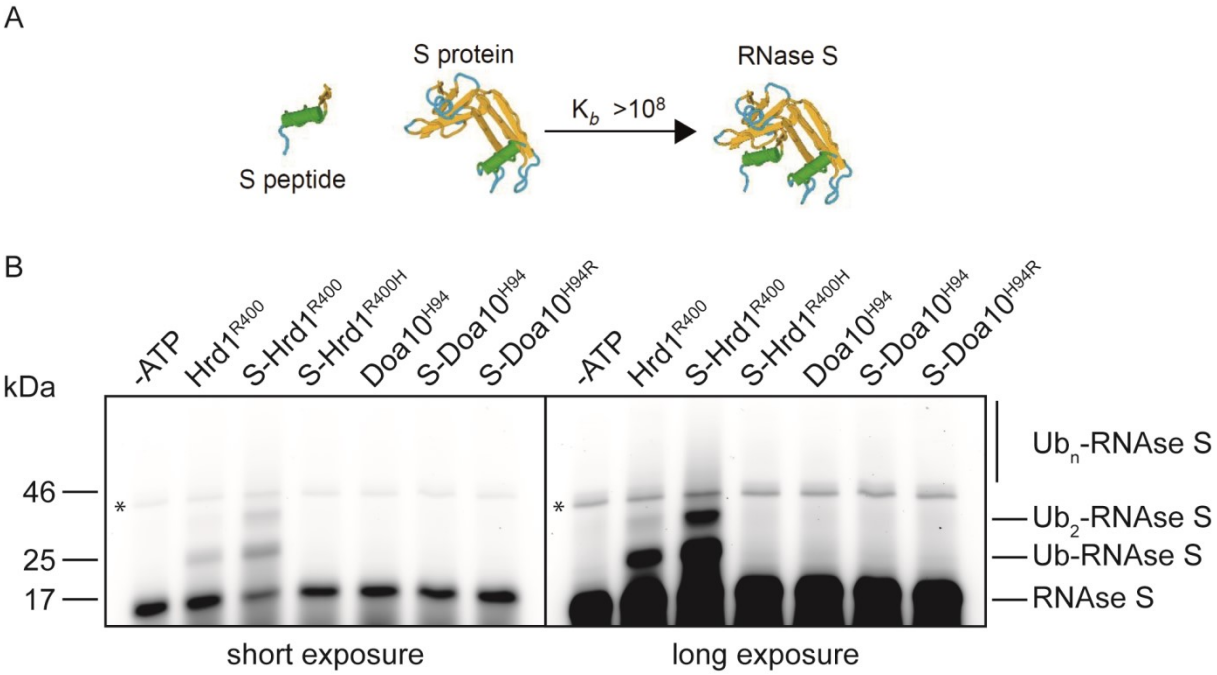

Figure 2-10: *In vitro* ubiquitination of the S protein by Ubc4. (A) S peptide harbors a high affinity for the S protein, adopted from Bays *et al.*[74] (B) Fluorescence scan of *in vitro* ubiquitination reactions involving Ubc4 and different untagged and S peptide-tagged RING domain variants. Asterisks mark unspecific signals.

As described by Bays *et al.*[74], Ubc4 decorated RNase S with up to two Ub moieties in such reactions. Considering the known catalytic properties of Ubc4, the observed modifications most likely represent mono-ubiquitination on multiple lysine residues[78]. Obviously, Ubc4-mediated ubiquitination was strictly dependent on the presence of the wild type Hrd1 RING domain. Even in presence of Hrd1 lacking the S peptide, a significant portion of the S protein was decorated with Ub (Fig. 2-10, lane 2). This activity probably results from random interactions of the proteins in solution. An S peptide-Hrd1^{R400} RING domain construct significantly increased ubiquitination on the S protein and caused a decrease of the unmodified form (Fig. 2-10, lane 3). S-Hrd1^{R400H}, which contains a histidine at the linchpin position, did not facilitate substrate ubiquitination implying that the activation of Ubc4 strictly depends on linchpin allostery (Fig. 2-10, lane 4). Remarkably, none of the S peptide-Doa10 RING constructs promoted ubiquitination of the S protein and hence this ligase seems unable to stimulate the activity of Ubc4 (Fig. 2-10, lanes 5-7).

Next, Ubc7-mediated substrate modification was analyzed (Fig. 2-11). These experiments also contained Cue1^{WT} to activate Ubc7 and to allow the synthesis of poly-Ub chains.

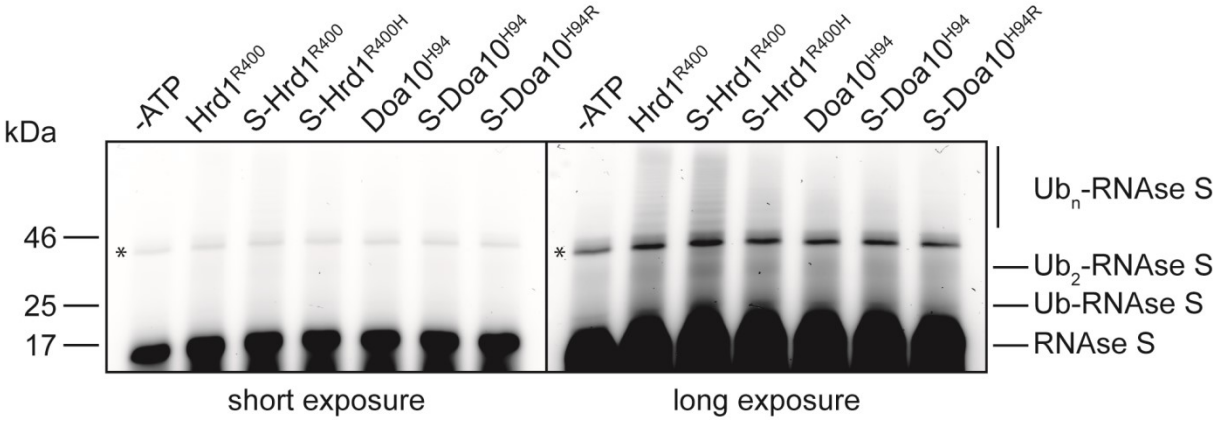

Figure 2-11: Ubc7-mediated *in vitro* substrate ubiquitination is Hrd1-dependent. Fluorescence scan of *in vitro* ubiquitination reactions involving Cue1^{WT}/Ubc7 and different untagged and S peptide-tagged RING domain variants. Asterisks mark unspecific signals.

Ubc7 weakly promoted chain formation on the S protein upon addition of the untagged Hrd1^{R400} RING domain (Fig. 2-11, lane 2), probably due to some unspecific association of the substrate with the RING construct and the E2. Specific recruitment of the RING domain via the S peptide increased the reactivity of Ubc7 towards the S protein (Fig. 2-11, lane 3). Substrate ubiquitination was largely dependent on the nature of the linchpin residue since the amount of ubiquitinated S protein was significantly lower in reactions containing S-Hrd1^{R400H} (Fig. 2-11, lane 4). Again, there was no substrate modification observed in presence of Doa10 RING domain variants (Fig. 2-11, lanes 5-7).

Taken together, *in vitro* ubiquitination of the S protein by Ubc7 required an arginine in the linchpin position of the Hrd1 RING domain. Given that Ub chain elongation is primarily accelerated by Cue1 (compare section 2.1.2.4), this indicates that the stimulation of Ubc7 by Hrd1 predominantly serves to facilitate the priming of substrates. Noteworthy, none of the Doa10 RING variants promoted ubiquitination by Ubc7. This result shows that the allosteric activation of Ubc7 by the linchpin residue relies on additional properties of the RING domain.

2.1.8 *In vitro* ubiquitination of proteins by Ubc6 does not require stimulation by a linchpin residue

Ubc6 is stimulated in discharge assays by Hrd1 and Doa10 RING domain variants regardless of the residue at the linchpin position (compare section 2.1.2.2). Still, this does not exclude that the transfer of Ub onto a protein by Ubc6 depends on allosteric activation via the linchpin residue. Thus, ubiquitination of the S protein by Ubc6 was analyzed (Fig. 2-12).

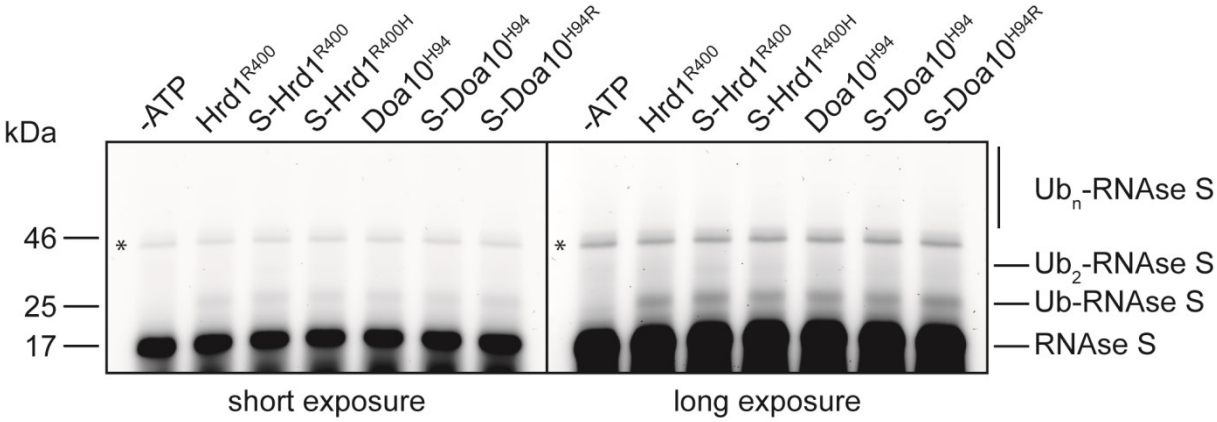

Figure 2-12: Ubc6-mediated *in vitro* substrate ubiquitination is linchpin-independent. Fluorescence scan of *in vitro* ubiquitination reactions involving Ubc6 and different untagged and S peptide-tagged RING domain variants. Asterisks mark unspecific signals.

Ubc6 was shown to efficiently prime client proteins with Ub, but lacks the capacity to form Ub chains on these substrates[20]. Concordantly, Ubc6 readily attached single Ub moieties to the S protein in the *in vitro* assays. This process was equally efficient regardless of which RING domain variant was added. Obviously substrate modification by Ubc6 is not stimulated by linchpin allostery. Furthermore, the S peptide on the RING domain did not enhance substrate ubiquitination. These findings correlate with the inherent activity of Ubc6 to dispose Ub onto acceptor molecules even in the absence of a RING domain as observed in discharge assays.

In summary, substrate ubiquitination by Ubc6 does not rely on the nature of the linchpin residue in a RING domain. Preliminary results suggest that this process does not require activation by a RING domain (data not shown). However, to draw more profound conclusions, the substrate ubiquitination assay needs to be further optimized to increase the client turnover rates and thereby improve the quality of the data. Moreover, an experiment lacking a RING domain construct should be performed to analyze any inherent activity of Ubc6 in substrate ubiquitination.

2.2 ERAD ligases exploit different strategies of priming and elongation to ensure efficient substrate degradation

2.2.1 The linchpin residue in Hrd1 determines the degradation rate of client proteins

After a thorough *in vitro* analysis, the effect of RING-mediated E2 stimulation was investigated in *S. cerevisiae*. The ERAD system was intensely studied in this model organism and specific substrates for the Doa10 and Hrd1 Ub ligase complexes have been identified. Of note, key players of the ERAD pathway are well-conserved in all eukaryotes[79].

To gain insight into the relevance of linchpin allostery on the function of Hrd1, the degradation of two model substrates showing different topology was analyzed. The soluble protein PrA* is derived from the vacuolar proteinase yscA (PrA), but lacks a short sequence encompassing the processing site and is therefore removed by Hrd1-mediated ERAD from the ER lumen[80]. Conversely, HMG-CoA reductase (Hmg2) represents an integral enzyme of the ER membrane involved in sterol biosynthesis that is regulated by Hrd1-dependent proteolysis[81].

Pulse-chase assays were conducted to follow the degradation of these model substrates. To this end, PrA* and Hmg2 were fused to 3xHA and 6xMyc epitopes, respectively, to allow a specific enrichment during the procedure. PrA*-3xHA was expressed in yeast cells from plasmids, while the construct for Hmg2-6xMyc expression was stably integrated in the yeast genome and replaced the endogenous gene. Cells were provided with S^{35}-radiolabeled amino acids which are incorporated into newly synthesized proteins. Subsequently, the cells were chased with unlabeled amino acids. Aliquots of the samples were removed at regular time points and cell lysates were prepared. HA- and Myc-tagged proteins were isolated by immunoprecipitation and the recovered material was visualized by autoradiography (Fig. 2-13 A, B). The amount of radiolabeled substrate was then quantified and plotted against the chase time (Fig. 2-13 C, D). The amount of recovered PrA*-3xHA rapidly decreased over time indicative for a fast turnover of this protein. In strains lacking Hrd1 (*Δhrd1*) substrate decay was heavily impaired and could be restored

with a plasmid expressing wild type Hrd1 (Hrd1^{R400}). This demonstrates that PrA*-3xHA is degraded via the Hrd1 Ub ligase. Similarly, Hmg2-6xMyc was degraded over time but this process was not exclusively dependent on Hrd1, since a significant loss of substrate could be observed even in cells lacking this ligase.

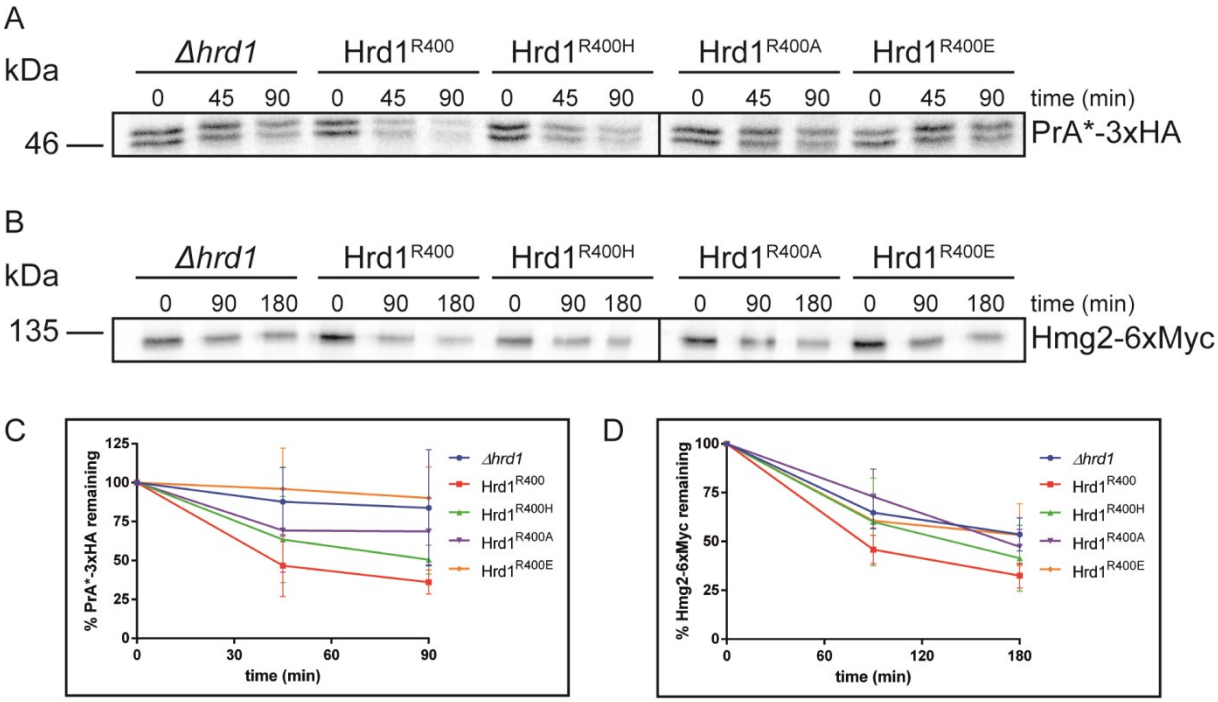

Figure 2-13: Degradation at the HRD ligase is linchpin-dependent. Representative autoradiography scans following the degradation of (A) PrA*-3xHA and (B) Hmg2-6xMyc. The upper species in the PrA*-3xHA scan represents the full-length construct. The lower species most likely results from premature translation termination and represents a variant with less than three HA epitopes. (C, D) Radioactive signals were quantified and plotted over time. Error bars represent the standard deviation of mean of at least three independent experiments.

Expression of appointed linchpin variants led to a gradual decrease in the turnover of both substrates. Remarkably, these results matched the effects observed in the Hrd1-stimulated Ubc7 discharge reactions (compare section 2.1.2.1). This implies that the nature of the linchpin residue affects protein degradation at the Hrd1 ligase irrespective of the topology of the substrate. Furthermore, these data suggest that Hrd1-mediated protein turnover mainly involves Ubc7.

2.2.2 Turnover of Doa10 target proteins does not involve the linchpin position

Doa10-mediated protein breakdown was analyzed by implementation of two Doa10 model substrates. An engineered cytosolic protein composed of the Doa10 target region Deg1 and two copies of the enhanced green fluorescent protein (Deg1-eGFP$_2$)[82] was expressed from a plasmid in yeast cells. Deg1 constitutes a degron

derived from the yeast transcriptional repressor Matalpha2 which is partially down-regulated by Doa10-mediated breakdown[48,83]. Therefore, fusion constructs containing Deg1 are degraded via the Doa10 pathway. In addition, an ER membrane-resident tail-anchored protein, which undergoes Doa10-dependent turnover, was studied. Sec61 β-subunit homologue 2 (Sbh2) is part of the trimeric Ssh1 (Sec61 homologue 1) translocon[84]. Unassembled Sbh2 subunits are rapidly removed via Doa10-mediated ubiquitination[85]. To increase the turnover of Sbh2, a FLAG epitope-marked version was expressed in yeast cells lacking its interaction partner Ssh1.

Addition of cycloheximide (CHX) to the growth medium blocks the synthesis of new proteins. The fate of already translated proteins can be followed by analyzing their amount in samples taken at regular time points after CHX addition and subsequent immunoblotting with specific antibodies (Fig. 2-14 A, B). To facilitate quantitative analysis, fluorescently labeled secondary antibodies were used and the obtained data for proteins amounts were plotted as a function of time (Fig. 2-14 C, D)

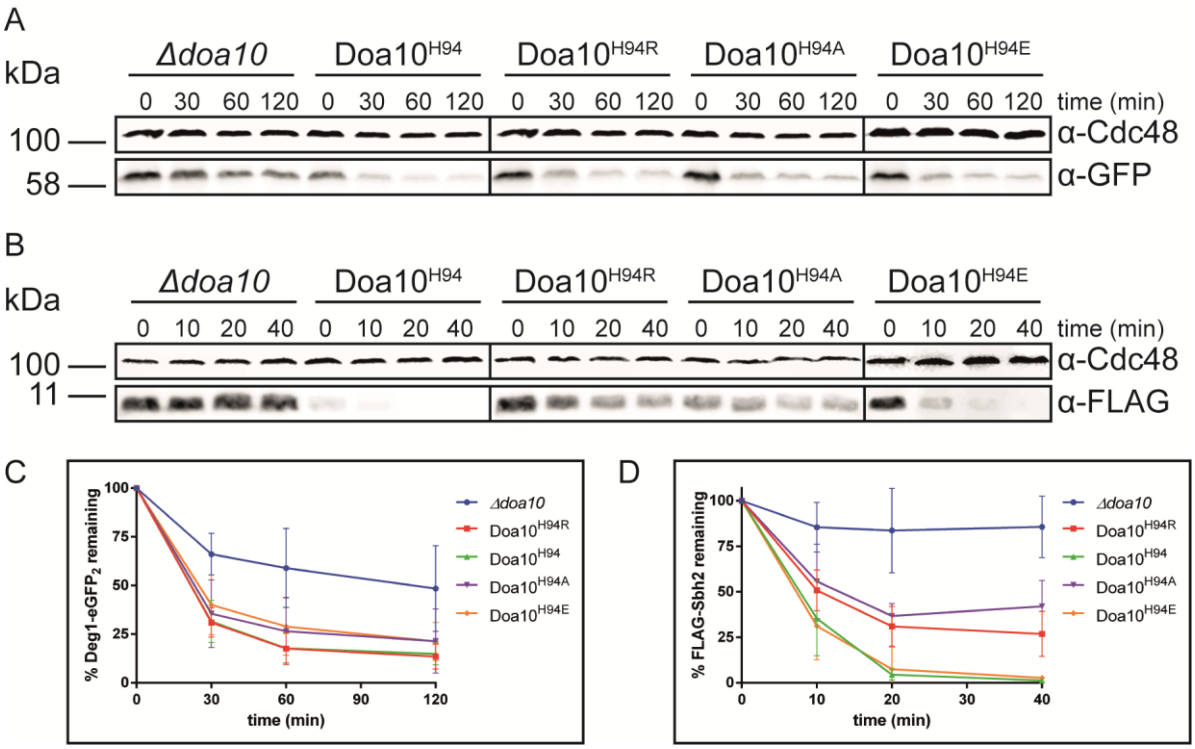

Figure 2-14: Degradation at the Doa10 ligase is linchpin-independent. Representative western blots following the decay of (A) Deg1-eGFP$_2$ and (B) FLAG-Sbh2. In both cases, Cdc48 served as loading control. Assays involving FLAG-Sbh2 were performed in cells deleted for Ssh1 (*Δssh1*). (C, D) Signals detected via fluorescently-labeled secondary antibodies were quantified and plotted over time. Error bars represent the standard deviation of mean of at least three independent experiments.

As seen in Figure 2-14, the amount of the Deg1-eGFP$_2$ signal rapidly decreases over time, indicative of fast proteolysis of the protein. Deg1 degron-containing proteins are in part degraded by pathways other than the Doa10 ligase, because the deletion of the *DOA10* gene (*Δdoa10*) did not fully abolish the turnover of Deg1-eGFP$_2$. In contrast, FLAG-Sbh2 decay was completely blocked in cells lacking Doa10. Degradation of Deg1-eGFP2 and FLAG-Sbh2 was then investigated in yeast strains expressing Doa10 variants with different amino acids at the linchpin position from the endogenous chromosomal locus. Strikingly, none of the Doa10 constructs affected the turnover of these substrates indicating that the processing of Doa10 client proteins commences without the stimulation of E2 enzymes via linchpin allostery.

2.2.3 The rate of Ub chain elongation does not restrict substrate degradation

In section 2.1.2.4, Ubc7-mediated Ub chain elongation was analyzed in molecular detail. Since both the Hrd1 and the Doa10 ligase cooperate with this E2, the impact of chain elongation on target breakdown was monitored in yeast cells. To this end, strains were constructed that express Cue1^{RGA} from the endogenous chromosomal locus or that completely lack Cue1 (*Δcue1*). In addition, different linchpin variants of Hrd1 or Doa10 were expressed in these cells.

To determine the relevance of chain elongation at the Hrd1 ligase, the proteolytic breakdown of PrA*-3xHA and Hmg2-6xMyc was followed in pulse-chase experiments (Fig. 2-15). While cells deleted for *CUE1* were unable to degrade these substrates (blue curves), cells expressing Cue1^{RGA} (red curves) were not affected in this process compared to wild type cells (black curves). The Cue1^{RGA} variant is impaired in Ub binding, but efficiently recruits Ubc7 to the Ub ligases in the ER membrane. Introduction of selected linchpin variants in these cells led to some variability during target turnover, but overall the decay of PrA*-3xHA and Hmg2-6xMyc followed the same pattern as observed in strains expressing the corresponding Hrd1 variants alone (compare Fig. 2-13). Since the CUE domain in Cue1 primarily serves to correctly align Ubc7 with growing Ub chains during poly-Ub synthesis, this indicates that the rate of chain elongation is not a limiting factor for the degradation of Hrd1 client proteins.

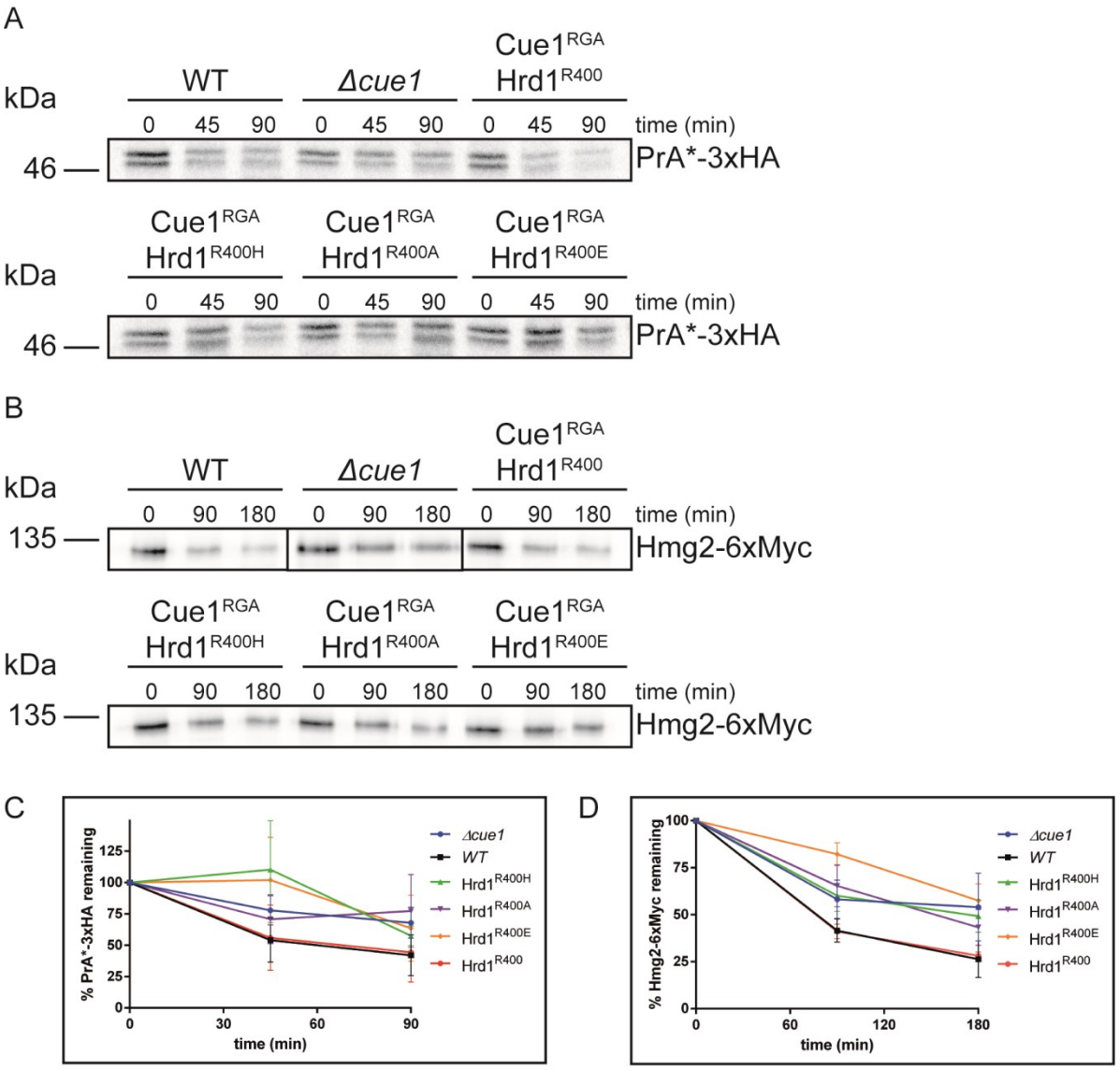

Figure 2-15: Introduction of Cue1^{RGA} does not exacerbate the degradation defects of the Hrd1 linchpin variants. Representative autoradiography scans following the degradation of (A) PrA*-3xHA and (B) Hmg2-6xMyc. The upper species in the PrA*-3xHA scan represents the full-length construct. The lower species most likely results from premature translation termination and represents a species with less than three HA epitopes. (C, D) Radioactive signals were quantified and plotted over time. Curves for Hrd1 linchpin variants (Hrd1^{R400x}) correspond to experiments in a Cue1^{RGA} strain background. Error bars represent the standard deviation of mean of at least three independent experiments.

The impact of Cue1^{RGA} on the processing of Doa10 substrates was also analyzed (Fig. 2-16). Deletion of *CUE1* only had a mild effect on Deg1-eGFP$_2$ breakdown, probably because the turnover of this protein only partially commences via the Doa10 ligase and the alternative degradation routes do not involve Cue1 function. In contrast, decay of FLAG-Sbh2 was completely abolished in absence of Cue1. Expression of the Cue1^{RGA} variant did not affect the processing of either substrate.

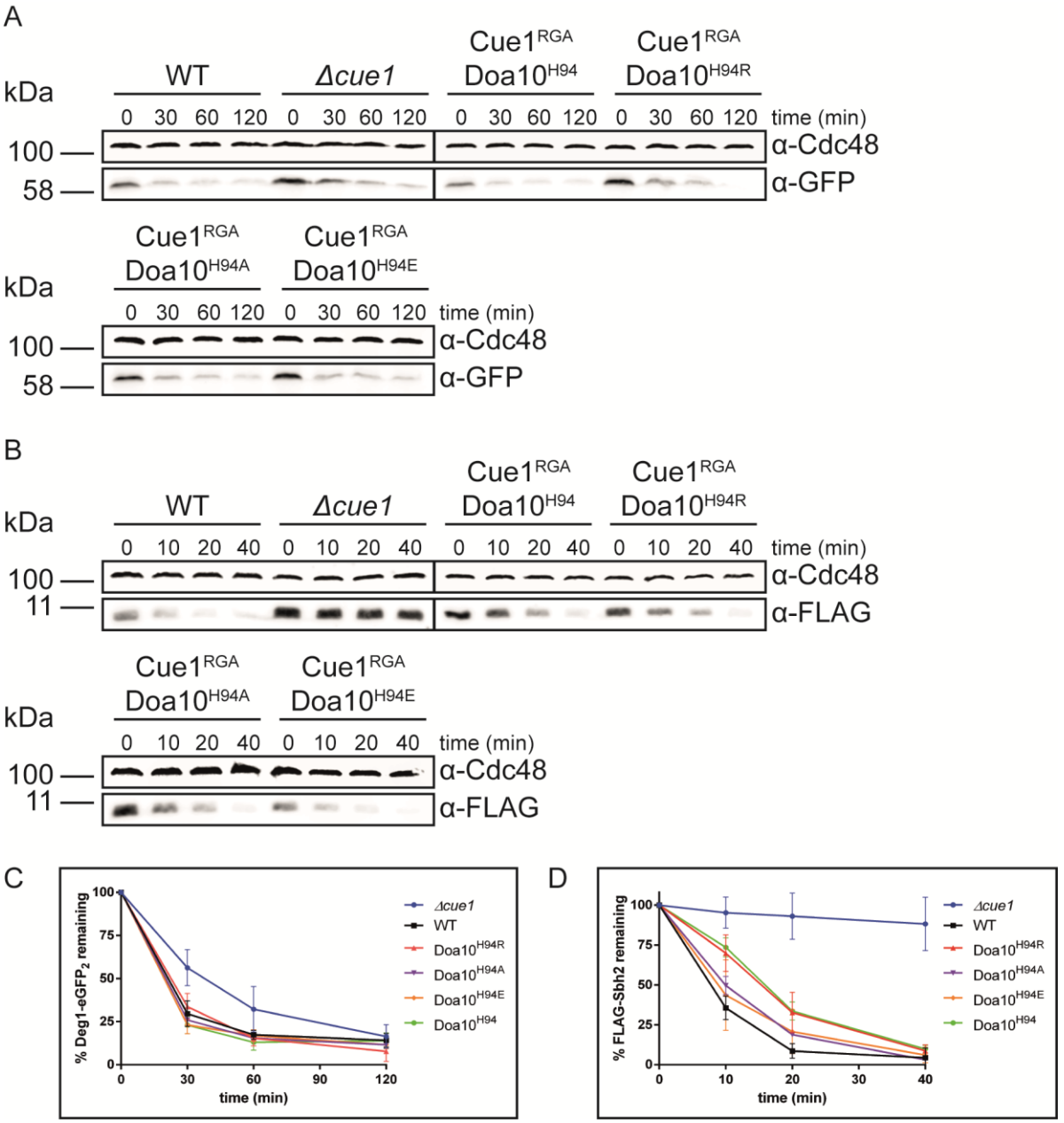

Figure 2-16: Degradation of Doa10 client proteins does not depend on the CUE domain of Cue1. Representative western blots following the decay of (A) Deg1-eGFP$_2$ and (B) FLAG-Sbh2. In both cases, Cdc48 served as loading control. Assays involving FLAG-Sbh2 were performed in cells deleted for Ssh1 (*Δssh1*). (C, D) Signals detected via fluorescently-labeled secondary antibodies were quantified and plotted over time. Curves for Doa10 linchpin variants (Doa10^{H94x}) correspond to experiments in Cue1^{RGA} strain background. Error bars represent the standard deviation of mean of at least three independent experiments.

Also the expression of the Doa10 linchpin variants in the Cue1^{RGA} cells did not cause significant changes in the turnover rates of Deg1-eGFP$_2$ or FLAG-Sbh2. Thus, similar to the results obtained with the Hrd1 ligase, degradation of Doa10 client proteins is not restricted by the rate of poly-Ub synthesis on the targets.

The impact of the Cue1^{RGA} variant on substrate decay was negligible although the efficient formation of K48-linked Ub chains by Ubc7 is thought to constitute a

prerequisite for proteasomal degradation. Therefore, the activity of the Hrd1 and Doa10 ligases was examined in cells lacking Ubc7 (Fig. 2-17).

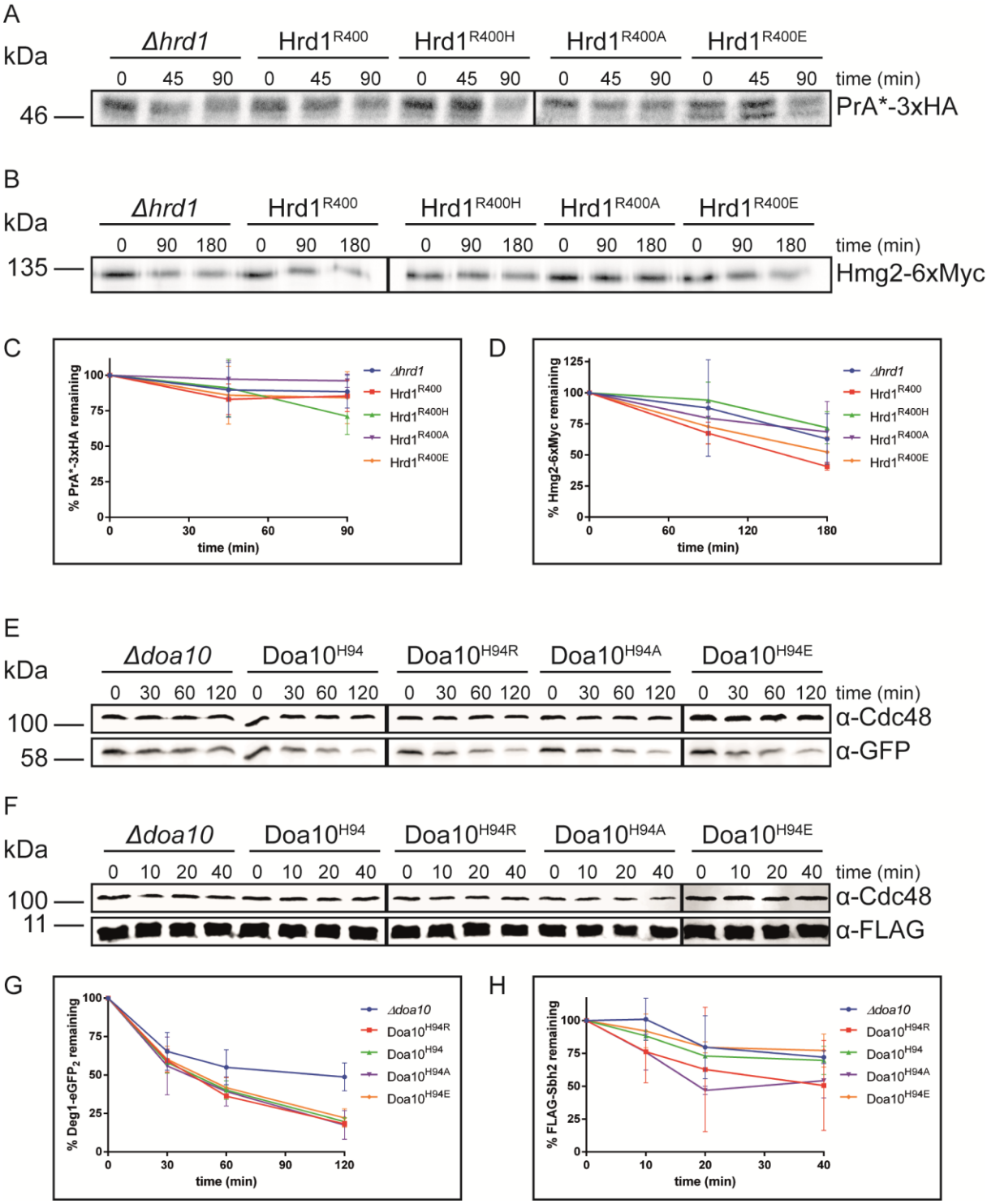

Figure 2-17: Degradation of Hrd1 and Doa10 target proteins relies on Ubc7. Representative autoradiography scans following the degradation of (A) PrA*-3xHA and (B) Hmg2-6xMyc and representative western blots following the decay of (E) Deg1-eGFP$_2$ and (F) FLAG-Sbh2. Experiments were performed in cells lacking Ubc7 (*Δubc7*). Cdc48 served as loading control in CHX chase experiments. Assays involving FLAG-Sbh2 were performed in cells deleted for Ssh1 (*Δssh1*). Radioactive (C, D) as well as fluorescent (G, H) signals were quantified and plotted over time. Error bars represent the standard deviation of mean of at least three independent experiments.

As expected, the decay of almost all tested substrates was heavily impaired in cells deleted for *UBC7* with the exception of Hmg2-6xMyc. In contrast to published data[86], degradation of this protein was only marginally slower in absence of Ubc7. Yet, Hmg2-6Myc breakdown proceeded differently in cells expressing individual Hrd1 RING linchpin variants indicating that also other E2 enzymes can initiate proteasomal degradation by synthesizing Ub chains onto this protein in a Hrd1-dependent manner. A promising candidate for this is Ubc4, since *in vitro* it could ubiquitinate a protein in a Hrd1-dependent manner and its activity in this assay was stimulated by linchpin allostery (compare Fig. 2-10). Degradation of the Hrd1 client protein, PrA*-3xHA was completely abolished in cells lacking Ubc7. This suggests that Ub signals that may be generated by other E2 enzymes in absence of Ubc7 are not efficiently initializing proteasomal breakdown of Hrd1 target proteins. Most likely, the Hrd1 ligase does not generally employ E2 enzymes other than Ubc7 to facilitate recognition of its substrates by the proteasome. The requirement of certain E2 enzymes in substrate processing may also originate from the distinct topology of the targets. The cytosolically exposed parts of membrane-bound Hmg2 may be directly accessible to Ubc4, while ubiquitination of PrA* may predominantly occur on regions which are selectively exposed to Ubc7 during retrotranslocation.

In summary, the rate of chain elongation seems to not constitute a limiting factor for the degradation of Hrd1 and Doa10 client proteins *in vivo*, even though the efficient synthesis of a K48-linked Ub signal on proteins is a prerequisite for proteasomal processing.

2.2.4 Priming of proteins with Ub is a rate-limiting step for their degradation

If chain elongation is not rate-limiting for substrate degradation, priming might be. Doa10 employs two E2 enzymes, Ubc6 and Ubc7, during substrate ubiquitination. Ubc6 first primes a target by attaching single Ub moieties which are then elongated to K48-linked poly-Ub chains by Ubc7[20,87]. The impact of priming on substrate turnover at the Doa10 ligase was investigated in CHX decay assays (Fig. 2-18).

In these experiments the deletion of *UBC6* abolished the degradation of Deg1-eGFP$_2$ irrespective of the Doa10 RING variant supplied. This demonstrates that the priming of a Doa10 substrate with Ub moieties strictly relies on Ubc6. Even a Doa10 variant

exposing an arginine at the linchpin position, which significantly stimulated Ubc7 activity in the *in vitro* discharge assays (compare section 2.1.2.1), did not bypass the requirement for Ubc6 *in vivo*.

Degradation of FLAG-Sbh2 was not completely abolished in cells lacking Ubc6, indicating that this substrate can be primed by Ubc7 or other E2s. Still, degradation succeeded noticeably slower in *Δubc6* than in wild type cells (compare Fig. 2-14). Expression of the Doa10 RING variants had no further impact on the turnover rate.

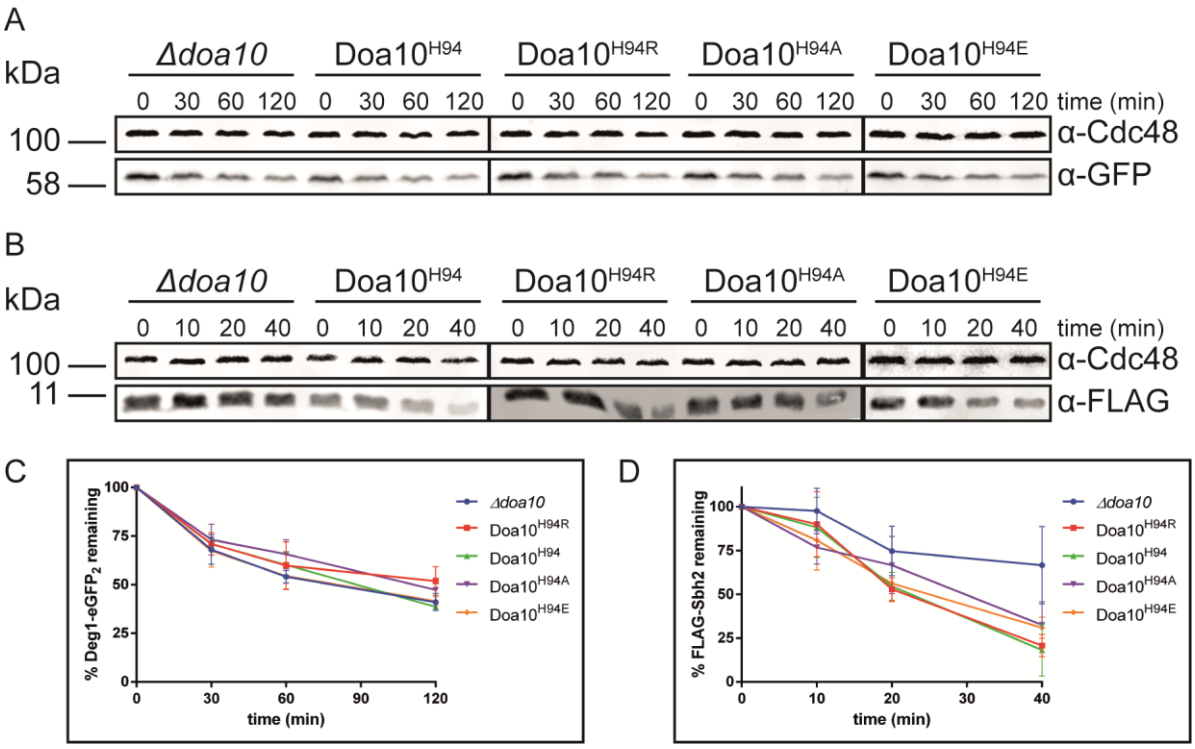

Figure 2-18: Impaired substrate priming slows down degradation at the Doa10 ligase. Representative western blots following the decay of (A) Deg1-eGFP$_2$ and (B) FLAG-Sbh2. Experiments were performed in cells lacking Ubc6 (*Δubc6*). Cdc48 served as loading control. Assays involving FLAG-Sbh2 were performed in cells deleted for Ssh1 (*Δssh1*). (C, D) Signals detected via fluorescently-labeled secondary antibodies were quantified and plotted over time. Error bars represent the standard deviation of mean of at least three independent experiments.

In contrast to the Doa10 ligase, the exchange of the linchpin residue in the Hrd1 RING affected substrate turnover. This most likely accounts for a reduced capability to stimulate the activity of Ubc7. Obviously, the activation of Ubc7 by a RING domain via linchpin allostery requires an arginine at the linchpin position. As revealed in the experiments employing the Cue1^{RGA} mutant, the synthesis of K48-linked poly-Ub chains by Ubc7 seems to proceed fast enough to allow efficient substrate degradation even in the absence of an appropriate residue at the linchpin site. These results imply that the Hrd1 linchpin mutants should be less efficient to allow the

priming of substrates with Ub by Ubc7. Therefore, the question arose whether target priming may be facilitated by another E2 apart from Ubc7 in cells harboring partially limited Hrd1 variants. Ubc6 is a priming enzyme which was stimulated by the Hrd1 RING *in vitro* (compare Fig. 2-4) and was already implicated in the degradation of a Hrd1-dependent model substrate[88]. Accordingly, protein breakdown at the Hrd1 ligase was analyzed in cells lacking Ubc6 (Fig. 2-19).

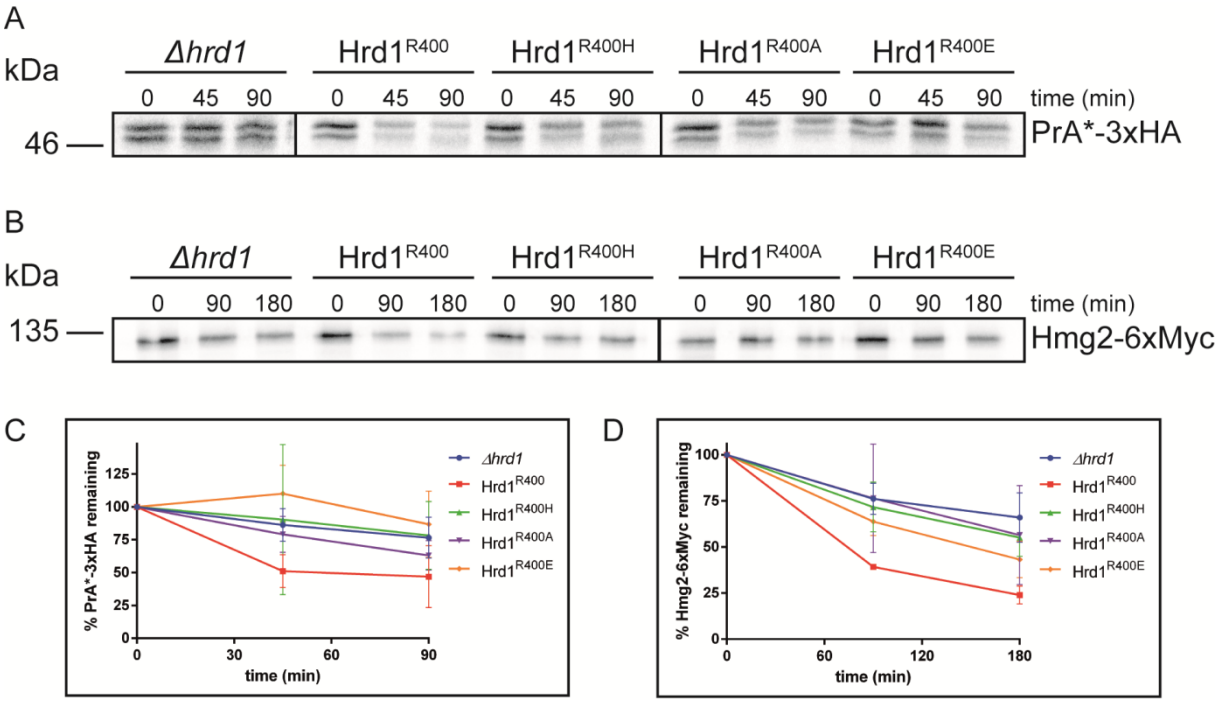

Figure 2-19: Ubc6 facilitates priming at the HRD ligase when Ubc7 is incapable thereof. Representative autoradiography scans following the degradation of (A) PrA*-3xHA and (B) Hmg2-6xMyc. Experiments were performed in cells lacking Ubc6 (*Δubc6*). (C, D) Radioactive signals were quantified and plotted over time. Error bars represent the standard deviation of mean of at least three independent experiments.

In cells lacking Hrd1, the deletion of *UBC6* (Δubc6) did not delay substrate degradation further (blue curves, compare Fig. 2-13). Likewise, the turnover of the Hrd1 client proteins was not affected in wild type cells deleted for *UBC6* alone (red curves). Remarkably, deletion of *UBC6* in cells expressing the Hrd1 RING linchpin mutations substantially impaired the degradation of both model substrates. This implies that Ubc6 can decorate Hrd1 client proteins with Ub. In situations, where Hrd1 fully activates Ubc7 for the transfer of Ub directly onto target proteins, the Ubc6 activity at Hrd1 does not significantly contribute to substrate turnover. However, once Hrd1 fails to stimulate Ubc7 activity, e.g. due to an exchange of the linchpin residue in the Hrd1 RING domain, Ubc6 activity promotes the degradation of at least a fraction of the Hrd1 client proteins.

Taken together, these results show that the attachment of the first Ub moiety to a protein, the so-called priming step, represents the rate-limiting event of the poly-ubiquitination process. Subsequent elongation by the conjugation of additional Ub molecules is a prerequisite for proteasomal breakdown, but does not necessarily limit the rate of degradation. To meet different requirements for the priming and elongation reaction, ERAD ligases employ distinct mechanisms. Doa10 cooperates with specialized E2 enzymes for substrate priming (Ubc6) and for Ub chain elongation (Ubc7). In some instances, Ubc7 may also serve as a priming E2 at this ligase. The Hrd1 ligase utilizes a single E2, Ubc7, for priming and elongation. This ligase can activate Ubc7 via linchpin allostery to facilitate the conjugation of Ub directly to target proteins. Still, Ubc6 can also prime Hrd1 client proteins with Ub, although with significantly reduced efficiency.

2.2.5 Hrd1 employs Ubc6 for non-canonical ubiquitination of client proteins

In the early days of ERAD research, a mutant form of the vacuolar carboxypeptidase yscY (CPY) termed CPY* was established as a Hrd1 target[80]. A single point mutation (G255R) close to the catalytic center prevents the delivery of this protein to the vacuole and routes it to ERAD via Hrd1. More recently, a version of CPY* devoid of all lysine residues (CPY*_noK-HA) was also shown to be efficiently degraded via the Hrd1pathway[89].

In all experiments so far, Ubc7 fails to attach Ub to amino acid residues other than lysine. Therefore, priming of CPY*_noK-HA with Ub should involve the activity of another E2. Ubc6 was shown to ubiquitinate not only lysines, but also hydroxylated amino acids on client proteins[20]. Moreover, this E2 enzyme attaches Ub to Hrd1 target proteins. Therefore, pulse chase assays were performed to investigate any involvement of Ubc6 in the turnover of CPY*_noK-HA (Fig. 2-20).

Degradation of CPY*_noK-HA depended on Hrd1, because it was heavily impaired in *Δhrd1* cells. Strikingly, Ubc6 was also strictly required for CPY*_noK-HA decay even in cells harboring wild type Hrd1 (*Δubc6*). Nonetheless, Doa10 was not involved in CPY*_noK-HA degradation. Cells deleted for *DOA10* (*Δdoa10*) even displayed a slightly accelerated turnover rate compared to the wild type, maybe due to a lack of competition of Hrd1 and Doa10 for Ubc6 binding. Another experiment revealed that

the disposal of lysine-free CPY* is still dependent on Ubc7 (data not shown) suggesting that the degradation signal is built up by a cooperative effort of Ubc6 and Ubc7. Analogous to their activity at the Doa10 ligase, Ubc6 may prime the substrate with Ub before Ubc7 can form a chain on the first Ub moiety.

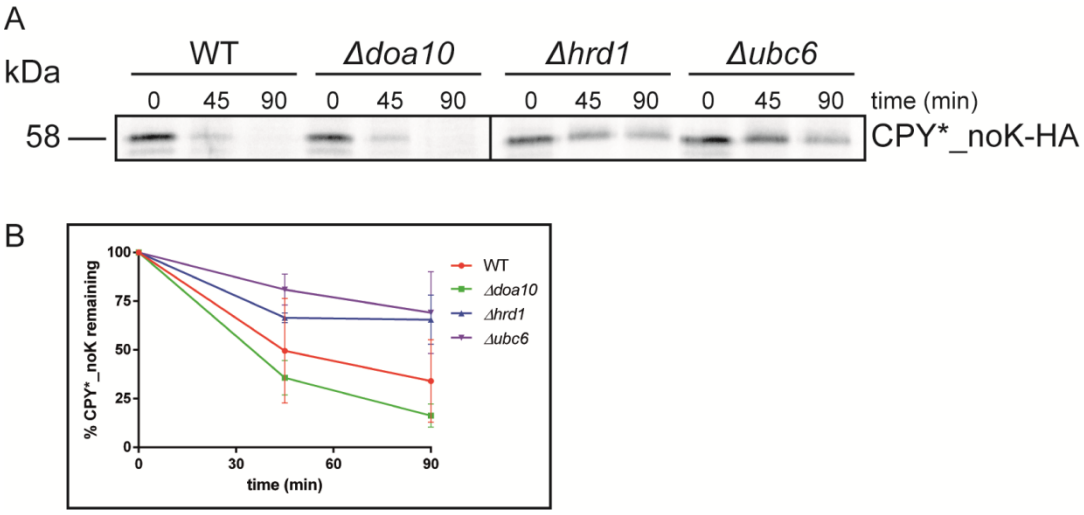

Figure 2-20: Hrd1 employs Ubc6 for ubiquitination of a lysine-free substrate. (A) Representative autoradiography scan following the degradation of CPY*_noK-HA. (B) Radioactive signals were quantified and plotted over time. Error bars represent the standard deviation of mean of at least three independent experiments.

In conclusion, Ubc6 and Ubc7 can initiate the degradation of Hrd1 target proteins by priming them with Ub. Still, most Hrd1 clients are not efficiently ubiquitinated by Ubc6. When the priming activity of Ubc7 is compromised or when substrates lack appropriate acceptor sites, the activity of Ubc6 suffices for the priming of at least a fraction of the Hrd1 substrates. This backup mechanism increases the flexibility of the ERAD system required to remove highly diverse misfolded proteins from cells and thereby prevent their cytotoxic accumulation.

2.3 Molecular analysis of the Asi complex at a glimpse

2.3.1 Establishment of a novel Asi model substrate

Up to this point, two different E3 ligases have been analyzed in molecular detail. Hrd1 harbors a canonical arginine at the linchpin position while Doa10 comprises an atypical histidine at this site. Recently, a third membrane-bound E3 ligase complex, termed the Asi complex, has been described in yeast. This ligase is involved in quality control at the inner nuclear membrane and the nucleus[50,51,56,57]. Two subunits of this complex expose nucleoplasmic domains containing a RING fold at their very C-terminus. Interestingly, the Asi1 RING harbors an arginine while the Asi3 RING holds an aspartate at the linchpin position. This unusual setup raised the question, how each of these different RING domains contributes to the ubiquitination reaction of the E3 ligase complex.

To address this issue, a novel Asi-dependent model substrate was constructed. Amongst others, the Asi complex regulates the activity of transcription factors Stp1 and Stp2[50,51]. A region in Stp1 comprising amino acids 16-50 has been identified as an Asi-dependent degron[55]. To analyze the ability of this degron to direct proteins to the Asi complex, Stp1$^{16-50}$ was fused to a triple HA epitope tag attached to the stable "superfolder green fluorescent protein" (sfGFP-3xHA)[90]. Degradation of plasmid-borne sfGFP-3xHA or the sfGFP construct containing the Stp1 degron (Stp1-sfGFP-3xHA) was monitored in wild type yeast by CHX decay assays (Fig. 2-21).

Noteworthy, the fusion of the Stp1 degron to sfGFP induced rapid removal of the otherwise stable protein from the cell.

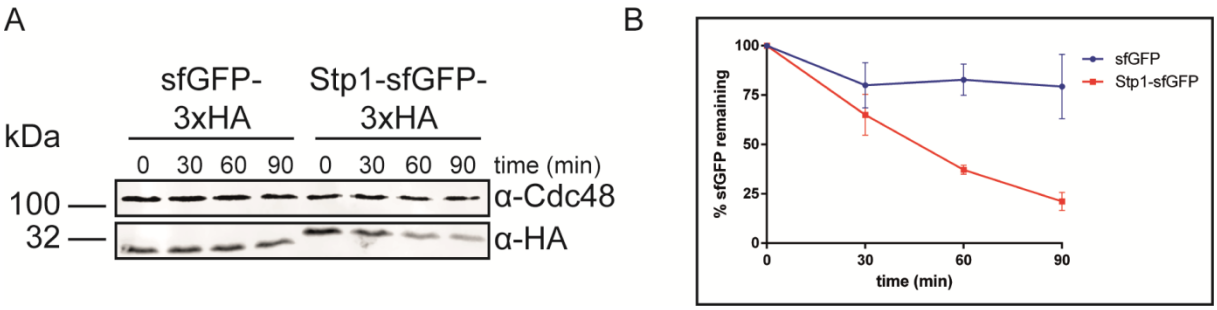

Figure 2-21: sfGFP is rapidly degraded after fusion to the Stp1 degron. (A) Representative western blot following the decay of two versions of sfGFP. Cdc48 served as a loading control. (B) Signals detected via fluorescently-labeled secondary antibodies were quantified and plotted over time. Error bars represent the standard deviation of mean of at least three independent experiments.

2.3.2 Each Asi subunit directly contributes to the function of the complex

To test if the Asi complex is involved in the degradation of Stp1-sfGFP-3xHA, CHX decay assays were performed. In these experiments, the turnover of another Asi target that adopts a different cellular topology was also investigated. The amount of lanosterol 14-α-demethylase (Erg11), a membrane-bound enzyme of the inner nucleus involved in ergosterol biosynthesis[91], has been shown to be subject to Asi-mediated regulation[56]. A construct for the expression of Erg11 harboring a triple HA epitope tag was integrated into the genomic locus of the *ERG11* gene to allow detection via immunoblotting. CHX chase assays in cells lacking single Asi subunits are shown below (Fig. 2-22).

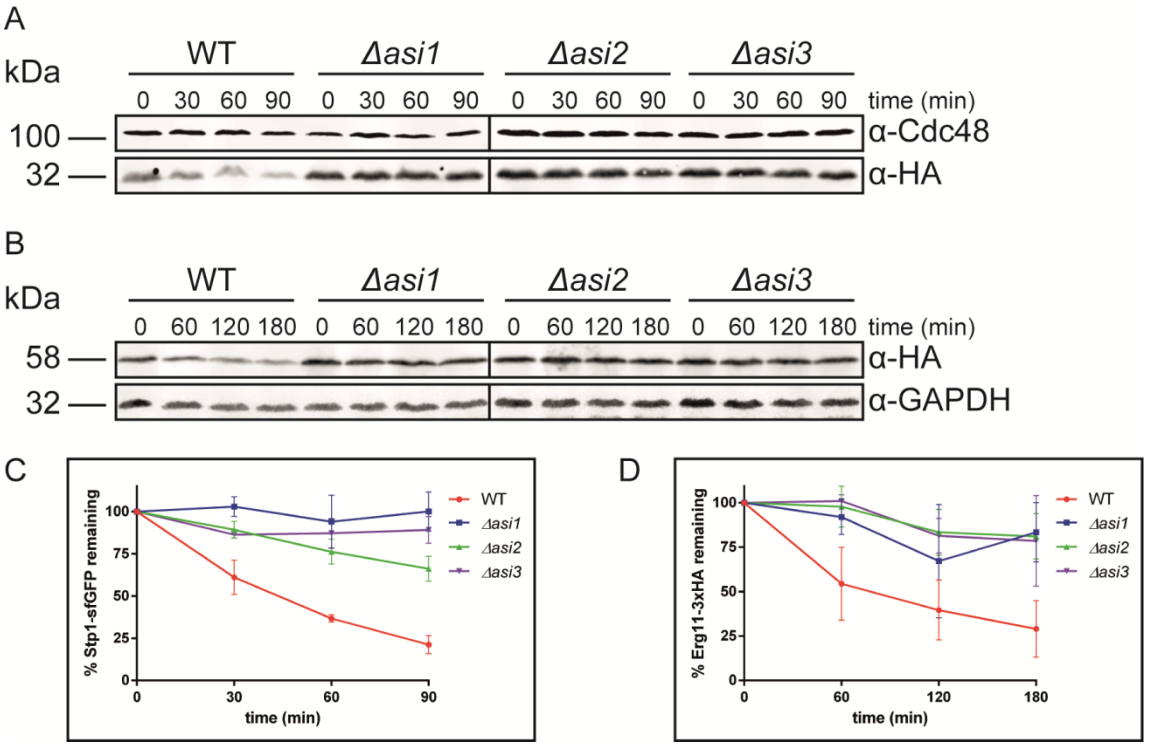

Figure 2-22: All Asi subunits contribute to the function of the complex. Representative western blots following the decay of (A) Stp1$^{16-50}$-sfGFP-3xHA and (B) Erg11-3xHA. Cdc48 and GAPDH served as loading controls, respectively. (C, D) Signals detected via fluorescently-labeled secondary antibodies were quantified and plotted over time. Error bars represent the standard deviation of mean of at least three independent experiments.

Stp1-sfGFP-3xHA and Erg11-3xHA were efficiently degraded in wild type yeast whereas cells lacking any component of the Asi complex displayed defects in their processing. This shows that both proteins constitute substrates of the Asi complex and that each Asi subunit contributes to their degradation.

2.3.3 The subunits of the Asi complex are tightly associated

Removal of individual subunits may cause the dissociation of the Asi complex and thereby indirectly affect substrate processing. Thus, binding of the Asi proteins to the complex was analyzed. To this end, plasmids that encode epitope-tagged versions of each component of the Asi complex were generated. Because the Asi proteins are probably synthesized with an amino-terminal signal sequence that targets them to the inner nuclear membrane, constructs for 3xHA, 3xMyc, or 3xFLAG epitope tags were inserted 30 codons downstream of the start codons of the *ASI* genes. These plasmids were then transformed into yeast cells deleted for the endogenous copies of all *ASI* genes. Non-denaturing immunoprecipitation (IP) using antibody-conjugated magnetic beads then allowed the isolation of individual subunits of the Asi complex and the associated partner proteins (Fig. 2-23).

IPs were performed for the purification of 3xHA-Asi1 (Fig. 2-23 A), 3xMyc-Asi2 (Fig. 2-23 B) or 3xFLAG-Asi3 (Fig. 2-23 C) and the retrieved material was analyzed by immunoblotting. The relative amount of the epitope tagged Asi proteins slightly varied in the samples, probably due to aberrations of the plasmid copy numbers in these cells. None of the Asi proteins unspecifically bound to the beads (first lane of Fig. 2-23 IP blots). Moreover, each Asi protein was co-purified with the other Asi subunits (last lane of each IP blot). In absence of the other subunits all Asi proteins were efficiently expressed and enriched in the pull-down experiments (lane 2 of Fig. 2-23 IP blots). This suggests that the Asi proteins constitute stable proteins even when the formation of the ligase is impaired and that unassembled complex partners are not necessarily removed by a cellular protein quality control pathway as previously described[92,93]. Remarkably, all Asi proteins were co-purified with any other subunit in absence of the third component (lanes 3 and 4 of each IP blot). This implies that each subunit of the Asi complex individually forms tight interactions with the other two elements.

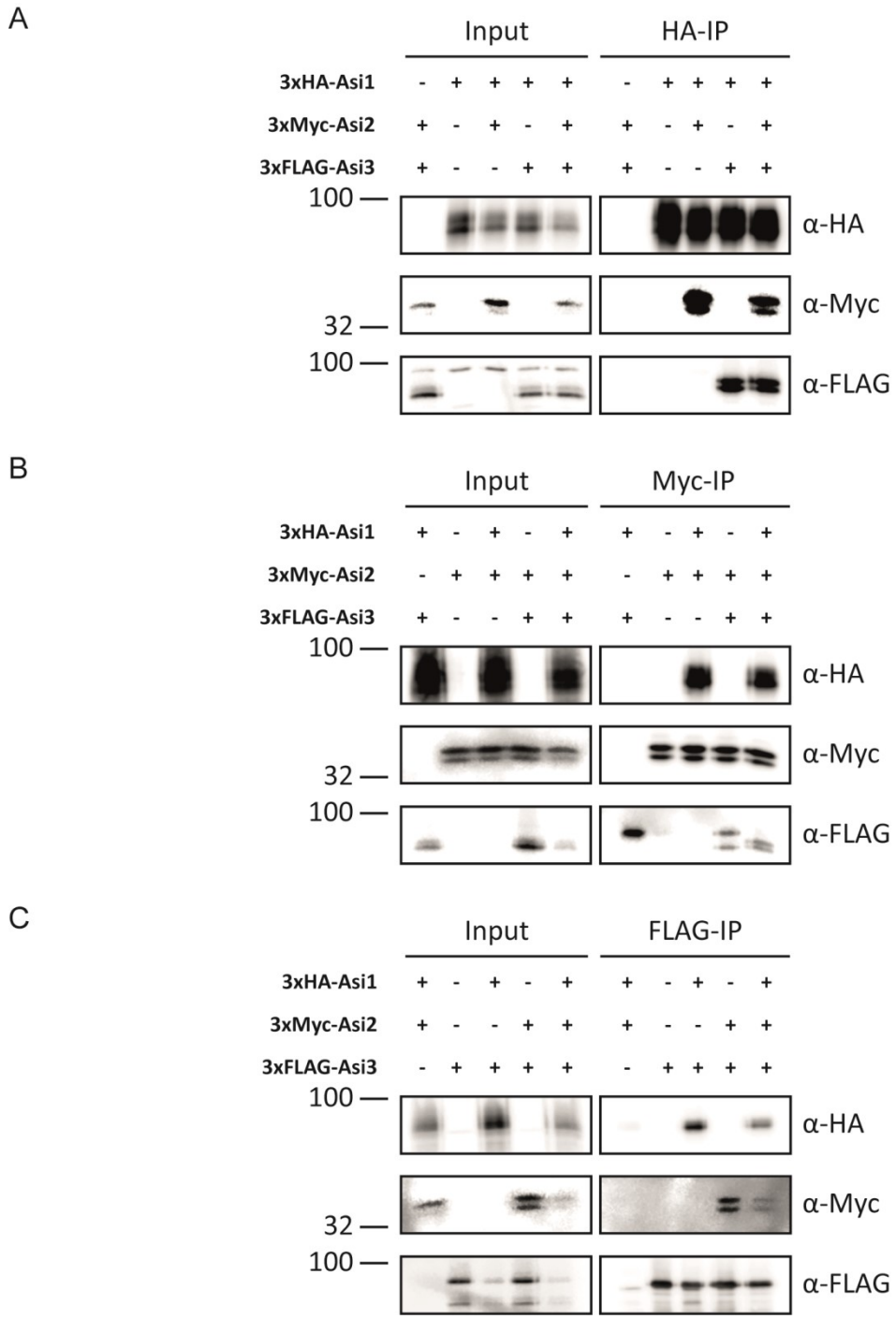

Figure 2-23: Tight binding of the subunits of the Asi complex. Representative blots of IP experiments enriched for (A) 3xHA-Asi1, (B) 3xMyc-Asi2 or (C) 3xFLAG-Asi3. Experiments were performed in cells deleted for all Asi complex proteins (*Δasi1/Δasi2/Δasi3*).

Taken together, these data show that the defects in substrate breakdown observed in the deletion mutants (compare Fig. 2-22) are not caused by an overall inability to form a functional complex, but rather indicate the requirement of still elusive functions administered by every single subunit of the complex.

2.3.4 Binding of the Asi subunits involves their nucleoplasmic domains

In the near future, *in vitro* ubiquitination assays need to be established to analyze the Asi complex in molecular detail. A prerequisite for a functional assay is the interaction of the soluble nucleoplasmic domains. If binding is primarily mediated by the transmembrane regions, the addition of dimerization domains needs to be considered during expression construct design[94]. Accordingly, the interaction interfaces of the complex proteins were mapped. To this end, truncation constructs of every subunit were created and analyzed for their interaction with the remaining complex subunits. First, IP experiments using various constructs of Asi1 consisting of either transmembrane or nucleoplasmic sections were conducted (Fig. 2-24).

Asi1 truncation variants (Fig. 2-24 A) were expressed from plasmids along with epitope tagged full-length Asi2 and Asi3 in cells deleted for all *ASI* genes. The N-terminal half of Asi1 encompasses several membrane-spanning regions while the C-terminal part comprises a large soluble domain exposed to the nucleoplasm. While constructs spanning different parts of the transmembrane region should still localize to the inner nuclear membrane due to their inherent N-terminal signal sequence, constructs harboring fragments of the nucleoplasmic domain were fused to the nuclear localization sequence of the simian virus 40 large T antigen (SV40 NLS)[95] to direct them to the compartment of interest. Unfortunately, nucleoplasmic constructs could neither be detected in the input nor after immunoprecipitation showing that expression of these was not successful in yeast (Fig. 2-24 B). Nevertheless, constructs covering the Asi1 transmembrane region were stably expressed and efficiently enriched during the IP procedure. While full-length Asi1 efficiently co-immunoprecipitated Asi2 and Asi3, the fragments comprising the N-terminal 99 or 199 amino acids of Asi1 displayed no detectable interaction with the remaining complex partners. Solely, the construct spanning the first 299 amino acids of the protein maintained a weak affinity for Asi2 suggesting that part of the interaction interface between Asi1 and Asi2 is located in the C-terminal fraction of the Asi1 transmembrane region. However, the amount of precipitated Asi2 was diminished in comparison to full-length Asi1 and Asi3 was not enriched at all using any of the transmembrane fragments. This indicates that binding of the other complex subunits to Asi1 is mainly facilitated by its nucleoplasmic portion.

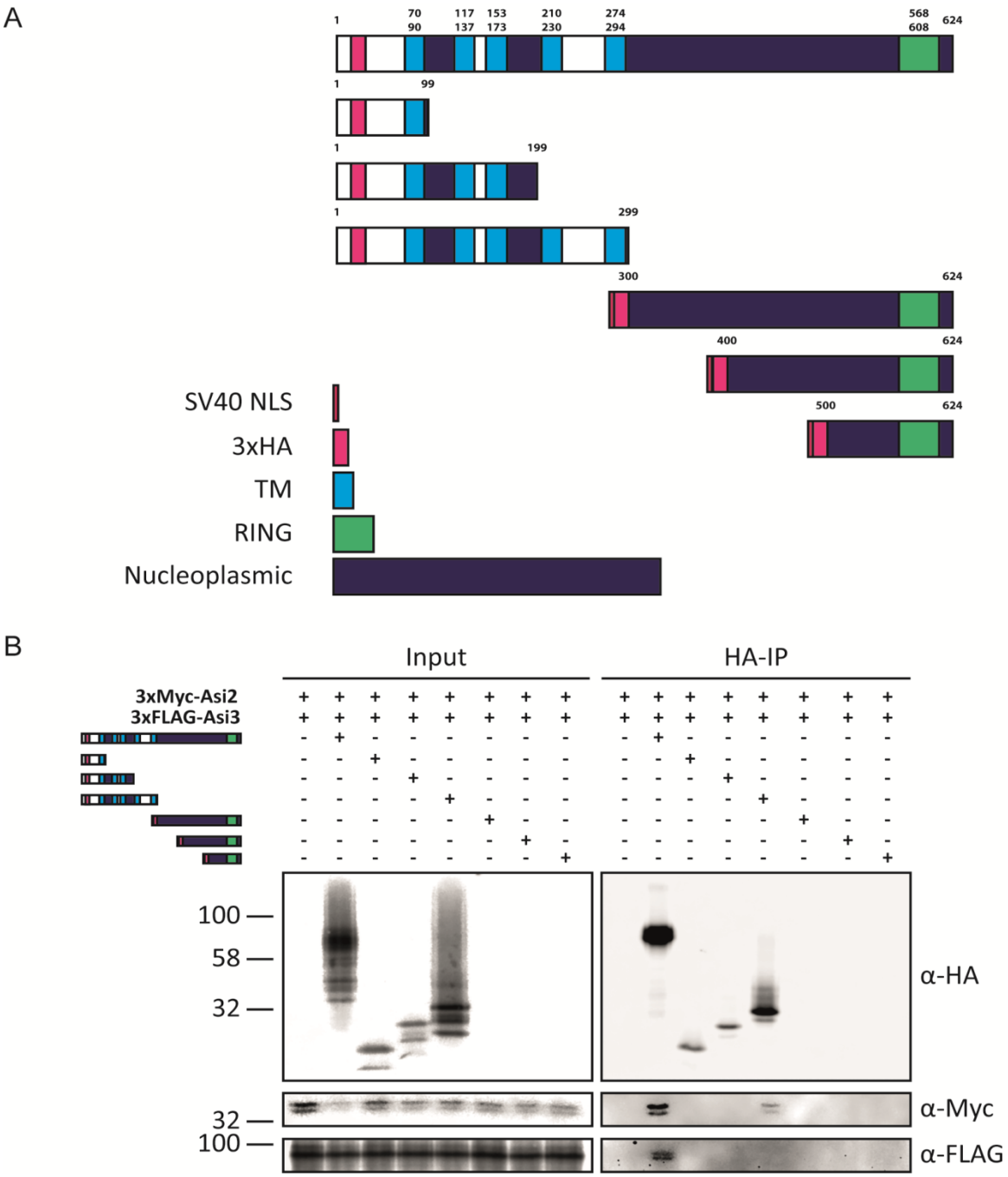

Figure 2-24: Asi1 shows only weak interactions with other complex partners through its transmembrane region. (A) Schematic presentations of the domain structure of full-length Asi1 and the created truncation constructs. Domain assignment was conducted using the UniProt[96] Asi1 entry (#P54074) (B) Shown are representative blots of IP experiments enriched for 3xHA-tagged Asi1 constructs of varying length. Experiments were performed in cells deleted for all Asi complex proteins (*Δasi1/Δasi2/Δasi3*).

Next, 3xMyc-tagged Asi2 truncation variants were created and analyzed for their ability to pull down the remaining complex partners. Experiments were performed as before for Asi1 in cells deleted for all Asi subunits and rescued with plasmids expressing different variants of Asi2 in addition to full-length Asi1 and Asi3 proteins (Fig. 2-25).

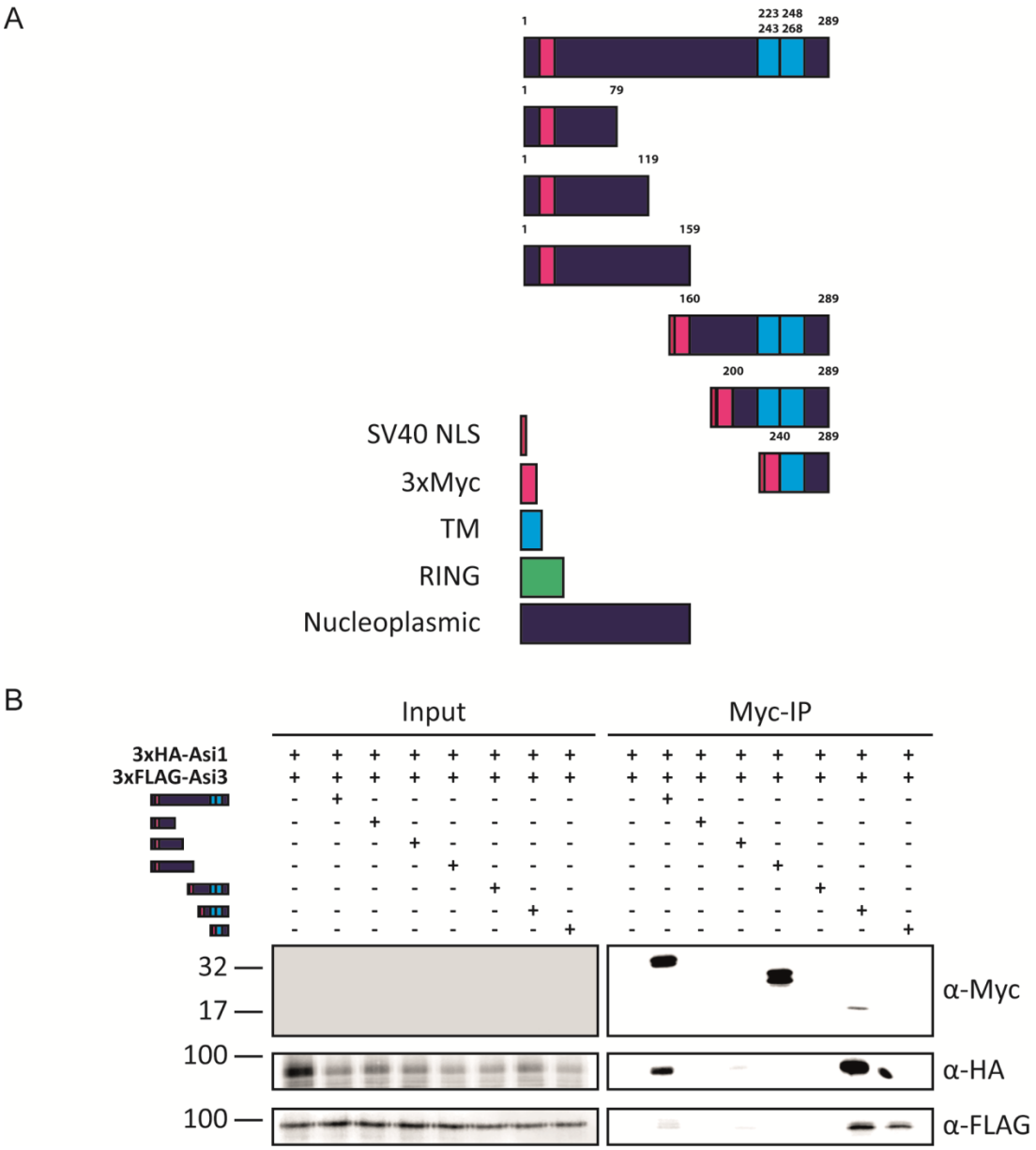

Figure 2-25: Interactions between Asi2 and other subunits are governed by its C-terminal region. (A) Schematic presentations of the domain structure of full-length Asi2 and the created truncation constructs. Domain assignment was conducted using the UniProt[96] Asi2 entry (#P53895) (B) Shown are representative blots of IP experiments enriched for 3xMyc-tagged Asi2 constructs of varying length. Experiments were performed in cells deleted for all Asi complex proteins (*Δasi1/Δasi2/Δasi3*).

Although the expression of the transformed Asi2 constructs could not be detected on input blots, luckily the full-length protein and some truncated variants were enriched after IPs directed against the 3xMyc epitope. Asi1 and Asi3 could only be co-immunoprecipitated using full-length Asi2 and constructs harboring its C-terminal part made up of the last transmembrane helix and a short nucleoplasmic tail. Interestingly, precipitated amounts of Asi1 and Asi3 using those fragments were increased compared to full-length Asi2, suggestive of a tight interaction in this region.

Thirdly, IP experiments using 3xFLAG epitope-marked Asi3 truncation variants were performed just as before for Asi1 and Asi2 to map specific interactions to corresponding regions of the Asi3 subunit (Fig. 2-26).

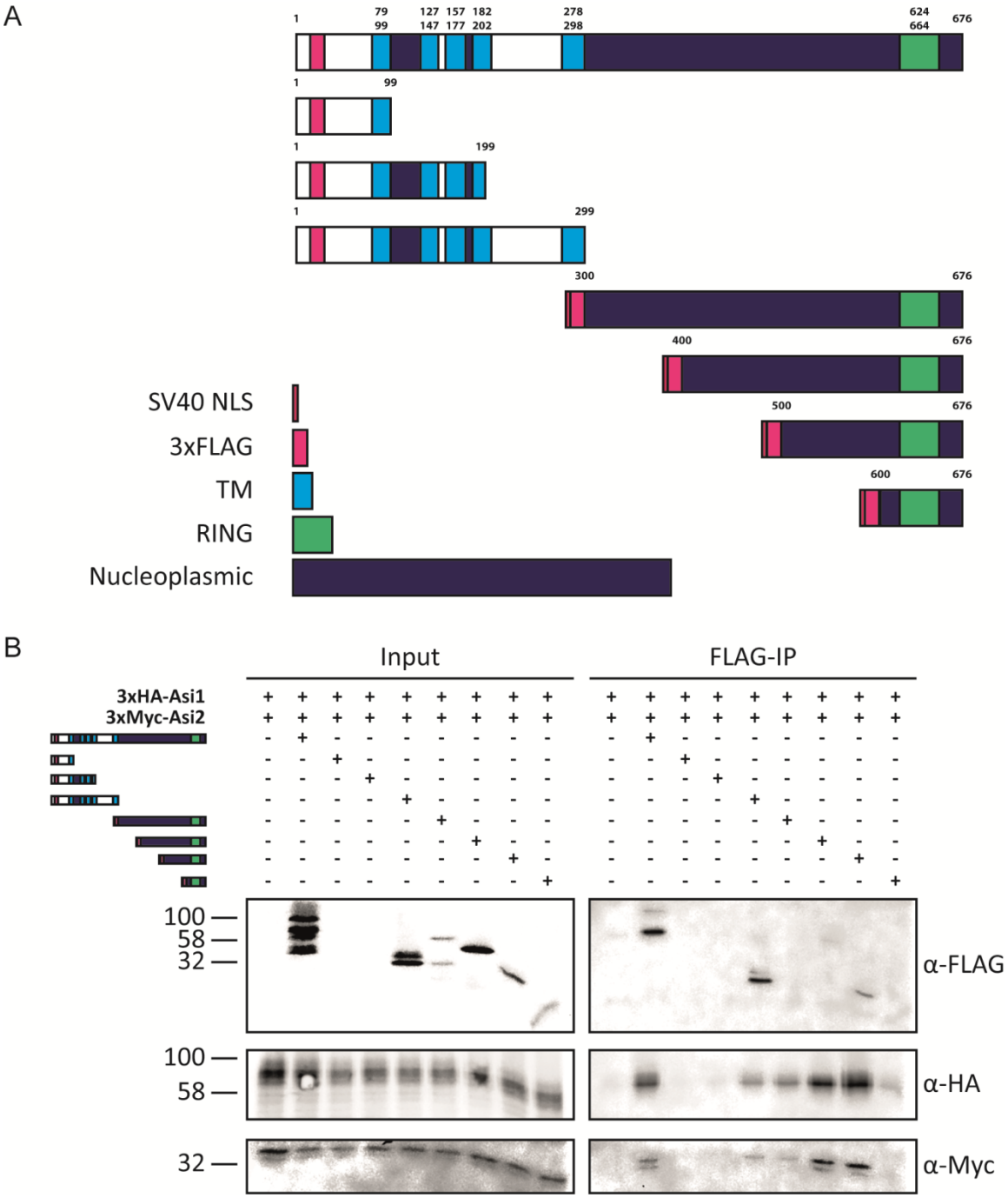

Figure 2-26: Asi3 mainly interacts with other complex partners through its nucleoplasmic portion. (A) Schematic presentations of the domain structure of full-length Asi3 and the created truncation constructs. Domain assignment was conducted using the UniProt[96] Asi3 entry (#P53983) (B) Shown are representative blots of IP experiments enriched for 3xFLAG-tagged Asi3 constructs of varying length. Experiments were performed in cells deleted for all Asi complex proteins (*Δasi1/Δasi2/Δasi3*).

In contrast to Asi1, expression of the transmembrane constructs failed while the soluble fragments were produced as seen on the input blot (Fig. 2-26 B). Pull-downs of Asi1 and Asi2 were readily visualized, even though immunoprecipitated Asi3 constructs were only partially detected. Observed interactions between the utilized constructs and the remaining Asi complex partners were clearly mapped to the nucleoplasmic region of Asi3. A fragment spanning the C-terminal 176 amino acids co-immunoprecipitated the whole complex, while further truncation resulted in reduced interaction, suggesting that the minimal interaction motif comprises the last 76 up to 176 amino acids.

All in all, the observed intermolecular interactions building up the Asi complex were mainly mapped to the nucleoplasmic regions of the Asi subunits. This is strongly supported by the incapability of Asi1 transmembrane constructs to bind partner proteins and by the strong enrichment of Asi complex subunits when soluble Asi3 fragments were used. Since it is rather unlikely to observe tight interactions between soluble and transmembrane domains, the detected interactions between the C-terminal part of Asi2 and its interaction partners might be mediated by the short nucleoplasmic tail of Asi2 rather than the two transmembrane helices. This interaction mapping experiment provides first insights into Asi complex architecture and may be used in future experiments to design constructs suitable for *in vitro* ubiquitination studies involving the Asi complex.

2.3.5 The Asi complex employs Ubc4 and Ubc7 for ubiquitination

Another prerequisite for the establishment of *in vitro* ubiquitination assays is the knowledge on the E2 enzymes that cooperate with an E3 ligase. Previous studies indicated a physical and functional interaction of the Asi complex with the E2s Ubc4, Ubc6 and Ubc7[56,57]. In this thesis, this was re-evaluated by studying the degradation of the model substrates Erg11-3xHA and Stp1-sfGFP-3xHA. CHX chase assays in cells lacking Ubc4 (*Δubc4*), Ubc6 (*Δubc6*), Ubc7 (*Δubc7*) or appointed combinations thereof were performed (Fig. 2-27).

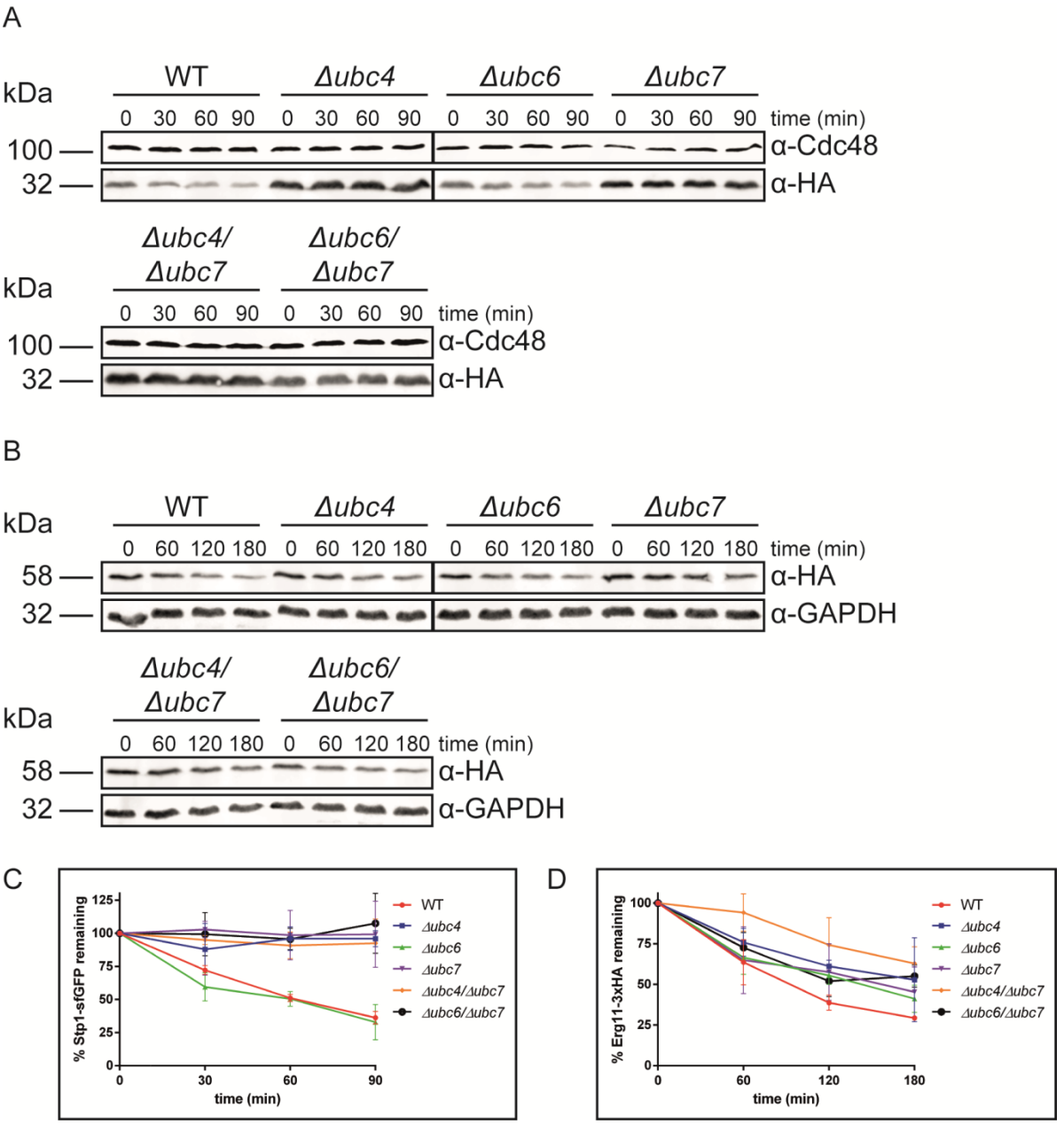

Figure 2-27: The Asi complex mainly cooperates with Ubc4 and Ubc7. Representative western blots following the decay of (A) Stp1$^{16-50}$-sfGFP-3xHA and (B) Erg11-3xHA. Cdc48 and GAPDH served as loading controls, respectively. (C, D) Signals detected via fluorescently-labeled secondary antibodies were quantified and plotted over time. Error bars represent the standard deviation of mean of at least three independent experiments.

In these experiments, Ubc4 and Ubc7 were strictly required for the turnover of Stp1-sfGFP-3xHA. The combined deletion of both genes did not cause additive effects suggesting that Ubc4 and Ubc7 operate in the same pathway for Stp1-sfGFP-3xHA ubiquitination. Noteworthy, Ubc6 did not contribute to the removal of the soluble Asi target. Degradation of Erg11-3xHA was only moderately affected by single E2 deletions. Simultaneous knockouts of Ubc6 and Ubc7 did not impair the target turnover beyond the level observed in the single mutants. The yeast strain deleted for *UBC4* and *UBC7* displayed the most pronounced defect in client removal. However,

in contrast to Stp1-sfGFP-3xHA, an additive effect compared to single knockouts was detected for the turnover of the membrane-bound Erg11-3xHA protein. This indicates that Ubc4 and Ubc7 act in separate pathways to degrade Erg11. A similar observation was made by Foresti *et al.*[56], even though they found Erg11 to be completely stable in cells lacking Ubc4 and Ubc7.

In summary, the presented data show a functional requirement of Ubc4 and Ubc7 for the removal of Asi complex client proteins, while Ubc6 seems to be mostly dispensable for this process.

2.3.6 Degradation of Asi client proteins involves both RING domains and a correctly situated linchpin residue

The contribution of the Asi1 and Asi3 RING domains to ligase function was analyzed by studying substrate degradation in cells expressing mutated versions of these proteins. Asi1 variants were expressed from plasmids in cells deleted for the *ASI1* gene (*Δasi1*) and the turnover of Stp1-sfGFP-3xHA or Erg11-3xHA was determined in CHX decay assays (Fig. 2-28). Plasmid-encoded Asi1^{WT} at least partially rescued degradation of Stp1-sfGFP-3xHA and Erg11-3xHA in *ASI1*-deleted cells (compare Fig. 2-22).

Following this, two mutated versions of Asi1 were assayed for their ability to complement the *ASI1* deletion. Asi1$^{CC583/585SS}$ harbors serine residues at the position of two cysteines, which contribute to the coordination of Zinc within the RING domain, and hence this protein should be inactive for E3 ligase function. Concordantly, expression of this variant did not promote the degradation of Stp1-sfGFP-3xHA and Erg11-3xHA in the *Δasi1* strain background. In Asi1^{R608D}, the arginine in the linchpin position of the Asi1 RING domain was substituted with the aspartate which is found in the corresponding site in Asi3. This single amino acid exchange also fully impaired the activity of the Asi complex demonstrating a function of the Asi1 linchpin residue in substrate processing.

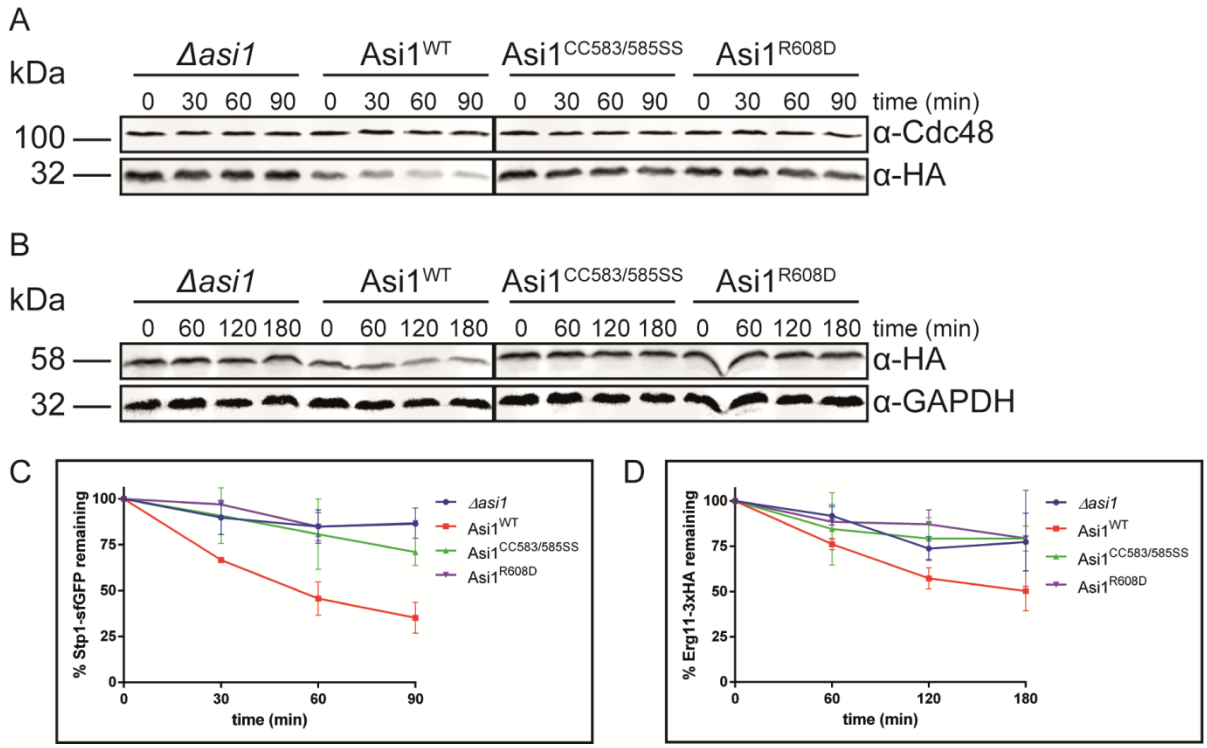

Figure 2-28: Substrate processing by the complex involves an activating residue at the linchpin position of the Asi1 RING domain. Representative western blots following the decay of (A) Stp1$^{16-50}$-sfGFP-3xHA and (B) Erg11-3xHA. Cdc48 and GAPDH served as loading controls, respectively. Experiments were performed in cells deleted for Asi1 (*Δasi1*). (C, D) Signals detected via fluorescently-labeled secondary antibodies were quantified and plotted over time. Error bars represent the standard deviation of mean of at least three independent experiments.

Analogous RING domain variants of the Asi3 protein were expressed in cells lacking endogenous Asi3 and the degradation of client proteins was monitored in CHX chase assays (Fig. 2-29). While plasmid-encoded wild type Asi3 efficiently restored Erg11-3xHA degradation in *Δasi3* cell, the amount of Stp1-sfGFP-3xHA apparently did not decrease over time in these cells. However, the steady state level of Stp1-sfGFP-3xHA was substantially reduced upon expression of Asi3 compared to cells lacking this complex subunit (see inset in Fig. 2-29 C for quantification) indicating that this Asi3 construct was at least partly functional. Turnover of both substrates was impaired in cells expressing an Asi3 variant harboring replacements of cysteine residues in the RING domain (Asi3$^{CC624/627SS}$). Interestingly, the substitution of the aspartate residue at the Asi3 linchpin position with an arginine (Asi3^{D664R}) fully complemented the degradation defect of the *ASI3*-deleted yeast strain. This indicates that substrate processing by the Asi complex does not depend on the nature of the amino acid in the Asi3 RING linchpin position. Therefore it can be concluded that this RING domain does not stimulate the activity of an E2 enzyme via linchpin allostery.

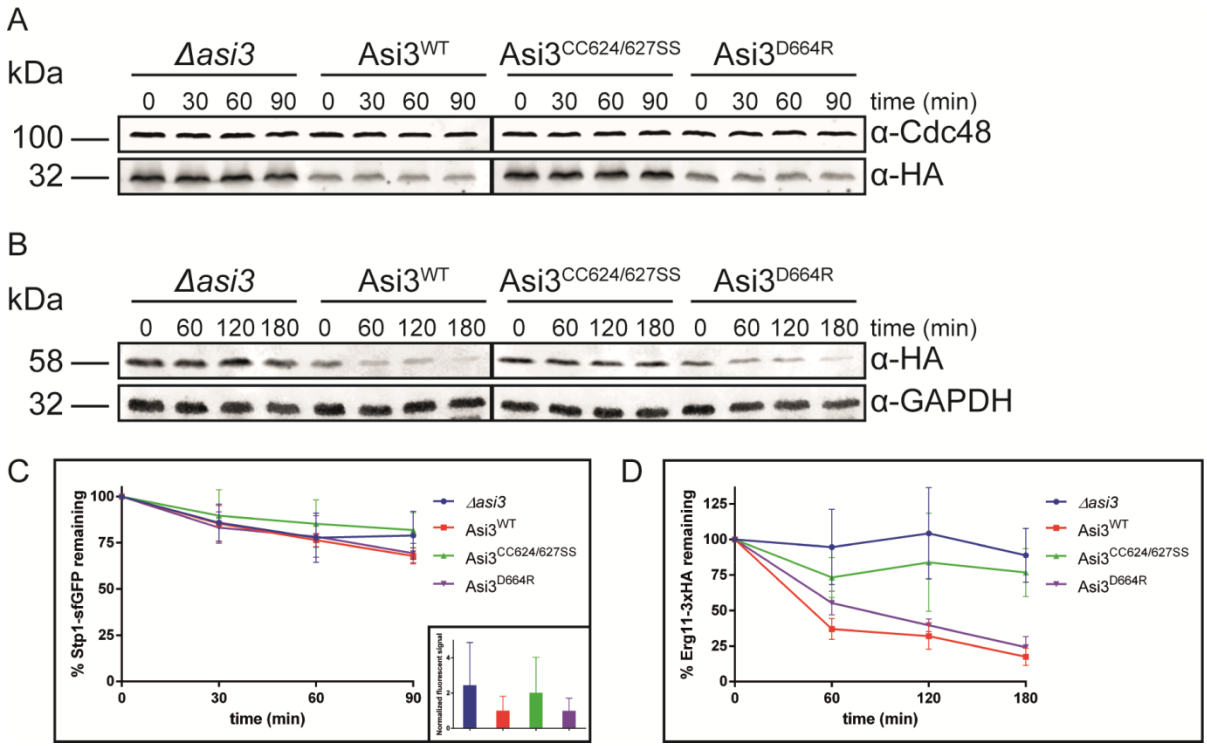

Figure 2-29: The function of the Asi complex does not depend on an activating amino acid in the linchpin position of the Asi3 RING domain. Representative western blots following the decay of (A) Stp1$^{16-50}$-sfGFP-3xHA and (B) Erg11-3xHA. Cdc48 and GAPDH served as loading controls, respectively. Experiments were performed in cells deleted for Asi3 (*Δasi3*). (C, D) Signals detected via fluorescently-labeled secondary antibodies were quantified and plotted over time. Error bars represent the standard deviation of mean of at least three independent experiments.

Next, it was tested if the introduction of a potent linchpin in the Asi3 RING domain could rescue the defect observed for an Asi1 variant incapable of providing linchpin allostery (Fig. 2-30). The expression of wild type Asi1 and Asi3 constructs rescued the deletion of both genes as determined by comparing steady state levels and degradation kinetics of Stp1-sfGFP-3xHA and Erg11-3xHA. Notably, an Asi1 variant harboring an aspartate in the linchpin position in combination with a version of Asi3 containing an arginine at the corresponding site rendered the complex inactive towards substrate degradation. Thus, the allosteric activation of an E2 enzyme by Asi1 probably relies on additional properties of the RING domain aside from the appropriate amino acid in the linchpin position.

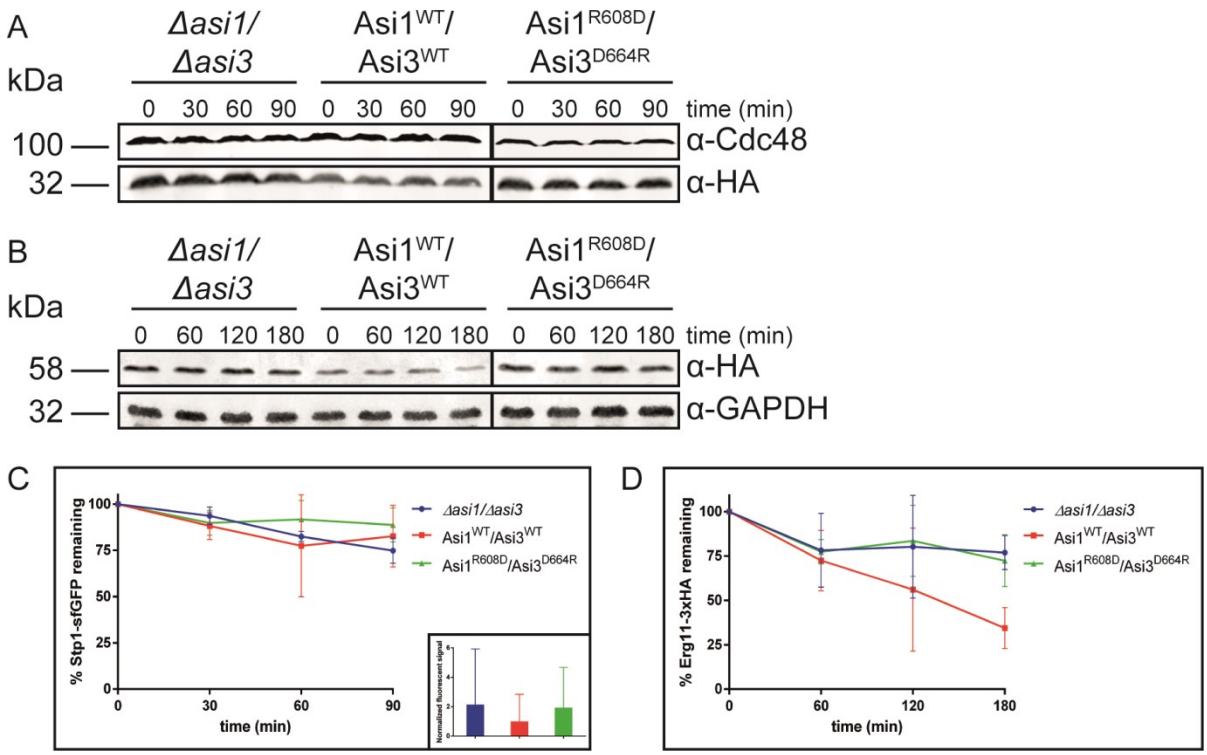

Figure 2-30: Linchpin allostery needs to be conferred by the Asi1 RING domain. Representative western blots following the decay of (A) Stp1$^{16-50}$-sfGFP-3xHA and (B) Erg11-3xHA. Cdc48 and GAPDH served as loading controls, respectively. Experiments were performed in cells deleted for Asi1 and Asi3 (*Δasi1/Δasi3*). (C, D) Signals detected via fluorescently-labeled secondary antibodies were quantified and plotted over time. Error bars represent the standard deviation of mean of at least three independent experiments.

In summary, it has been shown that Asi complex client removal strictly requires two functionally folded RINGs. Furthermore, linchpin allostery is a prerequisite for efficient target turnover. Interestingly, the location of the linchpin is of utter importance since it was observed that only a linchpin-harboring Asi1 RING induces substrate degradation while the Asi3 RING is not able to provide linchpin allostery. A possible model accommodating the presented findings could be one where in a fully functional Asi complex Asi3 recruits cooperating E2 enzymes via its RING domain which are then passed over to the Asi1 RING domain for stimulation of their inherent activity.

3. Discussion

In all eukaryotic cells a quality control process termed “endoplasmic reticulum-associated protein degradation” (ERAD) removes misfolded polypeptides from the secretory pathway and thereby ensures maintenance of protein homeostasis. Central to ERAD are the Hrd1 and Doa10 Ub ligases. Although Hrd1 and Doa10 target different sets of clients, they both employ the Ub conjugating enzymes Ubc6 and Ubc7. Strikingly though, Doa10 and Hrd1 display fundamental differences in how they cooperate with these E2 enzymes[33,48,88,97]. At the Doa10 ligase, ubiquitination of most substrates requires the initial attachment of single Ub moieties by Ubc6 which are then elongated to lysine 48-linked poly-Ub chains by Ubc7[20]. Contrarily, Ubc7 alone suffices for the efficient processing of the majority of Hrd1 client proteins.

Recently, another membrane-embedded Ub ligase, termed the Asi complex, was shown to be involved in maintaining protein homeostasis at the inner nuclear membrane and in the nucleus[50,51]. Aside from Ubc7, this ligase also seems to cooperate with Ubc4 and Ubc6[56,57]. Remarkably, the Asi complex harbors two closely related, yet different, RING-finger proteins but their contribution to substrate processing is unclear.

The aim of this study was to investigate how the ERAD RING-finger ligases Hrd1 and Doa10 stimulate the activity of their cognate E2 enzymes Ubc6 and Ubc7. Of particular interest were the impact of linchpin allostery and other interactions of the RING-finger domain with Ub on this process. Via these contacts the RING drives an E2~Ub conjugate into a closed conformation thereby facilitating the transfer of Ub onto a client. The RING-finger domains of Hrd1 and Doa10 harbor different amino acid residues at their linchpin positions and this work shows that both enzymes appear to stimulate their cognate E2 enzymes in a slightly diverse manner. Consequently, the Doa10 and Hrd1 ligases follow different approaches to mediate efficient poly-ubiquitination of client proteins. Doa10 employs distinct E2 enzymes for the priming and elongation steps during poly-Ub formation while Hrd1 is capable of stimulating Ubc7 activity via linchpin allostery for both reactions. Moreover, this work revealed that both RING-finger proteins in the Asi complex are required for substrate processing and that each of them also appears to activate E2 enzymes in different ways.

In summary, this thesis demonstrates that individual RING-finger ligases stimulate their cognate E2 enzymes via different mechanisms. This most likely accounts for divergent strategies to meet the distinct requirements of individual steps during the poly-ubiquitination reaction or of particular biological processes.

3.1 Differential stimulation of Ubc6 and Ubc7 by the Hrd1 and Doa10 RING-finger domains

3.1.1 Different stimulation of Ubc6 and Ubc7 activity by linchpin allostery

In absence of a RING-finger domain, Ubc7 was rather inactive for the transfer Ub to targets in the *in vitro* discharge assays. The addition of such a stimulating cofactor significantly increased the activity of the E2 enzyme. However, this stimulatory effect strictly relied on an appropriate amino acid in the linchpin position of the RING domains. While an arginine residue at this site in the Hrd1 RING-finger was absolutely mandatory for full activation, the Doa10 RING domain proved to be more flexible. Here, an arginine or histidine at the linchpin position displayed similar stimulatory effects on Ubc7. This suggests that the activation of an E2 enzyme by the Hrd1 RING mainly occurs via linchpin allostery while an additional mechanism supports the stimulation of E2 enzymes by the Doa10 RING-finger.

The deployment of a non-canonical histidine residue at the linchpin position of the Doa10 RING domain may be related to its tight functional interplay with Ubc6. This E2 enzyme was already quite reactive in reactions lacking a RING-finger domain and the stimulation of its activity by a RING did not involve the linchpin residue.

Interestingly, the human Doa10 homologue MARCH6 harbors a lysine residue at its linchpin site. This suggests that linchpin allostery is involved in the activation of its cognate E2 enzyme UBE2J2, a homologue of Ubc6[98]. Although Ubc6 and UBE2J2 share similar catalytic properties[20], we lack detailed knowledge on how the human E2 enzyme is stimulated by its Ub ligase. The activation of UBE2J2 might rely on linchpin allostery, which explains why the MARCH6 RING domain harbors a canonical lysine residue at this site. Still, further studies are required to analyze the functional interplay of UBE2J2 and MARCH6 in more detail.

Several other yeast E3 RING-finger ligases expose non-canonical amino acids at their linchpin sites. These enzymes are often associated with processes that do not involve the formation of a Ub chain. Hence, the inability of certain RING-finger Ub ligases to stimulate the activity of their E2 enzymes via linchpin allostery may prevent the formation of Ub chains and facilitate the generation of mono-Ub signals on their client proteins. Mono-ubiquitination of histone H2B involves the Rad6 ubiquitin conjugating enzyme and the Bre1 RING-finger ligase. This Ub signal specifically initiates the methylation of histone H3 which in turn is associated with active chromatin[99,100]. When associated with the E3 enzyme Rad18, Rad6 facilitates the mono-ubiquitination of PCNA[101]. Interestingly, Bre1 and Rad18 harbor non-canonical asparagine and leucine residues at their corresponding linchpin positions. Importantly though, Rad6 is proficient to catalyze the formation of poly-Ub when associated with other E3 enzymes[102].

Recycling of the cargo receptor Pex5 after peroxisomal import is triggered by mono-ubiquitination[103]. This is facilitated by the E2 enzyme Pex4 in concert with the RING-finger ligase Pex12. Pex12 harbors an alanine at its linchpin position, which may again represent an adaptation to avoid the poly-ubiquitination of the Pex5 protein.

In another context, the stimulation of E2 activity via linchpin allostery may also be counterproductive for the function of a ubiquitinating enzyme. Structural work revealed that RBR-type Ub ligases actively force their cognate E2 enzymes into an open state to favor the transfer of Ub onto the cysteine of the catalytic active RING2 domain and prevent direct ubiquitination of substrates[104]. In line with this, the RING-finger domains in RBR enzymes do not contain appropriate amino acids at their linchpin positions that are capable of facilitating stimulation of E2 enzymes by linchpin allostery.

The Doa10 RING-finger ligase does not contain a canonical linchpin residue for the activation of E2 enzymes. This ligase employs the specialized E2 enzyme Ubc6 in the priming step. This E2 does not require activation via linchpin allostery for its function. However, the activity of Ubc6 apparently must be regulated because a Doa10 RING-finger variant harboring a stimulating canonical arginine at its linchpin site affects the processing of client proteins.

3.1.2 RING/Ub contacts contribute to E2 stimulation

The stimulation of the catalytic activity of Ubc6, independent of linchpin allostery, indicated a second, so far unknown mechanism for the activation of this enzyme by a RING-finger protein. This work unraveled that binding of the RING to the Ub moiety in the Ubc6~Ub conjugate contributes to stimulate the transfer of Ub. Those contacts seemed to stabilize a closed conformation of the E2 enzyme and to enhance its inherent activity. The contact sites map to a non-conserved loop region in the Doa10 RING-finger. This suggests that Doa10 stimulates the activity via a novel and so far uncharacterized mechanism (Fig. 3-1).

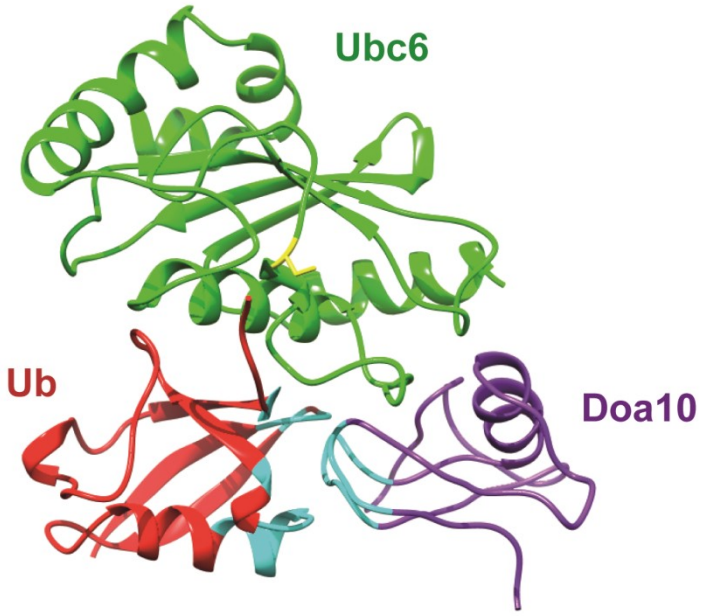

Figure 3-1: A non-conserved, yet dedicated loop in Doa10 mediates interaction with Ub. Shown is a rigid body model of Doa10 RING/Ubc6~Ub complex primed for catalysis. The model is based on PDB: 4AP4. Putative contacts between Doa10 and Ub are colored in cyan. The figure was adopted from Dr. Tobias Ritterhoff.

Contacts of the RING-finger domain with Ub were particularly prominent in the NMR samples containing Doa10 and the Ubc6~Ub conjugate, but also in the other experimental setups such interactions were readily observed. Previous work reports on other contacts of RING-finger domains with Ub in E2~Ub conjugates, indicating that such interactions are generally involved in the stimulation of ubiquitin conjugating enzymes[60,71,105]. Still, some RING-finger domains do not expose apparent Ub-interacting elements[58].

Additional work will reveal the detailed mechanisms of how the contacts of a RING-finger domain to Ub in the E2~Ub conjugates accelerates the ubiquitination reaction. This requires the thorough investigation of appropriate RING variants that are specifically impaired in the establishment of such interactions.

3.1.3 Stimulation of E2 enzymes by the RING-finger is mainly required for early steps in Ub chain synthesis

The analysis of Ubc7 function during the formation of K48-linked poly-Ub allowed a detailed look on the requirements for the individual steps in this reaction. The first attachment of Ub on another Ub molecule, which gives rise to a di-Ub species, clearly required stimulation of Ubc7 by a RING-finger domain. The subsequent steps in this process were also accelerated by the RING, however to a lesser degree. Consequently, the impact of the RING domain on the elongation reaction declines and the binding of Ubc7 to the poly-Ub chain via Cue1 becomes the more important factor. Thus, the catalytic stimulation of E2 enzymes by E3 ligases seems to primarily support the priming of client proteins and early events during the Ub chain elongation, but does not necessarily contribute to the formation of longer poly-Ub molecules. Those results are in line with previous studies describing the Cue1/Ubc7 chain elongation system as a self-accelerating machinery which requires di-ubiquitin as a minimal substrate for the binding to Cue1[41,42]. Cue1 positions Ubc7 on poly-Ub and thereby facilitates the addition of more Ub molecules. The CUE domain of Cue1 only weakly binds to the Ub chains, which allows a dynamic sliding of the Cue1/Ubc7 complex along a growing poly-Ub molecule. A slightly higher binding affinity for the penultimate Ub moiety in a chain suffices to place Ubc7 preferentially at the tip of the chain and thereby substantially increases the chance for the attachment of another Ub moiety. A more recent study demonstrated the structural flexibility of K48-linked poly-Ub[73]. Cue1 appears to actively select for open conformations within these molecules that allow a perfect positioning of Ubc7.

The results from the discharge and chain elongation assays were directly confirmed in a reconstituted *in vitro* ubiquitination assay. Again, the formation of a poly-Ub signal on a reporter protein by Ubc7 was strongly enhanced when the Hrd1 RING-finger construct contained a canonical arginine at its linchpin position. Neither a Hrd1

RING construct harboring a histidine at this site nor any of the tested Doa10 RING-finger variants facilitated poly-ubiquitination of the substrate. This implies that the transfer of Ub from Ubc7 to a client protein is substantially stimulated by linchpin allostery via the Hrd1 RING-finger domain. Although Doa10 can activate Ubc7 via the linchpin residue, this does not suffice to allow the priming of a substrate with Ub.

3.1.4 A refined model describing RING-mediated E2 stimulation

The results of this work allow a refinement of our current ideas on RING-finger-mediated stimulation of E2 activity (Fig. 3-2). This new “four-point-interaction model” describes, how distinct contacts of a RING-finger domain to an E2~Ub conjugate stabilize closed conformations of the intermediate and thereby trigger the transfer of Ub.

In Ubc7~Ub conjugates, the position of the Ub moiety is highly flexible. Binding of this intermediate by a RING-finger allows the interaction with an appropriate amino acid in the linchpin position, which restricts the movement of Ub and drives the Ubc7~Ub conjugate into a more closed conformation. Contacts of Ub with the E2 and the RING domain then further stabilize this compact configuration and thereby support the transfer of Ub to client proteins.

In contrast, the Ubc6~Ub conjugate inherently adopts a more closed conformation. The interaction of the RING-finger domain with Ub in the intermediate induces only minor changes, which slightly increases the stability of the reactive conformation. Linchpin allostery is not necessary for the stabilization of the Ubc6~Ub intermediate. In consequence, the association with a RING-finger domain only weakly stimulates the catalytic activity of Ubc6.

This model serves as a general draft of how RING-finger Ub ligases stimulate the catalytic activity of associated E2 enzymes. Other pairs of E2 enzymes and RING-finger proteins may employ only some aspects of the presented model to obtain a closed conformation of the E2~Ub intermediate. Under certain circumstances, the excessive stimulation of an E2 enzyme may counteract its cellular function. Thus, individual RING-finger ligases most likely have adapted their mode of E2 activation to the general requirements of the biological process they are involved in.

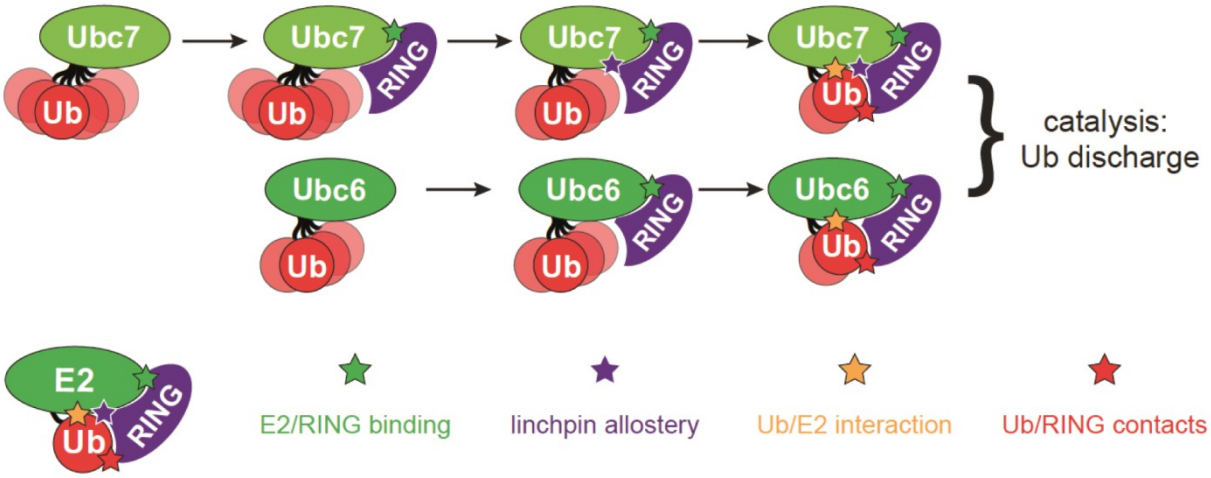

Figure 3-2: Four-point-interaction model for RING-mediated E2 stimulation. E2/RING binding, linchpin allostery, Ub/E2 interaction and Ub/RING contacts contribute to the stabilization of closed E2~Ub conjugate conformations that actively promote Ub transfer. The figure was adopted from Dr. Tobias Ritterhoff.

3.2 ERAD ligases employ different strategies in the priming and elongation reactions

3.2.1 ERAD ligases display different requirements regarding linchpin allostery

Processing of Hrd1 client proteins relies on particular amino acids in the linchpin position of the RING-finger domain, whereas the nature of the linchpin residue is not important for the degradation of Doa10 targets. This difference is correlated with diverging strategies for the priming of substrates with Ub. Still, both E3 ligase complexes employ Ubc7 for Ub chain formation. Unexpectedly, changes in the CUE domain of Cue1, which specifically impaired the elongation of Ub chains *in vitro*, did not generally affect the turnover of ERAD substrates *in vivo*.

However, this may not apply to all ERAD substrates. In yeast cells, Ubc6 is constitutively degraded via a Doa10-dependent pathway. Proteolysis of this particular ERAD substrate is affected by changes in the CUE domain of Cue1 that impair the association with poly-Ub[42]. However, the turnover of Ubc6 is unorthodox in some respects. Ubc6 auto-ubiquitinates itself and a large fraction of the protein modified with mono-Ub can be readily detected in cell extracts[20]. Therefore, degradation kinetics of this specific target may not be limited by its priming with mono-Ub, but rather by the rate of poly-Ub chain synthesis.

A puzzling observation was encountered during the analysis of Hmg2-6xMyc degradation. Processing of this protein was not completely abrogated in absence of Hrd1 or Ubc7. It is therefore feasible to speculate that cytosolic PQC pathways contribute in part to the turnover of this target. A recent study in human cells demonstrated the degradation of an ERAD-M substrate by a cytosolic protein quality control pathway[106]. Processing of INSIG1-GFP is mediated by the ER membrane-bound E3 ligase AMFR, but also required the activity of a cytosolic E2 enzyme and Ub ligase.

3.2.2 Backup mechanisms ensure efficient substrate removal

The Hrd1 and Doa10 ERAD ligases display clear preferences on how they prime their client proteins with Ub. Remarkably data in this thesis imply that both ligases can employ alternative priming mechanisms to handle specific subsets of substrates. Degradation of unassembled Sbh2 via Doa10 does not entirely rely on Ubc6 function. Obviously, also Ubc7 is able to prime this target with Ub in the context of the Doa10 RING-finger enzyme. However, the over-stimulation of Ubc7 activity by placing a canonical arginine into the linchpin position of the Doa10 RING-finger domain did not restore Sbh2 turnover in cells lacking Ubc6. This suggests that priming of Doa10 substrates by Ubc7 is not facilitated by linchpin allostery, but depends on other properties of the RING domain.

The degradation of Hrd1 client proteins was gradually impaired in mutants of the RING-finger domain that did not support full stimulation of Ubc7. Importantly, the turnover of these proteins was further delayed in absence of Ubc6. This demonstrates that Ubc6 is able to attach Ub onto Hrd1 substrates. In wild type cells, the priming activity of Ubc7 at the Hrd1 Ub ligase outperforms that of Ubc6. Once the stimulation of Ubc7 via linchpin allostery is compromised, the residual Ubc6 priming activity suffices to allow the degradation of at least a fraction of the Hrd1 substrates. Importantly, the processing of particular Hrd1 clients, like a variant of CPY* devoid of all lysine residues, may completely depend on priming by Ubc6. This shows that also the Hrd1 Ub ligase can employ a specialized E2 enzyme for the priming of certain target proteins with Ub, which most likely contributes to broaden the flexibility of this ERAD enzyme in the disposal of defective polypeptides.

In human cells, the Hrd1 homologue, SYVN1, cooperates with the homologues of Cue1 and Ubc7, AUP1 and UBE2G2, respectively[106,107]. In addition, several studies show a physical and functional interaction of SYVN1 and the Ubc6 homologue UBE2J1[106,108,109]. Obviously, the interplay of Hrd1 with a specialized priming E2 enzyme is conserved from yeast to human. Interestingly, human cells harbor two homologues of Ubc6. Each of those is functionally connected with either human Hrd1 or the homologue of Doa10. Human cells might therefore equip each of those ERAD Ub ligases separately with a highly flexible and versatile Ub priming enzyme to facilitate the ubiquitination of their client proteins.

In conclusion, the poly-ubiquitination of ERAD substrates is largely delimited by the priming reaction. To this end, two distinct strategies have evolved to ensure the efficient attachment of the initial Ub moieties (Fig. 3-3). The Doa10 ligase employs a specialized E2 enzyme for priming and utilizes another one for the formation of Ub chains. Accordingly, the Doa10 RING-finger domain binds both enzymes equally well. It accommodates a non-canonical amino acid residue at its linchpin position and thus does not stimulate the activity of the priming enzyme via linchpin allostery. Nevertheless, it is capable to support poly-Ub formation by Ubc7.

Hrd1 primarily cooperates with Ubc7 in the priming and elongation reactions. Nevertheless, Ubc6 can be utilized for the initial ubiquitination of appointed client proteins. Thus, these ERAD Ub ligases employ two fundamentally different strategies to promote the efficient degradation of their targets, but maintain a high degree of versatility to target unorthodox client proteins.

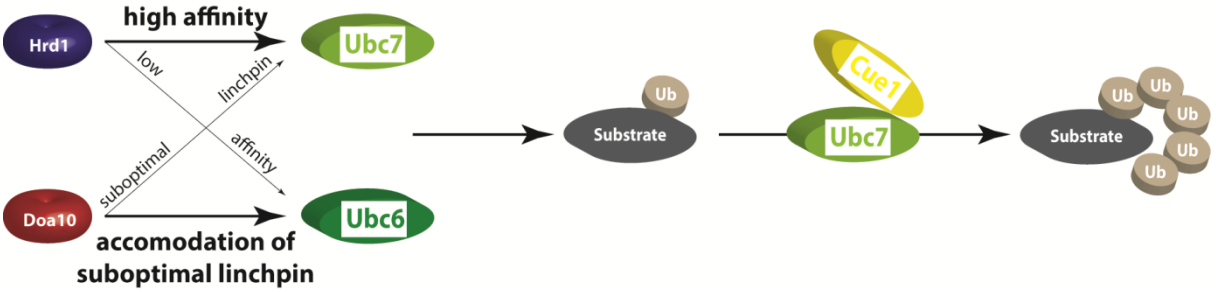

Figure 3-3: Interaction model of ERAD ligases and their cognate E2 enzymes during substrate priming and chain elongation. Distinct interactions between E3's and E2's serve the purpose of high processivity while backup mechanisms provide vast versatility.

3.3 Molecular analysis of the Asi complex at a glimpse

A novel Asi model substrate was established based on the very stable superfolder GFP[90]. Fusion of sfGFP to an Asi-regulated degron robustly recruited the engineered protein towards Asi-mediated quality control in yeast cells. With this tool in hand, several published and so far uninvestigated contributions to Asi complex function were dissected.

Foresti *et al.*[56] proved a strong interaction between Asi1 and Asi3 in absence of Asi2 and argued for the existence of different subcomplexes. Work in this thesis reveals that any two of the Asi subunits robustly interact with each other independent of the third complex partner. This still opens the possibility for the presence of distinctly active subcomplexes. However, the strict requirement for every single subunit of the complex regarding substrate degradation suggests that active Asi complexes comprise all three interaction partners.

In line with results from Foresti *et al.*[56], ubiquitination of Asi clients was facilitated by Ubc4 and Ubc7. Deletion of Ubc6 had only minor effects. While Khmelinskii *et al.*[57] provided data that show a physical interaction between Ubc6 and the Asi1 and Asi3 RING-finger domains, a clear indication for a functional partnership is missing. Thus, this physical interaction might solely result from close proximity since Ubc6, together with Doa10, also localizes to the inner nuclear membrane to regulate Asi2 protein levels[92,110].

In the final part of this thesis, the distinct contributions of the Asi1 and Asi3 RING-finger domains to target breakdown were analyzed. This study reveals that both RING domains are required for efficient substrate processing at the Asi complex. Furthermore, it proves that spatially regulated linchpin allostery is necessary for modification of client proteins.

An intriguing model accommodating the presented results is based on the consecutive action of the Asi1 and Asi3 RING domains. Cooperating E2 enzymes could be recruited to the complex by the Asi3 RING domain. Then, E2s would be passed over to the Asi1 RING domain for stimulation and Ub transfer to client molecules. To validate this hypothesis, a “RING-swapping” experiment could be conducted. To this end, fusion proteins consisting of Asi1 and Asi3 proteins harboring the corresponding RING domain of the other subunit could be used. If E2 recruitment

and stimulation is solely facilitated by the RING domains, the complex should still be functional. Additionally, the residues at the linchpin positions could be substituted by the corresponding one in the other RING domain to investigate if the observed effects are due to spatial issues or if other features of the RINGs are important. Spatial regulation may also be connected to substrate recruitment to the Asi complex, which unfortunately, has not yet been studied in detail. Even though, all Asi subunits have been shown to efficiently precipitate substrate molecules[56], they might only come in close proximity to E2 enzymes at the Asi1 RING.

Another model explaining the necessity of two correctly folded RING domains emerges from the heterodimeric BRCA1/BARD1 Ub ligase complex. The BRCA1/BARD1 ligase harbors two RING-carrying subunits. NMR studies proved that interaction between the complex and E2 enzymes is exclusively promoted by the BRCA1 RING, but not the BARD1 RING[111]. Nevertheless, interaction of the RINGs is strictly required for complex function. The authors claimed that the BARD1 RING stabilizes active BRCA1 conformations in the context of the active ligase complex. This could also apply to the Asi complex. To test this hypothesis, the effect of single point mutations in conserved residues, which are important for RING heterodimerization could be analyzed.

Another, albeit doubtful model features Asi1 as the only active subunit needed for substrate turnover. In this case, Asi2 and Asi3 would only partially contribute to substrate recruitment to the complex. Lack of those should then be covered by Asi1 overexpression. A similar mechanism was proposed for the Hrd1 ligase where it has been shown that overexpression of Hrd1 suppresses the need of other subunits of the Hrd1 ligase complex[112]. Experiments implementing overexpression of single Asi subunits in different deletion backgrounds could be performed to examine this idea.

Future work is needed to deepen the understanding of the Asi complex. Unfortunately, due to technical difficulties, the establishment an *in vitro* assay to monitor Asi-dependent E2 stimulation was not successful, so far. The newly established model substrate Stp1-sfGFP-3xHA may help in this regard by providing the means to directly follow substrate modification in solution.

3.4 Mechanisms of priming and elongation during Ub chain formation

Substrate priming with Ub and elongation of chains on previously attached Ub moieties display two fundamentally different processes. During priming, E2 enzymes are faced with the challenge to detect and modify accessible residues in a highly varying substrate pool. Targets of different topology are probably presented to the Ub conjugating enzymes in a many different ways leading to a manifold of different environments surrounding the amino acid side chains that will be modified. During elongation, E2 enzymes are repeatedly encountered with virtually the same interface on the client Ub. This is often achieved by distinct Ub binding domains aligning the Ub chain with the catalytic center of the E2 allowing for efficient Ub transfer.

To overcome these different challenges, versatile systems have been identified that uncouple substrate priming from chain elongation. With the Doa10 ligase to begin with, two different E2 enzymes are employed for either process[20]. This is particularly important in protein quality control since involved E3 ligases are challenged with a highly heterogeneous substrate pool[113].

A comparable mechanism is found at the anaphase-promoting complex (APC). The APC controls cell cycle progression to ensure equal distribution of sister chromatids to the daughter cells during mitosis. This in turn contributes to the maintenance of a healthy genome. Therefore, rapid removal of cell cycle inhibitors, like securin and cyclin B1, at a given time point must be guaranteed. To achieve this, the APC teams up with Ubc4 and Ubc1 for target priming and elongation of K48-linked chains[78]. Another example is found in the NF-κB pathway, in which modification of IκBα by the $SCF^{\beta TrCP2}$ complex is facilitated by sequential polyubiquitination[114]. The SCF ligase cooperates with the human Ubc4 homologue UbcH5c to prime IκBα with Ub, which is then elongated by Cdc34 to induce proteasomal degradation.

3.5 Concluding remarks

Mechanisms of priming and elongation are widely spread in nature and come to play whenever substrates need to be rapidly and efficiently removed to induce signaling pathways or prevent cells from proteotoxic stress. Therefore, the detailed mechanisms of priming and elongation in various Ub-related systems need to be investigated in molecular detail to understand target modification with Ub.

This study provides insight into the different strategies that E3 ligases employ to overcome the challenges of priming and elongation and proposes a refined model of E3-mediated E2 stimulation. This is not only limited to ERAD ligases, but can be extended to other systems. By analyzing the interactions between distinct E2/E3 pairs, we may be able to predict how they fulfill their functions in their given cellular context.

4. Material and methods

4.1 Material

4.1.1 Chemicals

All chemicals and reagents used in this study were purchased from Sigma, VWR or Roth, unless otherwise noted. Restriction enzymes were acquired from *New England Biolabs* (NEB). All buffer solutions were prepared using deionized H_20 which has been passed through a Milli-DI ® system (Millipore).

4.1.2 Bacterial strains

XL1-Blue (Agilent Technologies)

E. coli recA1 endA1 gyrA96 thi-1 hsdR17(r_K^- m_K^+) *supE44 relA1 lac* [F´ *proAB lacI*^{q}*ZΔM15* Tn*10* (Tet^r)]

BL21-Gold(DE3) (Agilent Technologies)

E. coli B F$^-$ *ompT hsdS*(r_B^- m_B^-) *dcm*$^+$ Tet´*gal* λ(DE3) *endA* Hte [pLysS Cam^r]

4.1.3 Yeast strains

All strains used in this study are haploid descendants of the diploid *S. cerevisiae* strain DF5[115]. Haploid YWO1 and YWO2 strains serve as wild type standards. Deviations from their genotypes for strains used in this study are listed below. Strains termed “YAWxxx” were constructed by Dr. Annika Weber as a contribution to this study, unless otherwise noted.

Table 4-1: Relevant yeast strains used in this thesis

Strain	Genotype	Reference
YWO1	*trp1-1 (am), his-Δ200, ura3-52, lys2-801, leu2-3, -112, MATα*	Seufert *et al.*[116]
YWO2	*trp1-1 (am), his-Δ200, ura3-52, lys2-801, leu2-3, -112, MATa*	Seufert *et al.*[116]
YWO13	*Δubc4::HIS3, MATα*	Seufert *et al.*[116]
YBM74	*Δdoa10::kanMX6, MATα*	Birgit Meusser
YBM77	*Δdoa10::kanMX6, Δubc7::LEU2, MATα*	Birgit Meusser
YJU3	*Δubc7::LEU2, MATα*	Jörg Urban
YJU4	*Δubc4::HIS3, Δubc7::LEU2, MATα*	Jörg Urban
YTX115	*Δcue1::LEU2, MATα*	Laboratory of Prof. Sommer
YTX190	*Δubc7::LEU2, MATα*	Laboratory of Prof. Sommer
YTX996	*Δubc6::HIS3, MATα*	Weber *et al.*[20]
YTX997	*Δubc6::HIS3, Δubc7::LEU2, MATα*	Katrin Bagola
YAW018	*Δdoa10::kanMX6, Δubc6::HIS3, MATα*	Annika Weber
YAW032	*Δdoa10::kanMX6, Δssh1::HIS3, MATa*	Weber *et al.*[20]
YAW068	*Δdoa10::kanMX6, Δssh1::HIS3, Δubc6::LEU2, MATa*	Annika Weber
YAW102	*Doa10 H94E, MATα*	This study
YAW109	*Doa10 H94E, Δubc6::HIS3, MATα*	This study
YAW110	*Doa10 H94E, Δubc7::LEU2, MATα*	This study
YAW111	*Doa10 H94E, Δssh1::HIS3, Δubc7::LEU2, MATα*	This study
YAW112	*Doa10 H94E, Δssh1::HIS3, MATa*	This study
YAW116	*Doa10 H94E, Δssh1::HIS3, Δubc6::HIS3, MATα*	This study
YCL005	*Erg11-3xHA::TRP1, MATα*	This study
YCL006	*Erg11-3xHA::TRP1, MATa*	This study
YCL007	*Δasi1::kanMX6, MATa*	This study
YCL010	*Δasi2::URA3, MATa*	This study
YCL013	*Δasi3::HIS3, MATa*	This study
YCL014	*Erg11-3xHA::TRP1, Δubc7::LEU2, MATα*	This study
YCL015	*Erg11-3xHA::TRP1, Δubc6::HIS3, MATα*	This study
YCL016	*Erg11-3xHA::TRP1, Δubc6::HIS3, Δubc7::LEU2, MATa*	This study
YCL018	*Erg11-3xHA::TRP1, Δasi1::kanMX6, MATa*	This study
YCL020	*Erg11-3xHA::TRP1, Δasi2::URA3, MATa*	This study
YCL022	*Erg11-3xHA::TRP1, Δasi3::HIS3, MATa*	This study
YCL036	*Erg11-3xHA::TRP1, Δubc4::HIS3, MATα*	This study
YCL057	*Δasi1::kanMX6, Δasi3::HIS3, MATα*	This study
YCL062	*Erg11-3xHA::TRP1, Δasi1::kanMX6, Δasi3::HIS3, MATa*	This study
YCL065	*Δasi1::kanMX6, Δasi2::URA3, Δasi3::HIS3, MATa*	This study
YCL070	*Erg11-3xHA::TRP1, Δubc4::HIS3, Δubc7::LEU2, MATα*	This study
YCL111	*Δhrd1::TRP1, Δubc6::HIS3, MATa*	This study
YCL114	*Δhrd1::TRP1, MATα*	This study

YCL123	*Δhrd1::TRP1, Δubc7::LEU2, MATa*	This study
YCL137	*Δhrd1::TRP1, Δubc6::HIS3, 6xMyc-Hmg2::URA3, MATa*	This study
YCL138	*Δhrd1::TRP1, Δubc7::LEU2, 6xMyc-Hmg2::URA3, MATa*	This study
YCL153	*Δssh1::HIS3, Δubc6::HIS3, MATα*	This study
YCL155	*Δdoa10::kanMX6, Δssh1::HIS3, Δubc7::LEU2, MATa*	This study
YCL156	*Δssh1::HIS3, Δubc7::LEU2, MATa*	This study
YCL157	*Δssh1::HIS3, MATa*	This study
YCL169	*Δhrd1::TRP1, Δcue1::LEU2, MATα*	This study
YCL178	*Δssh1::HIS3, Cue1 LAP(76-78)RGA, MATa*	This study
YCL180	*Δssh1::HIS3, Δcue1::LEU2, MATa*	This study
YCL183	*Δhrd1::TRP1, Cue1 LAP(76-78)RGA, MATa*	This study
YCL185	*Cue1 LAP(76-78)RGA, MATα*	This study
YCL201	*Δhrd1::TRP1, 6xMyc-Hmg2::URA3, MATα*	This study
YCL202	*Δhrd1::TRP1, Cue1 LAP(76-78)RGA, 6xMyc-Hmg2::URA3, MATα*	This study
YCL207	*Doa10 H94E, Δssh1::HIS3, Cue1 LAP(76-78)RGA, MATa*	This study
YCL210	*Doa10 H94E, Cue1 LAP(76-78)RGA, MATa*	This study
YCL250	*Doa10 H94R, MATα*	This study
YCL252	*Doa10 H94A, MATα*	This study
YCL253	*Doa10 H94R, Δssh1::HIS3, MATα*	This study
YCL255	*Doa10 H94A, Δssh1::HIS3, MATα*	This study
YCL256	*Doa10 H94R, Δssh1::HIS3, Δubc6::HIS3, MATα*	This study
YCL258	*Doa10 H94A, Δssh1::HIS3, Δubc6::HIS3, MATa*	This study
YCL259	*Doa10 H94R, Δubc6::HIS3, MATα*	This study
YCL260	*Doa10 H94A, Δubc6::HIS3, MATα*	This study
YCL261	*Doa10 H94R, Δubc7::LEU2, MATα*	This study
YCL263	*Doa10 H94A, Δubc7::LEU2, MATα*	This study
YCL264	*Doa10 H94R, Δssh1::HIS3, Δubc7::LEU2, MATα*	This study
YCL266	*Doa10 H94A, Δssh1::HIS3, Δubc7::LEU2, MATa*	This study
YCL274	*Doa10 H94R, Cue1 LAP(76-78)RGA, MATα*	This study
YCL276	*Doa10 H94R, Δssh1::HIS3, Cue1 LAP(76-78)RGA, MATα*	This study
YCL277	*Doa10 H94A, Cue1 LAP(76-78)RGA, MATα*	This study
YCL279	*Doa10 H94A, Δssh1::HIS3, Cue1 LAP(76-78)RGA, MATα*	This study

4.1.4 Plasmids

Plasmids used in this study are listed in table 4-2. Yeast expression plasmids encode for the endogenous promoter of the respective gene, unless otherwise noticed. pToR plasmids were constructed and provided by Dr. Tobias Ritterhoff from Rachel Klevit's laboratory as a contribution to this study. pAW plasmids were constructed by Dr. Annika Weber as a contribution to this study, unless otherwise noted.

Table 4-2: Relevant plasmids used in this thesis

Plasmid	Insert	Backbone	Reference
	Bacterial Expression Plasmids		
pAW039	GST-HRV3C-Ubc6 (2-230)	pGEX-6p1	Weber *et al.*[20]
pLP016	GST-HRV3C-Ubc4 K91R	pGEX-6p1	Lukas Pluska
pMD10	hUb	pETM60	Rogov et al.[117]
pMD11	hUb-His_6	pETM60	von Delbrück *et al.*[42]
pMD12	hUb S20C	pETM60	von Delbrück *et al.*[42]
pMD26	GST-HRV3C-Cdc34	pGEX-6p1	von Delbrück *et al.*[42]
pTX249	GST-HRV3C-Ubc7 (2-165)	pGEX-6p1	Bagola *et al.*[41]
pTX410	GST-HRV3C-Cue1-His_6 (24-203)	pGEX-6p1	Bagola *et al.*[41]
pTX411	GST-HRV3C-Cue1 LAP(76-78)RGA-His_6 (24-203)	pGEX-6p1	Bagola *et al.*[41]
pTX481	Uba1-His_6	pET32	Berndsen & Wolberger[118]
pToR1	His_6-SUMO3-Hrd1 (325-412)	pET28	This study
pToR3	GST-HRV3C-Doa10 (19-102)	pGEX-6p1	This study
pToR4	GST-HRV3C-Doa10 H94R (19-102)	pGEX-6p1	This study
pToR5	GST-HRV3C-Doa10 H94A (19-102)	pGEX-6p1	This study
pToR6	GST-HRV3C-Doa10 H94E (19-102)	pGEX-6p1	This study
pCL151	His_6-SUMO3-Hrd1 R400E (325-412)	pET28	This study
pCL153	His_6-SUMO3-Hrd1 R400A (325-412)	pET28	This study
pCL160	His_6-SUMO3-Hrd1 R400H (325-412)	pET28	This study
pCL166	His_6-SUMO3-S-Hrd1 (325-412)	pET28	This study
pCL167	GST-HRV3C-S-Doa10 (19-102)	pGEX-6p1	This study
pCL172	GST-HRV3C-RNase A-TUB (42-150)	pGEX-6p1	This study
pCL173	His_6-SUMO3-S-Hrd1 R400H (325-412)	pET28	This study
pCL176	GST-HRV3C-S-Doa10 H94R (19-102)	pGEX-6p1	This study
	Yeast Expression Plasmids		
pRB256	CPY*_noK-HA	pRS315	Baldridge & Rapoport[89]
pTR1646	FLAG-Sbh2	pRS414	Weber *et al.*[20]
pUL038	Deg1-$eGFP_2$	pRS414	Lenk & Sommer[82]
pAW183	Hrd1 R400H	pRS416	This study
pCL023	Asi1	pRS415	This study
pCL026	Asi1 CC583/585SS	pRS415	This study
pCL030	3xHA-Asi1	pRS415	This study
pCL068	3xMyc-Asi2	pRS317	This study
pCL069	3xFLAG-Asi3	pRS414	This study
pCL075	3xMYC Asi2 (1-159)	pRS317	This study
pCL076	3xFLAG-Asi3 (1-299)	pRS414	This study
pCL077	3xHA-Asi1 (1-299)	pRS415	This study
pCL080	SV40 NLS-3xHA-Asi1 (300-624)	pRS415	This study

pCL081	SV40 NLS-3xMyc-Asi2 (160-289)	pRS317	This study
pCL082	SV40 NLS-3xFLAG-Asi3 (300-676)	pRS414	This study
pCL083	Hrd1	pRS416	this study
pCL084	Hrd1 R400A	pRS416	this study
pCL087	3xHA-Asi1 (1-199)	pRS415	This study
pCL088	3xHA-Asi1 (1-99)	pRS415	This study
pCL089	3xMyc-Asi2 (1-119)	pRS317	This study
pCL090	3xMyc-Asi2 (1-79)	pRS317	This study
pCL091	3xFLAG-Asi3 (1-199)	pRS414	This study
pCL092	3xFLAG-Asi3 (1-99)	pRS414	This study
pCL099	SV40 NLS-3xHA-Asi1 (400-624)	pRS415	This study
pCL100	SV40 NLS-3xHA-Asi1 (500-624)	pRS415	This study
pCL101	SV40 NLS-3xMyc-Asi2 (200-289)	pRS317	This study
pCL102	SV40 NLS-3xMyc-Asi2 (240-289)	pRS317	This study
pCL103	SV40 NLS-3xFLAG-Asi3 (400-676)	pRS414	This study
pCL104	SV40 NLS-3xFLAG-Asi3 (500-676)	pRS414	This study
pCL105	SV40 NLS-3xFLAG-Asi3 (600-676)	pRS414	This study
pCL138	$Stp1^{16\text{-}50}$-sfGFP-3xHA	pRS424	This study
pCL139	sfGFP-3xHA	pRS424	This study
pCL142	Hrd1	pRS317	This study
pCL143	Hrd1 R400A	pRS317	This study
pCL149	PrA*-3xHA	pRS317	This study
pCL152	Hrd1 R400E	pRS317	This study
pCL157	Hrd1 R400E	pRS416	This study
pCL161	Hrd1 R400H	pRS317	This study
pCL165	Asi3	pRS416	This study
pCL168	Asi1 R608D	pRS415	This study
pCL169	Asi3 CC624/627SS	pRS416	This study
pCL171	Asi3 D664R	pRS416	This study

4.1.5 Oligonucleotides

Oligonucleotides used in this study are listed in table 4-3. All oligonucleotides were supplied by BioTeZ Berlin-Buch GmbH. Forward and reverse primers are indicated as “fwd” and “rev”, respectively. Primers for amplification of promoter and terminator regions upstream and downstream of genes are indicated as “up” and “down” respectively. Primers AWxxx were designed by Annika Weber as a contribution to this study. RF corresponds to primers used for Restriction-Free cloning[119].

Table 4-3: Relevant oligonucleotides used in this thesis

Oligonucleotide	Sequence 5' → 3'	Target gene	Description
AW278	GGA TGT TAA ATG TGA CAT CTG TCG CTA TCC CAT TCA ATT C	Doa10	Doa10 H94R fwd
AW279	GAA TTG AAT GGG ATA GCG ACA GAT GTC ACA TTT AAC ATC C	Doa10	Doa10 H94R rev
AW280	CTC AGA CTT GTC CTA TTT GTG CAT TGC CTG TCT TTG ATG	Hrd1	Hrd1 R400A fwd
AW281	CAT CAA AGA CAG GCA ATG CAC AAA TAG GAC AAG TCT GAG	Hrd1	Hrd1 R400A rev
AW350	CTC AGA CTT GTC CTA TTT GTC ACT TGC CTG TCT TTG ATG	Hrd1	Hrd1 R400H fwd
AW351	CAT CAA AGA CAG GCA AGT GAC AAA TAG GAC AAG TCT GAG	Hrd1	Hrd1 R400H rev
AW352	GGA TGT TAA ATG TGA CAT CTG TGC TTA TCC CAT TCA ATT C	Doa10	Doa10 H94A fwd
AW353	GAA TTG AAT GGG ATA AGC ACA GAT GTC ACA TTT AAC ATC C	Doa10	Doa10 H94A rev
AW356	GGA TGT TAA ATG TGA CAT CTG TGA GTA TCC CAT TCA ATT C	Doa10	Doa10 H94E fwd
AW357	GAA TTG AAT GGG ATA CTC ACA GAT GTC ACA TTT AAC ATC C	Doa10	Doa10 H94E rev
AW363	CTC AGA CTT GTC CTA TTT GTG AAT TGC CTG TCT TTG ATG	Hrd1	Hrd1 R400E fwd
AW364	CAT CAA AGA CAG GCA ATT CAC AAA TAG GAC AAG TCT GAG	Hrd1	Hrd1 R400E rev
CL131	CTT TTT GTC GAC CAC AAT TAC GAA AAC TAT ATT GTT TTG	Asi1	SalI_+200bp up_Asi1 fwd
CL132	GAA AAA CTG CAG CTC CCA AAC GAA AAA CCT C	Asi1	Asi1_+50 bp down_PstI rev
CL133	CTT TTT GTC GAC CAT TGC TGT GCA GTT AAT CTT C	Asi2	SalI_+200bp up_Asi2 fwd
CL134	GAA AAA CTG CAG CGA CCA CAT GCG AAA G	Asi2	Asi2_+50 bp down_PstI rev
CL135	CTT TTT AAG CTT ATG TCT ACA AAT ATA TTG CAA CAT GTT AAG	Asi3	HindIII_Asi3 fwd
CL136	GAA AAA CTG CAG CAG ACT TGA GGT TGA ACA TAT CC	Asi3	Asi3_+50 bp down_PstI rev
CL149	ATA CAG TAT TAT GGC CCA GCC GAA GTT TTG CCA TTT GCG AG	Asi1	Asi1 CC583/585SS fwd
CL150	CTC GCA AAT GGC AAA ACT TCG GCT GGG CCA TAA TAC TGT AT	Asi1	Asi1 CC583/585SS rev
CL151	GTG GAG GAA ATG GAT CTC TCC AGC CTA ATC AGC AAA GTT AAT AAA AGA AAT AT	Asi3	Asi3 CC624/627SS fwd

CL152	ATA TTT CTT TTA TTA ACT TTG CTG ATT AGG CTG GAG AGA TCC ATT TCC TCC AC	Asi3	Asi3 CC624/627SS rev
CL155	ATG ATT ATC TGT TTC AGC GAT TTC TAG AAG AAT CGG AAC AAA AGT TGA TTT CTG AAG AAG	Asi2	RF 3xMyc-Asi2 fwd
CL156	GAA GGC TCT CTA CTA TGC CTC GTT TCG TTC AAG TCT TCT TCT GAG ATT AAT	Asi2	RF 3xMyc-Asi2 rev
CL165	ACA AGC CGT AAT CTC AGG TAA CTC CTA CCC ATA CGA TGT TCC TGA CT	Asi1	RF 3xHA-Asi1 fwd
CL166	AGT CTA TAA GGA AAG TTG ATA ACA TTT GCG AAA GTA GCG TAA TCT GGA ACG TCA T	Asi1	RF 3xHA-Asi1 rev
CL207	TTA GCT TTT TTC ACA ACA AGA CTG GAA ATC TTA ATG ACT ACA AGG ACC ACG ACG GTG ACT ACA AGG ACC ACG ACA TCG ACT ACA AGG ACG ACG ACG ACA AGT ACC TAG ATA ACA CAA CTC AGA AAC CGG	Asi3	RF 3xFLAG-Asi3 fwd
CL208	CCG GTT TCT GAG TTG TGT TAT CTA GGT ACT TGT CGT CGT CGT CCT TGT AGT CGA TGT CGT GGT CCT TGT AGT CAC CGT CGT GGT CCT TGT AGT CAT TAA GAT TTC CAG TCT TGT TGT GAA AAA AGC TAA	Asi3	RF 3xFLAG-Asi3 rev
CL222	CAT GCG TCA GCT GTC GTA GTG AGG TGA AGG G	Asi3	Asi3 D664R fwd
CL223	CCC TTC ACC TCA CTA CGA CAG CTG ACG CAT G	Asi3	Asi3 D664R rev
CL267	CTT TTT CTC GAG CAC AAT TAC GAA AAC TAT ATT GTT TTG AAC AG	Asi1	XhoI _Asi1-promoter fwd
CL268	CGT ATG GGT AGA CCT TTC TTT TCT TTT TTG GCA TGT CGA CAT TCT TAG CAT AGT TTC TTT GTA AAA AGA AG	Asi1	Asi1-promoter-SV40 NLS-3xHA rev
CL269	GTC GAC ATG CCA AAA AAG AAA AGA AAG GTC TAC CCA TAC GAT GTT CCT GAC	Asi1	SV40 NLS-3xHA fwd
CL270	ACT GTA AAA GTT CGC AAG AAT TAC GTG ATT TTC CAT GCA TAG CGT AAT CTG GAA CGT CA	Asi1	3xHA_NsiI_Asi1 (300-624) rev
CL271	TGA CGT TCC AGA TTA CGC TAT GCA TGG AAA ATC ACG TAA TTC TTG CG	Asi1	3xHA_NsiI_Asi1 (300-624) fwd
CL272	CTT TTT GGG CCC CAT TGC TGT GCA GTT AAT CTT CAT	Asi2	ApaI_Asi2-promoter fwd
CL273	ACT TTT GTT CGA CCT TTC TTT TCT TTT TTG GCA TGA ATT CTT TTT CTC ACT AAA TGC TTG TGA GG	Asi2	Asi2-promoter-SV40 NLS-3xMyc rev
CL274	GAA TTC ATG CCA AAA AAG AAA AGA AAG GTC GAA CAA AAG TTG ATT TCT GAA GAA GAT TTG	Asi2	SV40 NLS-3xMyc fwd

CL275	ATA TCT TGG CAA ATT TCC AGT ATC CCA CGA TAT GCA TGT TCA AGT CTT CTT CTG AGA TTA ATT TTT GTT C	Asi2	3xMyc_NsiI_Asi2 (160-289) rev
CL276	GAA GAC TTG AAC ATG CAT ATC GTG GGA TAC TGG AAA TTT G	Asi3	3xMyc_NsiI_Asi2 (160-289) fwd
CL277	CCT TGT AGT CGA CCT TTC TTT TCT TTT TTG GCA TAA GCT TAT TCT TAG CAT AGT TTC TTT GTA AAA AGA AG	Asi3	Asi1-promoter-SV40 NLS-3xFLAG rev
CL278	AAG CTT ATG CCA AAA AAG AAA AGA AAG GTC GAC TAC AAG GAC CAC GAC GG	Asi3	SV40 NLS-3xFLAG fwd
CL279	TAT ATC TTG AAT ATA ATG ATC GGA ACG GAT TAC TAT GCA TCT TGT CGT CGT CGT CC	Asi3	3xFLAG_NsiI_Asi3 (300-676) rev
CL280	ACG ACA AGA TGC ATA GTA ATC CGT TCC GAT CAT TAT ATT C	Asi3	3xFLAG_NsiI_Asi3 (300-676) fwd
CL281	GCT TAA TTA GAT GGG ATC CAT TTT GAA AAT CAC GTA ATT CTT GCG AA	Asi1	Asi1 299_STOP fwd
CL282	TTC GCA AGA ATT ACG TGA TTT TCA AAA TGG ATC CCA TCT AAT TAA GC	Asi1	Asi1 299_STOP rev
CL283	AAT ATC TTG GCA AAT TTC CAG TAT CCC ACT CAT TCG ATT ATA AAA TCA TTC TCT GAA AAG G	Asi2	Asi2 159_STOP fwd
CL284	CCT TTT CAG AGA ATG ATT TTA TAA TCG AAT GAG TGG GAT ACT GGA AAT TTG CCA AGA TAT T	Asi2	Asi2 159_STOP rev
CL285	CCT GAA GGC TTT GTT CAC CTG AAA TCC GTT CCG ATC ATT AT	Asi3	Asi3 299_STOP fwd
CL286	ATA ATG ATC GGA ACG GAT TTC AGG TGA ACA AAG CCT TCA GG	Asi3	Asi3 299_STOP rev
CL287	GAA AAA AAG CTT TCA AAG AAA AGG TTT AAT AGA CGA TAA ATT TCC	Hrd1	HindIII_+300bp up_Hrd1 fwd
CL288	CTT TTT GGA TCC CAG TAG TTT TTT TCT TTA AAA AAA ACT ATG TAT AAT ATA AAA C	Hrd1	Hrd1_+50 bp down_BamHI rev
CL294	GAA AAA ATG CAT CAA AGA TTT TTT TTA ATG TTT CCA AAA TCT ATA ATA TG	Asi1	NsiI_Asi1 (400-624) fwd
CL295	GAA AAA ATG CAT AAC GAA ACT CGG GAT GCC	Asi1	NsiI_Asi1 (500-624) fwd
CL296	GAA AAA ATG CAT TCT TCA CCT GTG ATA AAA CAT ATT ATG AAA AG	Asi2	NsiI_Asi2 (200-289) fwd
CL297	GAA AAA ATG CAT ATC TAT TTA GCT TAT GGC GTA AGT G	Asi2	NsiI_Asi2 (240-289) fwd
CL298	GAA AAA ATG CAT ACA TAT TTA GGC CTT TTT GAA TTA GTA AGA AC	Asi3	NsiI_Asi3 (400-676) fwd
CL299	GAA AAA ATG CAT TCA GAT GAA GAG TTT GAT AGT GAT ATG G	Asi3	NsiI_Asi3 (500-676) fwd

CL300	GAA AAA ATG CAT GAT GAC AAA TTA GAG TTC AAG TTT GAT TTT G	Asi3	NsiI_Asi3 (600-676) fwd
CL301	TCA TTG TTT GAA CTT TCG ATT CAG TTT TAT ACA ATG ACT AAT TAG AAT ACT AAA TTT TTA GAT TCT CC	Asi1	Asi1 199_STOP fwd
CL302	GGA GAA TCT AAA AAT TTA GTA TTC TAA TTA GTC ATT GTA TAA AAC TGA ATC GAA AGT TCA AAC AAT GA	Asi1	Asi1 199_STOP rev
CL303	GAA CCG GTT CGT TGT ATT TTA CTG AGT CCT TAA CAA CGG TTC CAG AC	Asi1	Asi1 99_STOP fwd
CL304	GTC TGG AAC CGT TGT TAA GGA CTC AGT AAA ATA CAA CGA ACC GGT TC	Asi1	Asi1 99_STOP rev
CL305	CAG AGC CCT CTC AGA ACT TTT CTT TGA AAT TTA TTC ATT TTA GAT TAC TT	Asi2	Asi2 119_STOP fwd
CL306	AAG TAA TCT AAA ATG AAT AAA TTT CAA AGA AAA GTT CTG AGA GGG CTC TG	Asi2	Asi2 119_STOP rev
CL307	TTC TAC TTC AAA TAT AAA TAG AGC AGC TAA TTA GGA TGC AAC CAC AAA CGG	Asi2	Asi2 79_STOP fwd
CL308	CCG TTT GTG GTT GCA TCC TAA TTA GCT GCT CTA TTT ATA TTT GAA GTA GAA	Asi2	Asi2 79_STOP rev
CL309	TTT TCC ATA TGG GGT TTA TCA TTG AAT CTT TAG ATC ATA TCC AAA ATG CC	Asi3	Asi3 199_STOP fwd
CL310	GGC ATT TTG GAT ATG ATC TAA AGA TTC AAT GAT AAA CCC CAT ATG GAA AA	Asi3	Asi3 199_STOP rev
CL311	TAT GTT TTA GTA CCG CCA TTA TTT TGT AAA GGT TGA CTG TAA TGT CTT CAT TG	Asi3	Asi3 99_STOP fwd
CL312	CAA TGA AGA CAT TAC AGT CAA CCT TTA CAA AAT AAT GGC GGT ACT AAA ACA TA	Asi3	Asi3 99_STOP rev
CL393	GAA AAA GTC GAC TTT ATA ATC AAA TTT TAG TGG TCT TTT CTA TTT TTA TTT G	Pra1	SalI_+200bp up_Pra1
CL394	GAA GTT TTG AGG TGG AGT ACC CAA AGT AAT GTC AGT GTA ATA CTT TTG GCC TAA ATG AGC TAA ATG	Pra1	Pra1 Y54 rev
CL395	TCA CTT TCG AGC AAC ATT TAG CTC ATT TAG GCC AAA AGT ATT ACA CTG ACA TTA CTT TGG GTA CTC	Pra1	Pra1 Y92 fwd
CL396	CTT TTT CTG CAG TCA AGC GTA ATC TGG AAC GTC ATA TGG ATA GGA TCC TGC ATA GTC CGG GAC GTC ATA GGG ATA GCC CGC ATA GTC AGG AAC ATC GTA TGG GTA AAT TGC TTT GGC CAA ACC AAC	Pra1	Pra1-3xHA_STOP_PstI rev
CL399	GAA AAA GGG CCC GCA TGC AAC TTC TTT TCT TTT TTT TTC	sfGFP	ApaI_ADH1 fwd
CL400	CTT TTT CTC GAG AGT TGA TTG TAT GCT TGG TAT AGC	sfGFP	ADH1_XhoI rev

CL401	GAA AAA GTC GAC ATG ATT CCA GGC AAG ATA TAC GCG TTC TTC AGA GAG CTC GTC AGC GGA GTT ATT ATA TCC AAG CCA GAT CTA AGT CAT CAT TAT TCT TGT GAA AAT GCG ACA AAG GAG CGT AAA GGC GAA GAG CTG	sfGFP	SalI_Stp1$^{16-50}$-sfGFP fwd
CL402	CTT TTT GAA TTC TCA AGC GTA ATC TGG AAC GTC ATA TGG ATA GGA TCC TGC ATA GTC CGG GAC GTC ATA GGG ATA GCC CGC ATA GTC AGG AAC ATC GTA TGG GTA TTT GTA CAG TTC ATC CAT ACC ATG C	sfGFP	sfGFP-3xHA_EcoRI rev
CL403	GAA AAA GTC GAC ATG CGT AAA GGC GAA GAG CTG	sfGFP	SalI_sfGFP fwd
CL445	CAG CAC TTG CGT ATG TTG TGA TAG TAA AGT TCA TGG GTA C	Asi1	Asi1 R608D fwd
CL446	GTA CCC ATG AAC TTT ACT ATC ACA ACA TAC GCA AGT GCT G	Asi1	Asi1 R608D rev
CL447	GTT CCA GCA GCA GAC GGG AGG TAA GGA AAC TGC AGC AGC CAA GTT TGA GCG GC	Hrd1	RF S-Tag-Hrd1 (325-412) fwd
CL448	TCG TCG AGC TGT TTC GGA TCC ATG GAG TCC ATG TGC TGC CGC TCA AAC TTG GCT	Hrd1	RF S-Tag-Hrd1 (325-412) rev
CL449	GGA AGT TCT GTT CCA GGG GCC CAA GGA AAC TGC AGC AGC CAA GTT TGA GCG GC	Doa10	RF S Tag-Doa10 (19-102) fwd
CL450	CCT CGT TTG CCA CGG ATC CCA GGG AGT CCA TGT GCT GCC GCT CAA ACT TGG CT	Doa10	RF S Tag-Doa10 (19-102) rev
CL452	GAA AAA GTC GAC TTA TTC TTC GCC TTC TTC TTC GCC TTC GCC TTC CAC GCT ATC CAC CAC TGA AGC ATC AAA GTG GAC	RNase A	RNase A (42-150)-TUB tag_SalI rev
CL455	GAA AAA GGA TCC AGC ACT TCC GCT GCC	RNase A	BamHI_RNase A (42-150) fwd

4.1.6 Antibodies

Antibody solutions were prepared in TBT buffer (50 mM Tris-HCl pH 7.5, 150 mM NaCl, 0.1 % (v/v) Tween®-20) supplemented with 0.05 % (w/v) NaN_3 and 5 % (w/v) skim milk powder or BSA. Species from which the antibodies were derived are mouse (m), rabbit (rb), goat (g) and donkey (d). All antibodies used in this study are listed in table 4-4.

Table 4-4: Relevant antibodies used in this thesis

Antibody	Dilution	Reference
	Primary antibodies	
Monoclonal α-FLAG (m)	1:2.000	Sigma-Aldrich F3165
Monoclonal α-GAPDH (m)	1:1.000	Sigma-Aldrich G8795
Monoclonal α-HA (m)	1:5.000	Sigma-Aldrich H9658
Monoclonal α-HA (rb)	1:1.000	Cell Signaling Technology C29F4
Monoclonal α-Myc (m)	1:2.000	Sigma-Aldrich M5546
Polyclonal α-Cdc48 (rb)	1:10.000	Neuber *et al.*[43]
Polyclonal α-FLAG (rb)	1:1.000	Cell Signaling Technology 2368S
Polyclonal α-GFP (rb)	1:1.000	Thermo Fisher Scientific A-11122
Polyclonal α-Myc (rb)	1:1.000	MBL International 562
	Secondary antibodies	
IRDye® 680RD α-m IgG (g)	1:10.000	LI-COR 926-68070
IRDye® 800CW α-m IgG (d)	1:10.000	LI-COR 926-32212
IRDye® 800CW α-rb IgG (g)	1:10.000	LI-COR 926-32211
Polyclonal HRP-conjugated α-m IgG (rb)	1:10.000	Sigma-Aldrich A9044
Polyclonal HRP-conjugated α-rb IgG (g)	1:10.000	Sigma-Aldrich A0545

4.2 Methods

4.2.1 Polymerase chain reaction (PCR)

PCR reactions were performed using the Phusion® High-Fidelity DNA Polymerase system (NEB). 150 ng of plasmid DNA or yeast genomic DNA were supplemented with 0.2 µM of forward and reverse oligonucleotides, 200 µM of dNTP's, 10 µl 5x Phusion® HF buffer, 1 µl of Phusion® DNA Polymerase (2U) and ddH_2O ad 50 µl. At first, DNA strands were denaturated for at 98 °C for 2 min. Subsequently, DNA was amplified in 30 cycles of denaturation at 98 °C for 30 s, oligonucleotide annealing at 53 °C for 1 min and DNA strand elongation at 72 °C for 1 min/kB. In a final elongation step at 72 °C for 5 min, immature strand ends were filled.

4.2.2 Site-directed mutagenesis

Point mutations were introduced using the *QuikChange Site-Directed Mutagenesis Kit* (Agilent Technologies) according to the manufacturer's instructions.

Epitope tags were introduced by Restriction-Free (RF) cloning[119].

4.2.3 Cloning, DNA purification and ligation

Amplified DNA fragments and target vectors were digested using restriction enzymes and appropriate buffers from NEB according to the manufacturer's protocol. Digested DNA was supplemented with Purple Gel Loading Dye (6x concentrate, NEB) and separated on agarose gels (1 - 2 % (w/v) agarose in TAE buffer (40 mM Tris-HCl, pH 8.2, 0.14 % (v/v) acetic acid, 1 mM EDTA)). For subsequent UV-mediated detection, the DNA-intercalating fluorophore *RedSafe*™ (iNtRON Biotechnology) was added during agarose gel preparation. Separated DNA fragments and linearized vectors were purified from gels using the *Wizard® SV Gel and PCR Clean-Up System* (Promega) followed by ligation involving T4 DNA ligase (NEB) at 37 °C for 1 h.

4.2.4 *Escherichia coli* (*E. coli*) cell culture

E. coli cells were grown in LB (lysogeny broth) medium (1 % (w/v) Bacto™ Tryptone, 0.5 % (w/v) Bacto™ yeast extract, 1 % (w/v) NaCl) containing appropriate antibiotics (50 µg/ml ampicillin or 25 µg/ml kanamycin) or on solid LB medium plates (LB medium supplemented with 2 % (w/v) agar) for cloning and plasmid amplification purposes. For heterologous expression of target genes, *E. coli* cells were grown in TB (terrific broth) medium (1.2 % (w/v) Bacto™ Tryptone, 2.4 % (w/v) Bacto™ yeast extract, 0.4 % (v/v) glycerol, 17 mM KH_2PO_4, 72 mM K_2HPO_4) containing appropriate antibiotics. The production of perdeuterated proteins for NMR studies was performed in minimal M9/D_2O medium (42,3 mM Na_2HPO_4, 22 mM KH_2PO_4, 17 mM NaCl, 1 mM $MgSO_4$, 100 µM $CaCl_2$, 7.5 µM thiamin, 37 µM $FeCl_3$, 0.4 % (w/v) glucose, 18.4 mM $^{15}NH_4Cl$ solved in 99.9 % D_2O) containing appropriate antibiotics.

4.2.5 *E. coli* transformation

Plasmid DNA was transformed into competent *E. coli* cells by electroporation. Therefore, 50 µl of cells were thawed on ice, supplemented with DNA and transferred to a precooled electroporation cuvette. After a short pulse at 2.5 MV, 25 µF and 200 Ω, cells were taken up in 200 µl of SOC medium (2 % (w/v) Bacto™ Tryptone, 0.5 % (w/v) Bacto™ yeast extract, 10 mM NaCl, 2.5 mM KCl, 10 mM $MgCl_2$, 0.2 % (w/v) glucose) and incubated at 37 °C for 30 min (ampicillin resistance) or 2 h (kanamycin resistance). Afterwards, cells were plated on solid LB medium containing antibiotics for the selection of the desired plamids and incubated at 37 °C overnight. XL1-blue cells were transformed for plasmid amplification. For heterologous expression of target genes BL21-Gold (DE3) cells were used.

4.2.6 Plasmid preparation and sequencing

Single colonies of transformed XL1-blue cells were picked from LB selection plates and inoculated in 3 ml LB medium at 37 °C and 200 rpm overnight. Plasmids were extracted from 2 ml per culture using the *Jetstar™ 2.0 Plasmid Purification Kits* (GENOMED GmbH) according to the manufacturer's instructions. Plasmid DNA was dissolved in 50 µl of ddH_2O and the concentration was measured at a micro-volume spectrophotometer (NanoDrop™ 2000, Thermo Fisher Scientific). For sequencing, the concentration was adjusted according to the recommended sample requirements prior to sample delivery to LGC Genomics GmbH.

4.2.7 Heterologous protein expression in *E. coli*

Transformed BL21-Gold (DE3) cells were grown in 50 ml LB medium at 37 °C and 200 rpm overnight. Overnight cultures were used to inoculate M9 or TB medium (typically, 2 l, starting OD_{600} of 0.1) which were then shaken at 37 °C and 90 rpm until an OD_{600} of 0.6 - 0.8 or 1 - 1.5, respectively was reached. Subsequently, cells were cooled to 16 °C for 30 min prior to induction of protein expression by addition of 1 mM IPTG. After 16 - 18 h, cells were harvested by centrifugation (6,000 x g, 30 min, 4 °C), washed with ddH_2O, transferred to 50 ml Falcon tubes and frozen in liquid nitrogen. Pellets were stored at -80 °C until further use.

4.2.8 *Saccharomyces cerevisiae* cell culture

Yeast cells were grown in YPD (yeast peptone dextrose) medium (2 % (w/v) Bacto™ Peptone, 1 % (w/v) Bacto™ yeast extract, 2 % (w/v) glucose, pH adjusted to 5.5 with HCl ± 250 µg/ml geneticin (G418)) or minimal SD (synthetic defined) medium (0.67 % (w/v) yeast nitrogen base without amino acids, 2 % (w/v) glucose, 20 mg/l adenine sulfate, 30 mg/l L-leucine, 30 mg/l L-lysine, 20 mg/l L-histidine, 20 mg/l L-tryptophan, 20 mg/l uracil). To prepare solid medium plates, above mentioned media were supplemented with 2 % (w/v) agar. For auxotrophic selection of plasmids or gene deletions, designated amino acids were left out when preparing SD medium.

4.2.9 Yeast transformation

For plasmid transformation, 1 OD_{600} of logarithmic growing yeast cells were harvested by centrifugation (2,000 x g, 3 min). The pellet was resuspended in 100 µl of transformation buffer A (10 mM Tris-HCl, pH 7.4, 1 mM EDTA, 100 mM LiOAc). 1 µg of plasmid DNA and denatured herring sperm DNA at a final concentration of 0.2 µg/µl were added. The solution was supplemented with 500 µl of transformation buffer B (10 mM Tris-HCl, pH 7.4, 1 mM EDTA, 100 mM LiOAc, 40 % (v/v) PEG 3350) and incubated at 30 °C for 30 min. After a heat shock at 42 °C for 15 min, cells were pelleted (2,000 x g, 3 min), resuspended in 100 µl of ddH_2O and plated on SD selection medium.

For genomic integration of amplified PCR fragments, the protocol was slightly changed. 25 OD_{600} of logarithmic growing cells were harvested and washed in 1 ml of transformation buffer A. The cell pellet was resuspended in 200 µl of buffer A and supplemented with denatured herring sperm DNA. PCR-amplified DNA was precipitated by addition of 400 mM NaOAc and 2.5 volumes of ethanol and centrifugation (20,000 x g, 15 min, 4 °C). The DNA pellet was resuspended in 15 µl of ddH_2O and added to the transformation solution. The solution was supplemented with 800 µl of transformation buffer B and incubated at 30 °C for 30 min. After heat shocking at 42 °C for 15 min, cells were either incubated for another 2 h at 30 °C to develop a resistance against G418 or for 30 min at 30 °C if auxotrophic marker cassettes were used. Following this regeneration step, 200 µl of the suspension were plated on YPD-G418 or SD selection medium, respectively.

4.2.10 Preparation of genomic yeast DNA

Yeast cells were inoculated in 3 ml YPD medium at 30 °C and 200 rpm overnight. Genomic DNA was extracted from 2 ml per culture (5 - 10 OD_{600}). Cells were harvested by centrifugation (2,000 x g, 3 min) and washed with 1 ml of ddH_2O. The cell pellet was resuspended in 200 µl of DNA extraction buffer (10 mM Tris-HCl, pH 8.0, 100 mM NaCl, 1 mM EDTA, 1 % (w/v) SDS, 2 % (v/v) Triton X-100). The suspension was supplemented with a mixture of phenol:chloroform:isoamyl alcohol (25:24:1). Glass beads were added and mechanical lysis was performed by vigorous shaking on a Vibrax VXR basic for 5 min. The lysate was diluted with 200 µl of TE buffer (10 mM Tris-HCl, pH 7.4, 1 mM EDTA) and centrifuged (20,000 x g, 5 min) for phase separation. The upper aqueous was transferred to a fresh tube containing 1 ml of cold ethanol and centrifuged (20,000 x g, 15 min, 4 °C) to precipitate nucleic acids. The resulting pellet was resuspended in 400 µl of TE buffer. To digest precipitated RNA, 30 µg of RNase A (Roth) were added and the solution was incubated at 37 °C for 5 min. DNA was precipitated by addition of ammonium acetate (final concentration 100 mM) and 1 ml of cold ethanol followed by centrifugation (20,000 x g, 15 min, 4 °C). The pellet was dried at room temperature and resuspended in 100 µl of ddH_2O.

4.2.11 Yeast strain crossing

Haploid yeast strains of different mating types (*MATa* or *MATα*) were inoculated in 3 ml YPD medium overnight. 500 µl of each culture were mixed in a tube bearing a small hole in its lid for oxygen supply. The cell suspension was incubated under constant stirring at room temperature for 4 - 5 h. Sedimented (diploid) cells were plated on SD plates selecting for auxotrophy markers from both initial haploid strains allowing only diploid cells to grow. After two days of incubation at 30 °C, diploid yeast cells were inoculated in 3 ml YPD medium overnight. 200 µl of this culture were supplemented with 3 ml of nutrient-rich pre-sporulation medium (0.3 % (w/v) Bacto™ Peptone, 0.8 % (w/v) Bacto™ yeast extract, 10 % (w/v) glucose) and incubated for at 30 °C and 200 rpm for 4 h. To initiate sporulation, 2 ml of this culture were harvested by centrifugation (2,000 x g, 3 min), washed twice with ddH_2O, resuspended in 3 ml of nutrient-poor sporulation medium (0.1 % (w/v) Bacto™ yeast extract, 0.05 % (w/v) glucose, 1 % (w/v) KOAc) and incubated for up to 4 days at 30 °C and 200 rpm.

Sporulation efficiency was checked using an optical microscope (Zeiss). For tetrad dissection, 1 ml of the sporulation reaction was harvested (2,000 x g, 3 min) and resuspended in 1ml of SED medium (18.2 % (w/v) sorbitol, 25 mM EDTA). 200 µl of this suspension were supplemented with 50 mM DTT and 200 µg zymolyase (MP Biomedicals) and incubated at room temperature for 20 min to digest the ascus wall. Subsequently, a small amount of this suspension was spread on a YPD plate using an inoculation loop. Individual spores of a tetrade were dissected at a micromanipulator (Singer Instruments). After 2 days of incubation at 30 °C, spores were analyzed regarding their genotype by replica plating on appropriate selection plates.

4.2.12 SDS-PAGE

Complex protein samples were analyzed using sodium dodecyl sulfate-polyacrylamide gel electrophoresis (SDS-PAGE)[120]. According to their molecular weight, proteins were separated in an electric field using gel electrophoresis systems (Hoefer Inc.) filled with Laemmli running buffer (LRB) (25 mM Tris, 192 mM glycine, 0.1 % (w/v) SDS). Therefore, proteins were focused in a 3 % stacking gel (125 mM Tris-HCl, pH 6.8, 3 % (v/v) acrylamide, 0.15 % (v/v) bisacrylamide, 0.1 % (w/v) SDS, 0.25 % (v/v) TEMED, 2.5 % (w/v) APS) at 80 V for 30 min. Subsequently, proteins were separated in 12 % or 18 % separating gels (500 mM Tris-HCl, pH 8.8, 12 % or 18 % (v/v) acrylamide, 0.006 or 0.009 % (v/v) bisacrylamide, 0.1 % (w/v) SDS, 0.25 % (v/v) TEMED, 2.5 % (w/v) APS) at 120 V until the buffer front reached the end of the gel. For protein detection, gels were subjected to Coomassie staining, fluorescence scanning, autoradiography or western blotting. To determine the molecular weight of detected proteins, a protein marker (*Color Prestained Protein Standard, Broad Range* (11 - 245 kDa), NEB) was applied to gels before electrophoresis.

4.2.13 Coomassie staining

To detect all proteins in complex protein mixtures, gels were incubated with Coomassie staining solution (10 % (v/v) acetic acid, 40 % (v/v) methanol, 0.25 % (w/v) Coomassie Brilliant Blue R-250) at room temperature for 30 min. Destaining was achieved either in ddH_2O, overnight or in destaining solution (10 % (v/v) acetic acid, 40 % (v/v) methanol) for several hours until stained proteins were clearly visible. The detection limit of Coomassie Brilliant Blue R-250 ranges around 0.2 - 0.5 µg of protein.

4.2.14 Fluorescence scanning

Alexa Fluor 488-labeled proteins were detected directly from SDS-PAGE gels. Therefore, the fluorophore was excited at 473 nm and emission was detected at 510 nm with a LPB filter (510LP) using a Typhoon FLA 9500 laser scanner (GE Healthcare). Fluorescent signals were quantified in ImageQuant TL 7.01 (GE Healthcare).

4.2.15 Autoradiography

Radioisotope-labeled substrates were visualized by autoradiography. Therefore, samples were fixed by incubating SDS-PAGE gels in 10 % (v/v) acetic acid. Gels were washed with ddH_2O and dried in a Model 583 gel dryer (Bio-Rad Laboratories, Inc.). Signals were transferred to BAS Storage Phosphor Screens (GE Healthcare) and detected using a Typhoon FLA 9500 laser scanner. Radioactive signals were quantified in ImageQuant TL 7.01.

4.2.16 Western Blotting/Immunoblotting

For the detection of selected proteins in complex samples separated proteins from SDS-PAGE gels were transferred to PVDF membranes (pore size 0.45 µm, Roth). To this ends, gels were placed on methanol-activated membranes and embedded in Whatman-paper. This assembly was placed in a TE22 Mighty Small Transfer Tank (Hoefer Inc.) filled with transfer buffer (25 mM Tris, 192 mM glycine, 15 % (v/v)

isopropanol). Transfer onto membranes was achieved by applying an electric current of 250 mA for 90 min. After the blotting procedure, unspecific binding sites were blocked by incubating the membranes at room temperature for 30 min in blocking solution (5 % (w/v) skim milk powder or BSA in TBT (50 mM Tris-HCl, pH 7.5, 150 mM NaCl, 0.1 % (v/v) Tween®-20). Primary antibody solutions were prepared as described (4.1.6) and applied to membranes prior to incubation at 4 °C overnight. Membranes were washed three times with 20 ml TBT and three times with 20 ml PBS (137 mM NaCl, 2.7 mM KCl, 10.1 mM Na_2HPO_4, 1.8 mM KH_2PO_4) for 10 min, each. Secondary antibody solutions were prepared as before and applied to membranes at room temperature for 1 h. After another washing procedure as described above, signals were detected either by application of *Western Lightning® Plus-ECL, Enhanced Chemiluminescence Substrate* (PerkinElmer, Inc.) for HRP-conjugated secondary antibodies or by instant scanning for fluorophore-conjugated IRDye® secondary antibodies (LI-COR Biosciences), both using an Odysee® Fc imaging system (LI-COR Biosciences). Fluorescent signals were quantified in Image Studio Lite 5.0 (LI-COR Biosciences).

4.2.17 *E. coli* cell lysis

Frozen cell pellets were thawed on ice and resuspended in 30 ml lysis buffer (50 mM Tris-HCl, pH 7.5, 150 mM NaCl, 1mM PMSF, 0.4 mg/ml lysozyme, 5 µg/ml DNase, 10 µg/ml RNase). Lysis was done by high pressure homogenization, passing the cell suspension three times through an EmulsiFlex-C5 homogenizer (AVESTIN Europe, GmbH) (4 °C, 1500 bar). The lysate was cleared by centrifugation (20,000 x g, 30 min, 4 °C).

4.2.18 Purifcation of GST-tagged proteins

Genes coding for Glutathione S-transferase (GST)-tagged proteins harbored a *Human Rhinovirus* (HRV) 3C protease cleavage site between the epitope and the target protein. All of the following steps were performed on ice or at 4 °C. Lysates of GST-tagged fusion proteins were supplemented with *Glutathione Sepharose® 4 Fast Flow* (GE Healthcare) (typically 2 ml slurry per liter of TB medium used for expression) and incubated for 4 h under constant shaking. Sepharose was washed 5

times with 15 ml of protease inhibitor-free lysis buffer. To elute bound proteins from the resin, self-made GST-tagged HRV 3C protease was added prior to overnight incubation. On the following day, the supernatant was collected and incubated with fresh sepharose for another hour to remove excess protease. After removing the resin, the protein solution was concentrated to 500 µl in centrifugal filters (*Amicon® Ultra*, Merck Millipore, MWCO corresponding to about 1/3 of the predicted MW of the target protein) and further purified by size exclusion chromatography (*Superdex™ 75 Increase 10/300 GL*, GE Healthcare) in SEC buffer (50 mM Tris-HCl, pH 7.5, 150 mM NaCl) using an ÄKTA™ pure chromatography system (GE Healthcare). Fractions containing the target protein, as judged by absorbance at 280 nm as well as SDS-PAGE and Coomassie staining, were pooled, concentrated, frozen in liquid nitrogen and stored at -80 °C until further use.

4.2.19 Purification of His_6-tagged proteins

Most hexa histidine (His_6)-tagged proteins were fused to SUMO3 (human small ubiquitin-related modifier 3) to increase solubility and expression. All of the following steps were performed on ice or at 4 °C. Lysates of those fusion proteins were supplemented with *Ni-NTA Agarose* (Qiagen) and incubated for 4 h under constant shaking. Agarose was washed 5 times with 15 ml of wash buffer (50 mM Tris-HCl, pH 7.5, 150 mM NaCl, 20 mM imidazole). To elute bound proteins from the resin, self-made His_6-tagged Ulp1 (yeast protease cleaving SUMO3 from target proteins) was added prior to overnight incubation. From here on, the supernatant was treated as described before (4.2.2.7).

The E1 enzyme (Uba1-His_6) was purified with a slightly changed protocol. During the whole procedure, the cell pellet and lysate were kept in 2 x PBS (274 mM NaCl, 5.4 mM KCl, 20.2 mM Na_2HPO_4, 3.6 mM KH_2PO_4). The lysate was applied to a *HisTrap™ Fast Flow Crude* column (GE Healthcare) using an ÄKTA™ pure. The column was washed with 10 column volumes of 2 x PBS including 20 mM Imidazol. Bound proteins were eluted by application of 2 x PBS containing 300 mM Imidazol. Size exclusion chromatography was performed on a *HiLoad™ 16/60 Superdex™ 200 prep grade*.

The purification of Ub-His_6 is described in section 4.2.2.9.

4.2.20 Purification of ubiquitin monomers.

Untagged ubiquitin monomers were purified by acidic precipitation. The stable fold of ubiquitin protected it from precipitation while other *E. coli* proteins aggregated. 300 µl of 70 % (v/v) perchloric acid were titrated to 30 ml of cleared cell lysates under vigorous stirring on ice. The precipitate was removed by centrifugation (20,000 x g, 20 min, 4 °C). The pH of the supernatant was adjusted to neutral range by addition of 10 M NaOH. The supernatant was concentrated to 2 ml and applied to a *HiLoad™ 26/60 Superdex™ 75 prep grade* size exclusion column in SEC buffer. Fractions were collected as described in 4.2.2.7.

Ub-His_6 was purified using *HisTrap™ Fast Flow Crude* columns equilibrated in lysis buffer. Columns were washed with lysis buffer containing 20 mM Imidazol. Proteins were eluted in lysis buffer containing 300 mM Imidazol. SEC was performed as described above.

The Ub^{S20C} variant was purified as before except for using 1 x PBS buffer during SEC.

4.2.21 Lowry protein assay

Protein concentration was determined based on the method established by Lowry[121]. Therefore, the *DC™ Protein Assay* (Bio-Rad Laboratories, Inc.) was used. A BSA concentration gradient served as standard curve to determine concentrations by measuring absorbance at 750 nm.

4.2.22 Synthesis and purification of K48-linked ubiquitin chains

Ubiquitin chains linked through lysine48 were enzymatically assembled on C-terminally blocked Ub-His_6. *In vitro* reactions included 1 µM E1, 20 µM Cdc34, 900 µM Ub, 600 µM Ub-His_6 in chain synthesis buffer (50 mM Tris-HCl, pH 8.0, 9 mM $MgCl_2$, 0.9 mM DTT, 20 mM ATP) and were performed by incubation at 37 °C overnight. His_6-tagged chains were enriched using *Ni-NTA Agarose*, concentrated to 2 ml and further purified by SEC (*HiLoad™ 26/60 Superdex™ 75 prep grade*) in SEC buffer. Chains of specific length were collected as described before (4.2.2.7).

4.2.23 Fluorescent labeling of Ub^{S20C}

Since Ub does not harbor any endogenous thiol groups, introduction of a cysteine at amino acid position 20 allowed for site-specific labeling of Ub with *Alexa Fluor™ 488 C_5 Maleimide* (Thermo Fisher Scientific). In a first step, the thiol group of Ub was reduced by addition of three-fold molar excess of TCEP in 1 x PBS at room temperature for 10 min. Subsequently, four-fold molar excess of fluorescent dye was added and the labeling reaction was performed at room temperature for 90 min in the dark. The reaction was quenched by addition of 10 mM β-mercaptoethanol and the labeling mix was desalted in two steps using *NAP™-5 columns* equilibrated in 50 mM Tris-HCl, pH 8.0 to remove excess reducing agent and dye. The eluate was concentrated to 300 µl. Labeling efficiency was determined by the ratio of dye concentration (absorbance at 493 nm) and protein concentration (4.2.2.10). Labeled Ub^{488} was stored at -80 °C until further use.

4.2.24 Fluorescent labeling of S protein

The S protein was modified with 3-Azido-L-tyrosine (Iris Biotech GmbH) by use of the previously reported TUB-tag labeling approach[76]. Therefore, 75 µM of the S protein were mixed with 1.8 mM of 3-Azido-L-tyrosine, 5 µM of tubulin tyrosine ligase (TTL), 2.5 mM ATP and 5 mM GSH in TTL buffer (20 mM MES, pH 7.0, 100 mM KCl, 10 mM $MgCl_2$) and incubated for two hours at 37 °C. Unconjugated 3-Azido-L-tyrosine was removed by SEC on a *HiTrap™ Desalting column* (GE Healthcare). Protein-carrying fractions were pooled, concentrated to 300 µl and protein concentration was determined as before (4.2.2.10). Subsequently, strain-promoted azide-alkyne cycloaddition[77] (SPAAC) was initiated by addition of dibenzocyclooctyne (DBCO)-strained *Alexa Fluor™* 488 (Jena Bioscience) in 30-fold molar excess and incubation at 30 °C for four hours. After another desalting step, labeled S $protein^{488}$ was treated as described before for Ub^{488} (4.2.2.12).

4.2.25 Reconstituted ubiquitination reactions involving purified components

Discharge assays were performed in two subsequent steps. Charging reactions included 33 µM of the designated E2 (Ubc6 or U7BR/Ubc7), 132 µM Ub (Ub^{WT} for Ubc6 or Ub^{K48R} for U7BR/Ubc7), 3.3 µM or 0.55 µM E1 (for Ubc6 or U7BR/Ubc7, respectively), 5 mM ATP and 5 mM $MgCl_2$ in PBS. Reactions were incubated at 37 °C (3 min for Ubc6 or 2.5 min for U7BR/Ubc7), quenched by addition of 50 mM EDTA and discharge was started by dilution into ethanolamine (in PBS, final concentration of 100 mM) in absence or presence of E3 RING domains (final concentration 30 µM Doa10 variants for either enzyme, 45 µM Hrd1 variants for Ubc6 and 10 µM Hrd1 variants for U7BR/Ubc7). Discharge reactions were incubated at room temperature or 37 °C (for U7BR/Ubc7 and Doa10). Samples were collected after 0, 1, 2.5, 6 and 15.5 min in non-denaturing sample buffer (125 mM Tris-HCl, 8 % (w/v) SDS, 25 % (v/v) glycerol, 0.05 % (w/v) bromophenol blue) and analyzed by SDS-PAGE and Coomassie staining.

Single-turnover chain elongation reactions included 0.15 µM E1, 2 µM Cue1 (WT/RGA), 2 µM Ubc7, 2 µM RING domain variants (Hrd1/Doa10), 14.8 µM acceptor Ub (His_6-blocked mono-Ub/Ub chains) and 0.2 µM donor Ub (fluorescent Ub^{488}) in *in vitro* reaction buffer (50 mM Tris-HCl, pH 8.0, 4 mM $MgCl_2$, 0.5 mM DTT). Reactions were started by addition of 4 mM ATP and incubated at 30 °C. 15 µl samples were collected after 0, 1, 2, 3, 4, 5, 10, 30 and 60 min. Reactions were stopped with urea sample buffer (4 x concentrate: 200 mM Tris-HCl, pH 6.8, 8 M urea, 5 % (w/v) SDS, 0.1 mM EDTA, 1.5 % (w/v) DTT, 0.03 % (w/v) bromophenol blue) at the indicated time points. Samples were analyzed by SDS-PAGE and fluorescence scanning.

Ubiquitination reactions on the S protein included 0.3 µM E1, 5 µM E2 (Ubc4, Ubc6 or Cue1/Ubc7), 5 µM RING variants (Hrd1/Doa10, S peptide-tagged or untagged), 5 µM S $protein^{488}$ and 50 µM Ub^{WT} in *in vitro* reaction buffer. Reactions were started by addition of 4 mM ATP and incubated at 30 °C for 30 min. Reactions were stopped with urea sample buffer and analyzed by SDS-PAGE and fluorescence scanning.

4.2.26 NMR titration experiments

E2~Ub conjugates were prepared prior to NMR measurements. Therefore, Ub^{G76C} was activated by supplementation with a 5-fold molar excess of DTNB and incubated on ice for 5 min. Subsequently, the reaction was desalted by SEC. Conjugates were formed by addition of a 2-fold molar excess of Ub^{G76C}-TNB to the designated E2 enzymes and incubation for 30 min at room temperature. Conjugates were purified by SEC (*Superdex™ 75 Increase 10/300 GL*, GE Healthcare) in NMR buffer (25 mM Na_2HPO_4, pH 7.0, 150 mM NaCl, 10 % D2O).

Heteronuclear single quantum coherence-transverse relaxation-optimized spectroscopy (HSQC-TROSY) measurements were conducted with 200 µM labeled proteins at 295 K. Data was collected on a 500 MHz Bruker Avance II (University of Washington), processed using NMR-Pipe and visualized with NMRView.

4.2.27 Pulse-chase assay

Degradation of Hrd1-dependent model substrates PrA*-3xHA and Hmg2-6xMyc was observed in yeast cells by pulse-chase analysis. Therefore, 15 OD_{600} (5 OD_{600} per time point) of logarithmic growing cells were harvested (2,000 x g, 3 min) and resuspended in 1 ml SD selective medium. Newly synthesized proteins were labeled with radioisotopes by addition of 3 MBq *EasyTag™ EXPRESS^{35}S Protein Labeling Mix* (PerkinElmer, Inc.) and incubation at 30 °C for 8 min. Cells were pelleted (8.000 x g, 30 s), resuspended in 3.5 ml of label-free chase mix (SD medium, 3.3 mM $(NH_4)_2SO_4$, 0.013 % (w/v) L-methionine, 0.01 % (w/v) L-cysteine) and incubated at 30 °C. At designated time points (0, 45, 90 min for PrA*-3xHA and 0, 90, 180 min for Hmg2-6xMyc) 1 ml samples were collected and degradation was stopped by addition of 10 mM NaN_3. Cells were harvested (8,000 x g, 30 s) and resuspended in 100 µl lysis buffer (50 mM Tris-HCl, pH 7.5, 1 % (w/v) SDS, 1 mM PMSF). Glass beads were added and mechanical lysis was performed by vigorous shaking. The lysates were supplemented with 1 ml IP dilution buffer (50 mM Tris-HCl, pH 7.5, 165 mM NaCl, 5.5 mM EDTA, 1.1 % (v/v) Triton X-100) and incubated on ice for 30 min. After removing cell debris and glass beads by centrifugation (15,000 x g, 10 min, 4 °C), the supernatants were transferred to fresh tubes. To enrich for desired substrate proteins, 15 µl magnetic beads were added (*Pierce™ Anti-HA Magnetic Beads* for

PrA*-3xHA or *Pierce™ Anti-c-Myc Magnetic Beads* for Hmg2-6xMyc, Thermo Fisher Scientific) prior to overnight incubation at 4 °C under constant shaking. The next day, beads were washed three times with 1 ml IP buffer (50 mM Tris-HCl, pH 7.5, 150 mM NaCl, 5 mM EDTA, 0.1 % (w/v) SDS, 1 % (v/v) Triton X-100). Anti-HA beads were additionally treated with 10 µl deglycosylation mix (IP buffer, 1 % (v/v) β-mercaptoethanol, 0.4 U *PNGase F* (Roche)) for 1 h at 37 °C. Beads were supplemented with 20 µl SDS sample buffer (2x concentrate: 125 mM Tris/HCl, pH 6.8, 4 % (w/v) SDS, 20 % (v/v) glycerol, 0.1 % (w/v) bromophenol blue, 100 mM DTT), incubated for 15 min at 65 °C and analyzed by SDS-PAGE and autoradiography.

4.2.28 Cycloheximide decay assay

Degradation of Doa10-dependent model substrates FLAG-Sbh2 and Deg1-eGFP$_2$ was observed in yeast cells by cycloheximide decay assays. Therefore, 20 OD_{600} of logarithmic growing cells were harvested (2,000 x g, 3 min), resuspended in 4.5 ml SD selective medium and incubated at 30 °C. Protein translation was inhibited by addition of 0.33 mg/ml cycloheximide. At designated time points (0, 10, 20, 40 min for FLAG-Sbh2 and 0, 30, 60, 120 min for Deg1-eGFP$_2$) 1 ml samples were collected and degradation was stopped by addition of 10 mM NaN_3. Cells were harvested (20,000 x g, 2 min) and resuspended in 100 µl lysis buffer (50 mM Tris-HCl, pH 7.5, 1 % (w/v) SDS, 1 mM PMSF). Glass beads were added and mechanical lysis was performed by vigorous shaking. The lysates were supplemented with 80 µl SDS sample buffer (4x concentrate: 250 mM Tris-HCl, pH 6.8, 8 % (w/v) SDS, 40 % (v/v) glycerol, 0.2 % (w/v) bromophenol blue, 100 mM DTT) and incubated for 15 min at 65 °C. Cell debris and glass beads were removed by centrifugation (1,000 x g, 5 min) and the supernatants were transferred to fresh tubes. Samples were analyzed by SDS-PAGE and western blotting.

4.2.29 Non-denaturing immunoprecipitation

Yeast cells were grown to an OD_{600} of 1 - 1.5 in SD selective medium. 100 OD_{600} of cells were harvested (2,000 x g, 3 min), washed with 10 ml of cold ddH_2O (containing 1 mM PMSF) and resuspended in 1 ml IP15 buffer (50 mM Tris-HCl, pH 7.5, 480 mM KOAc, 1 mM EDTA, 10 % (v/v) glycerol). The suspension was transferred to a 2 ml tube, pelleted (2,000 x g, 3 min) and resuspended in 400 µl IP15 buffer. Glass beads were added and mechanical lysis was performed by vigorous shaking. The lysates were supplemented with 1 ml IP15 buffer and cell debris was removed (1,000 x g, 5 min). The supernatant was transferred to a 1 ml tube and membranes were pelleted (20,000 x g, 20 min). The membrane pellet was gently solubilized in IP15 buffer containing 1 % (w/v) LMNG and incubated for 1 h at 4 °C. The lysate was cleared (20,000 x g, 10 min) and the supernatant was transferred to a new 1 ml tube. 45 µl of lysate were removed and supplemented with 15 µl SDS sample buffer (4x concentrate: 250 mM Tris-HCl, pH 6.8, 8 % (w/v) SDS, 40 % (v/v) glycerol, 0.2 % (w/v) bromophenol blue, 100 mM DTT) as a loading control sample. The remaining lysate was diluted with an equal amount of IP15 buffer and supplemented with 30 µl of magnetic beads conjugated with antibodies directed against the desired epitope tags (HA/Myc/FLAG for 3xHA-Asi, 3xMyc-Asi2 and 3xFLAG-Asi3) prior to incubation overnight at 4 °C. The next day, beads were washed three times with 1 ml IP15 buffer. Beads were supplemented with 50 µl SDS sample buffer (1x concentrate: 62.5 mM Tris/HCl, pH 6.8, 2 % (w/v) SDS, 10 % (v/v) glycerol, 0.05 % (w/v) bromophenol blue, 100 mM DTT), incubated for 15 min at 65 °C and analyzed by SDS-PAGE and western blotting.

5. Appendix

5.1 Bibliography

1. Schlesinger DH, Goldstein G, Niall HD. Complete amino acid sequence of ubiquitin, an adenylate cyclase stimulating polypeptide probably universal in living cells. *Biochemistry*. 1975;14(10):2214-2218. doi:10.1021/bi00681a026

2. Hershko A, Ciechanover A, Rose IA. Resolution of the ATP-dependent proteolytic system from reticulocytes: a component that interacts with ATP. *Proc Natl Acad Sci*. 1979;76(7):3107-3110. doi:10.1073/pnas.76.7.3107

3. Hershko A, Ciechanover A, Heller H, Haas AL, Rose IA. Proposed role of ATP in protein breakdown: conjugation of protein with multiple chains of the polypeptide of ATP-dependent proteolysis. *Proc Natl Acad Sci*. 1980;77(4):1783-1786. doi:10.1073/pnas.77.4.1783

4. Hershko A, Ciechanover A, Rose IA. Identification of the active amino acid residue of the polypeptide of ATP-dependent protein breakdown. *J Biol Chem*. 1981;256(4):1525-1528. http://www.ncbi.nlm.nih.gov/pubmed/6257674.

5. Hetz C. The unfolded protein response: controlling cell fate decisions under ER stress and beyond. *Nat Rev Mol Cell Biol*. 2012;13(2):89-102. doi:10.1038/nrm3270

6. Thibaudeau TA, Smith DM. A Practical Review of Proteasome Pharmacology. Ma Q, ed. *Pharmacol Rev*. 2019;71(2):170-197. doi:10.1124/pr.117.015370

7. Finley D, Ulrich HD, Sommer T, Kaiser P. The Ubiquitin–Proteasome System of Saccharomyces cerevisiae. *Genetics*. 2012;192(2):319-360. doi:10.1534/genetics.112.140467

8. Kerscher O, Felberbaum R, Hochstrasser M. Modification of Proteins by Ubiquitin and Ubiquitin-Like Proteins. *Annu Rev Cell Dev Biol*. 2006;22(1):159-180. doi:10.1146/annurev.cellbio.22.010605.093503

9. Kostova Z, Tsai YC, Weissman AM. Ubiquitin ligases, critical mediators of endoplasmic reticulum-associated degradation. *Semin Cell Dev Biol*. 2007;18(6):770-779. doi:10.1016/j.semcdb.2007.09.002

10. O'Connor HF, Lyon N, Leung JW, et al. Ubiquitin-Activated Interaction Traps (UBAITs) identify E3 ligase binding partners. *EMBO Rep*. 2015;16(12):1699-1712. doi:10.15252/embr.201540620

11. Metzger MB, Hristova VA, Weissman AM. HECT and RING finger families of E3 ubiquitin ligases at a glance. *J Cell Sci*. 2012;125(3):531-537. doi:10.1242/jcs.091777

12. Wenzel DM, Klevit RE. Following Ariadne's thread: a new perspective on RBR ubiquitin ligases. *BMC Biol*. 2012;10(1):24. doi:10.1186/1741-7007-10-24

13. Dove KK, Stieglitz B, Duncan ED, Rittinger K, Klevit RE. Molecular insights into RBR E3 ligase ubiquitin transfer mechanisms. *EMBO Rep*. 2016;17(8):1221-1235. doi:10.15252/embr.201642641

14. Dove KK, Klevit RE. RING-Between-RING E3 Ligases: Emerging Themes amid the Variations. *J Mol Biol*. 2017;429(22):3363-3375. doi:10.1016/j.jmb.2017.08.008

15. Smit JJ, Sixma TK. RBR E3-ligases at work. *EMBO Rep*. 2014;15(2):142-154. doi:10.1002/embr.201338166

16. Amerik AY, Li S-J, Hochstrasser M. Analysis of the Deubiquitinating Enzymes of the Yeast Saccharomyces cerevisiae. *Biol Chem*. 2000;381(9-10). doi:10.1515/BC.2000.121

17. Mansour W, Nakasone MA, von Delbrück M, et al. Disassembly of Lys 11 and Mixed Linkage Polyubiquitin Conjugates Provides Insights into Function of Proteasomal Deubiquitinases Rpn11 and Ubp6. *J Biol Chem*. 2015;290(8):4688-4704. doi:10.1074/jbc.M114.568295

18. Leznicki P, Kulathu Y. Mechanisms of regulation and diversification of deubiquitylating enzyme function. *J Cell Sci*. 2017;130(12):1997-2006. doi:10.1242/jcs.201855

19. Tokarev AA, Munguia J, Guatelli JC. Serine-Threonine Ubiquitination Mediates Downregulation of BST-2/Tetherin and Relief of Restricted Virion Release by HIV-1 Vpu. *J Virol*. 2011;85(1):51-63. doi:10.1128/JVI.01795-10

20. Weber A, Cohen I, Popp O, et al. Sequential Poly-ubiquitylation by Specialized Conjugating Enzymes Expands the Versatility of a Quality Control Ubiquitin Ligase. *Mol Cell*. 2016;63(5):827-839. doi:10.1016/j.molcel.2016.07.020

21. Breitschopf K, Bengal E, Ziv T, Admon A, Ciechanover A. A novel site for ubiquitination: the N-terminal residue, and not internal lysines of MyoD, is essential for conjugation and degradation of the protein. *EMBO J*. 1998;17(20):5964-5973. doi:10.1093/emboj/17.20.5964

22. Carvalho AF, Pinto MP, Grou CP, et al. Ubiquitination of Mammalian Pex5p, the Peroxisomal Import Receptor. *J Biol Chem*. 2007;282(43):31267-31272. doi:10.1074/jbc.M706325200

23. Wauer T, Simicek M, Schubert A, Komander D. Mechanism of phospho-ubiquitin-induced PARKIN activation. *Nature*. 2015;524(7565):370-374. doi:10.1038/nature14879

24. Ohtake F, Saeki Y, Sakamoto K, et al. Ubiquitin acetylation inhibits polyubiquitin chain elongation. *EMBO Rep*. 2015;16(2):192-201. doi:10.15252/embr.201439152

25. Hendriks IA, D'Souza RCJ, Yang B, Verlaan-de Vries M, Mann M, Vertegaal ACO. Uncovering global SUMOylation signaling networks in a site-specific manner. *Nat Struct Mol Biol*. 2014;21(10):927-936. doi:10.1038/nsmb.2890

26. Komander D, Rape M. The Ubiquitin Code. *Annu Rev Biochem*. 2012;81(1):203-229. doi:10.1146/annurev-biochem-060310-170328

27. Swatek KN, Komander D. Ubiquitin modifications. *Cell Res*. 2016;26(4):399-422. doi:10.1038/cr.2016.39

28. Yau R, Rape M. The increasing complexity of the ubiquitin code. *Nat Cell Biol*. 2016;18(6):579-586. doi:10.1038/ncb3358

29. Dikic I, Wakatsuki S, Walters KJ. Ubiquitin-binding domains — from structures to functions. *Nat Rev Mol Cell Biol*. 2009;10(10):659-671. doi:10.1038/nrm2767

30. Balchin D, Hayer-Hartl M, Hartl FU. In vivo aspects of protein folding and quality control. *Science (80-)*. 2016;353(6294):aac4354. doi:10.1126/science.aac4354

31. Chiti F, Dobson CM. Protein Misfolding, Amyloid Formation, and Human Disease: A Summary of Progress Over the Last Decade. *Annu Rev Biochem*. 2017;86(1):27-68. doi:10.1146/annurev-biochem-061516-045115

32. Stevenson J, Huang EY, Olzmann JA. Endoplasmic Reticulum–Associated Degradation and Lipid Homeostasis. *Annu Rev Nutr*. 2016;36(1):511-542. doi:10.1146/annurev-nutr-071715-051030

33. Ruggiano A, Foresti O, Carvalho P. ER-associated degradation: Protein quality control and beyond. *J Cell Biol*. 2014;204(6):869-879. doi:10.1083/jcb.201312042

34. Gauss R, Jarosch E, Sommer T, Hirsch C. A complex of Yos9p and the HRD ligase integrates endoplasmic reticulum quality control into the degradation machinery. *Nat Cell Biol*. 2006;8(8):849-854. doi:10.1038/ncb1445

35. Horn SC, Hanna J, Hirsch C, et al. Usa1 Functions as a Scaffold of the HRD-Ubiquitin Ligase. *Mol Cell*. 2009;36(5):782-793. doi:10.1016/j.molcel.2009.10.015

36. Mehnert M, Sommer T, Jarosch E. Der1 promotes movement of misfolded proteins through the endoplasmic reticulum membrane. *Nat Cell Biol*. 2014;16(1):77-86. doi:10.1038/ncb2882

37. Biederer T, Volkwein C, Sommer T. Role of Cue1p in ubiquitination and degradation at the ER surface. *Science (80-)*. 1997;278(5344):1806-1809. doi:10.1126/science.278.5344.1806

38. Bazirgan OA, Hampton RY. Cue1p Is an Activator of Ubc7p E2 Activity in Vitro and in Vivo. *J Biol Chem*. 2008;283(19):12797-12810. doi:10.1074/jbc.M801122200

39. Ravid T, Hochstrasser M. Autoregulation of an E2 enzyme by ubiquitin-chain assembly on its catalytic residue. *Nat Cell Biol*. 2007;9(4):422-427. doi:10.1038/ncb1558

40. Metzger MB, Liang YH, Das R, et al. A Structurally Unique E2-Binding Domain Activates Ubiquitination by the ERAD E2, Ubc7p, through Multiple Mechanisms. *Mol Cell*. 2013;50(4):516-527. doi:10.1016/j.molcel.2013.04.004

41. Bagola K, vonDelbrück M, Dittmar G, et al. Ubiquitin Binding by a CUE Domain Regulates Ubiquitin Chain Formation by ERAD E3 Ligases. *Mol Cell*. 2013;50(4):528-539. doi:10.1016/j.molcel.2013.04.005

42. von Delbrück M, Kniss A, Rogov V V., et al. The CUE Domain of Cue1 Aligns Growing Ubiquitin Chains with Ubc7 for Rapid Elongation. *Mol Cell*. 2016;62(6):918-928. doi:10.1016/j.molcel.2016.04.031

43. Neuber O, Jarosch E, Volkwein C, Walter J, Sommer T. Ubx2 links the Cdc48 complex to ER-associated protein degradation. *Nat Cell Biol*. 2005;7(10):993-998. doi:10.1038/ncb1298

44. Jarosch E, Taxis C, Volkwein C, et al. Protein dislocation from the ER requires polyubiquitination and the AAA-ATPase Cdc48. *Nat Cell Biol*. 2002;4(2):134-139. doi:10.1038/ncb746

45. Ye Y, Meyer HH, Rapoport TA. The AAA ATPase Cdc48/p97 and its partners transport proteins from the ER into the cytosol. *Nature*. 2001;414(6864):652-656. doi:10.1038/414652a

46. Braun S, Matuschewski K, Rape M, Thoms S, Jentsch S. Role of the ubiquitin-selective CDC48(UFD1/NPL4)chaperone (segregase) in ERAD of OLE1 and other substrates. *EMBO J*. 2002;21(4):615-621. doi:10.1093/emboj/21.4.615

47. Kreft SG, Wang L, Hochstrasser M. Membrane Topology of the Yeast Endoplasmic Reticulum-localized Ubiquitin Ligase Doa10 and Comparison with Its Human Ortholog TEB4 (MARCH-VI). *J Biol Chem*. 2006;281(8):4646-4653. doi:10.1074/jbc.M512215200

48. Swanson R. A conserved ubiquitin ligase of the nuclear envelope/endoplasmic reticulum that functions in both ER-associated and Matalpha 2 repressor degradation. *Genes Dev*. 2001;15(20):2660-2674. doi:10.1101/gad.933301

49. Smoyer CJ, Jaspersen SL. Patrolling the nucleus: inner nuclear membrane-associated degradation. *Curr Genet*. April 2019. doi:10.1007/s00294-019-00971-1

50. Boban M, Zargari A, Andréasson C, Heessen S, Thyberg J, Ljungdahl PO. Asi1 is an inner nuclear membrane protein that restricts promoter access of two latent transcription factors. *J Cell Biol*. 2006;173(5):695-707. doi:10.1083/jcb.200601011

51. Zargari A, Boban M, Heessen S, Andréasson C, Thyberg J, Ljungdahl PO. Inner Nuclear Membrane Proteins Asi1, Asi2, and Asi3 Function in Concert to Maintain the Latent Properties of Transcription Factors Stp1 and Stp2. *J Biol Chem*. 2007;282(1):594-605. doi:10.1074/jbc.M609201200

52. Boer M d. Stp1p, Stp2p and Abf1p are involved in regulation of expression of the amino acid transporter gene BAP3 of Saccharomyces cerevisiae. *Nucleic Acids Res*. 2000;28(4):974-981. doi:10.1093/nar/28.4.974

53. Forsberg H, Ljungdahl PO. Sensors of extracellular nutrients in Saccharomyces cerevisiae. *Curr Genet*. 2001;40(2):91-109. http://www.ncbi.nlm.nih.gov/pubmed/11680826.

54. Abdel-Sater F, El Bakkoury M, Urrestarazu A, Vissers S, Andre B. Amino Acid Signaling in Yeast: Casein Kinase I and the Ssy5 Endoprotease Are Key Determinants of Endoproteolytic Activation of the Membrane-Bound Stp1 Transcription Factor. *Mol Cell Biol*. 2004;24(22):9771-9785. doi:10.1128/MCB.24.22.9771-9785.2004

55. Omnus DJ, Ljungdahl PO. Latency of transcription factor Stp1 depends on a modular regulatory motif that functions as cytoplasmic retention determinant and nuclear degron. Weis K, ed. *Mol Biol Cell*. 2014;25(23):3823-3833. doi:10.1091/mbc.e14-06-1140

56. Foresti O, Rodriguez-Vaello V, Funaya C, Carvalho P. Quality control of inner nuclear membrane proteins by the Asi complex. *Science (80-)*. 2014;346(6210):751-755. doi:10.1126/science.1255638

57. Khmelinskii A, Blaszczak E, Pantazopoulou M, et al. Protein quality control at the inner nuclear membrane. *Nature*. 2014;516(7531):410-413. doi:10.1038/nature14096

58. Metzger MB, Pruneda JN, Klevit RE, Weissman AM. RING-type E3 ligases: Master manipulators of E2 ubiquitin-conjugating enzymes and ubiquitination. *Biochim Biophys Acta - Mol Cell Res*. 2014;1843(1):47-60. doi:10.1016/j.bbamcr.2013.05.026

59. Dou H, Buetow L, Sibbet GJ, Cameron K, Huang DT. Essentiality of a non-RING element in priming donor ubiquitin for catalysis by a monomeric E3. *Nat Struct Mol Biol*. 2013;20(8):982-986. doi:10.1038/nsmb.2621

60. Dou H, Buetow L, Sibbet GJ, Cameron K, Huang DT. BIRC7–E2 ubiquitin conjugate structure reveals the mechanism of ubiquitin transfer by a RING dimer. *Nat Struct Mol Biol*. 2012;19(9):876-883. doi:10.1038/nsmb.2379

61. Koliopoulos MG, Esposito D, Christodoulou E, Taylor IA, Rittinger K. Functional role of TRIM E3 ligase oligomerization and regulation of catalytic activity. *EMBO J*. 2016;35(11):1204-1218. doi:10.15252/embj.201593741

62. Brzovic PS, Rajagopal P, Hoyt DW, King MC, Klevit RE. Structure of a BRCA1-BARD1 heterodimeric RING-RING complex. *Nat Struct Biol*. 2001;8(10):833-837. doi:10.1038/nsb1001-833

63. Vodermaier HC. APC/C and SCF: Controlling Each Other and the Cell Cycle. *Curr Biol*. 2004;14(18):R787-R796. doi:10.1016/j.cub.2004.09.020

64. Stewart MD, Ritterhoff T, Klevit RE, Brzovic PS. E2 enzymes: More than just middle men. *Cell Res*. 2016;26(4):423-440. doi:10.1038/cr.2016.35

65. Eletr ZM, Huang DT, Duda DM, Schulman BA, Kuhlman B. E2 conjugating enzymes must disengage from their E1 enzymes before E3-dependent ubiquitin and ubiquitin-like transfer. *Nat Struct Mol Biol*. 2005;12(10):933-934. doi:10.1038/nsmb984

66. Brown NG, Watson ER, Weissmann F, et al. Mechanism of Polyubiquitination by Human Anaphase-Promoting Complex: RING Repurposing for Ubiquitin Chain Assembly. *Mol Cell*. 2014;56(2):246-260. doi:10.1016/j.molcel.2014.09.009

67. Wenzel DM, Lissounov A, Brzovic PS, Klevit RE. UBCH7 reactivity profile reveals parkin and HHARI to be RING/HECT hybrids. *Nature*. 2011;474(7349):105-108. doi:10.1038/nature09966

68. Pruneda JN, Stoll KE, Bolton LJ, Brzovic PS, Klevit RE. Ubiquitin in Motion: Structural Studies of the Ubiquitin-Conjugating Enzyme~Ubiquitin Conjugate. *Biochemistry*. 2011;50(10):1624-1633. doi:10.1021/bi101913m

69. Pruneda JN, Littlefield PJ, Soss SE, et al. Structure of an E3:E2~Ub Complex Reveals an Allosteric Mechanism Shared among RING/U-box Ligases. *Mol Cell*. 2012;47(6):933-942. doi:10.1016/j.molcel.2012.07.001

70. Kostova Z, Mariano J, Scholz S, Koenig C, Weissman AM. A Ubc7p-binding domain in Cue1p activates ER-associated protein degradation. *J Cell Sci*. 2009;122(9):1374-1381. doi:10.1242/jcs.044255

71. Jaffray EG, Tatham MH, Naismith JH, Hay RT, Ring RNF. Structure of a RING E3 ligase and ubiquitin-loaded E2 primed for catalysis. *Nature*. 2012;489(7414):115-120. doi:10.1038/nature11376

72. Hershko A, Ciechanover A. THE UBIQUITIN SYSTEM. *Annu Rev Biochem*. 1998;67(1):425-479. doi:10.1146/annurev.biochem.67.1.425

73. Kniss A, Schuetz D, Kazemi S, et al. Chain Assembly and Disassembly Processes Differently Affect the Conformational Space of Ubiquitin Chains. *Structure*. 2018;26(2):249-258.e4. doi:10.1016/j.str.2017.12.011

74. Bays NW, Gardner RG, Seelig LP, Joazeiro CA, Hampton RY. Hrd1p/Der3p is a membrane-anchored ubiquitin ligase required for ER-associated degradation. *Nat Cell Biol*. 2001;3(1):24-29. doi:10.1038/35050524

75. Richards FM. on the Enzymic Activity of Subtilisin-Modified Ribonuclease. *Proc Natl Acad Sci*. 1958;44(2):162-166. doi:10.1073/pnas.44.2.162

76. Schumacher D, Lemke O, Helma J, et al. Broad substrate tolerance of tubulin tyrosine ligase enables one-step site-specific enzymatic protein labeling. *Chem Sci*. 2017;8(5):3471-3478. doi:10.1039/c7sc00574a

77. Agard NJ, Baskin JM, Prescher JA, Lo A, Bertozzi CR. A Comparative Study of Bioorthogonal Reactions with Azides. *ACS Chem Biol*. 2006;1(10):644-648. doi:10.1021/cb6003228

78. Rodrigo-Brenni MC, Morgan DO. Sequential E2s Drive Polyubiquitin Chain Assembly on APC Targets. *Cell*. 2007;130(1):127-139. doi:10.1016/j.cell.2007.05.027

79. Carvalho P, Goder V, Rapoport TA. Distinct Ubiquitin-Ligase Complexes Define Convergent Pathways for the Degradation of ER Proteins. *Cell*. 2006;126(2):361-373. doi:10.1016/j.cell.2006.05.043

80. FINGER A, KNOP M, WOLF DH. Analysis of two mutated vacuolar proteins reveals a degradation pathway in the endoplasmic reticulum or a related compartment of yeast. *Eur J Biochem*. 1993;218(2):565-574. doi:10.1111/j.1432-1033.1993.tb18410.x

81. Hampton RY, Gardner RG, Rine J. Role of 26S proteasome and HRD genes in the degradation of 3-hydroxy-3-methylglutaryl-CoA reductase, an integral endoplasmic reticulum membrane protein. *Mol Biol Cell*. 1996;7(12):2029-2044. http://www.ncbi.nlm.nih.gov/pubmed/8970163.

82. Lenk U, Sommer T. Ubiquitin-mediated Proteolysis of a Short-lived Regulatory Protein Depends on Its Cellular Localization. *J Biol Chem*. 2000;275(50):39403-39410. doi:10.1074/jbc.M006949200

83. Chen P, Johnson P, Sommer T, Jentsch S, Hochstrasser M. Multiple ubiquitin-conjugating enzymes participate in the in vivo degradation of the yeast MAT alpha 2 repressor. *Cell*. 1993;74(2):357-369. http://www.ncbi.nlm.nih.gov/pubmed/8393731.

84. Finke K, Plath K, Panzner S, et al. A second trimeric complex containing homologs of the Sec61p complex functions in protein transport across the ER membrane of S. cerevisiae. *EMBO J*. 1996;15(7):1482-1494. http://www.ncbi.nlm.nih.gov/pubmed/8612571.

85. Habeck G, Ebner FA, Shimada-Kreft H, Kreft SG. The yeast ERAD-C ubiquitin ligase Doa10 recognizes an intramembrane degron. *J Cell Biol*. 2015;209(2):261-273. doi:10.1083/jcb.201408088

86. Hampton RY, Bhakta H. Ubiquitin-mediated regulation of 3-hydroxy-3-methylglutaryl-CoA reductase. *Proc Natl Acad Sci*. 1997;94(24):12944-12948. doi:10.1073/pnas.94.24.12944

87. Ravid T, Kreft SG, Hochstrasser M. Membrane and soluble substrates of the Doa10 ubiquitin ligase are degraded by distinct pathways. *EMBO J*. 2006;25(3):533-543. doi:10.1038/sj.emboj.7600946

88. Hiller MM, Finger A, Schweiger M, Wolf DH. ER degradation of a misfolded luminal protein by the cytosolic ubiquitin-proteasome pathway. *Science*. 1996;273(5282):1725-1728. http://www.ncbi.nlm.nih.gov/pubmed/8781238.

89. Baldridge RD, Rapoport TA. Autoubiquitination of the Hrd1 Ligase Triggers Protein Retrotranslocation in ERAD. *Cell*. 2016;166(2):394-407. doi:10.1016/j.cell.2016.05.048

90. Pédelacq J-D, Cabantous S, Tran T, Terwilliger TC, Waldo GS. Engineering and characterization of a superfolder green fluorescent protein. *Nat Biotechnol*. 2006;24(1):79-88. doi:10.1038/nbt1172

91. Lees ND, Skaggs B, Kirsch DR, Bard M. Cloning of the late genes in the ergosterol biosynthetic pathway of Saccharomyces cerevisiae--a review. *Lipids*. 1995;30(3):221-226. http://www.ncbi.nlm.nih.gov/pubmed/7791529.

92. Boban M, Pantazopoulou M, Schick A, Ljungdahl PO, Foisner R. A nuclear ubiquitin-proteasome pathway targets the inner nuclear membrane protein Asi2 for degradation. *J Cell Sci*. 2014;127(16):3603-3613. doi:10.1242/jcs.153163

93. Pantazopoulou M, Boban M, Foisner R, Ljungdahl PO. Cdc48 and Ubx1 participate in a pathway associated with the inner nuclear membrane that governs Asi1 degradation. *J Cell Sci*. 2016;129(20):3770-3780. doi:10.1242/jcs.189332

94. Fernandez-Rodriguez J, Marlovits TC. Induced heterodimerization and purification of two target proteins by a synthetic coiled-coil tag. *Protein Sci*. 2012;21(4):511-519. doi:10.1002/pro.2035

95. Kalderon D, Roberts BL, Richardson WD, Smith AE. A short amino acid sequence able to specify nuclear location. *Cell*. 1984;39(3 Pt 2):499-509. http://www.ncbi.nlm.nih.gov/pubmed/6096007.

96. UniProt: a worldwide hub of protein knowledge. *Nucleic Acids Res*. 2019;47(D1):D506-D515. doi:10.1093/nar/gky1049

97. Meusser B, Hirsch C, Jarosch E, Sommer T. ERAD: The long road to destruction. *Nat Cell Biol*. 2005;7(8):766-772. doi:10.1038/ncb0805-766

98. Tan JME, Cook ECL, van den Berg M, Scheij S, Zelcer N, Loregger A. Differential use of E2 ubiquitin conjugating enzymes for regulated degradation of the rate-limiting enzymes HMGCR and SQLE in cholesterol biosynthesis. *Atherosclerosis*. 2019;281:137-142. doi:10.1016/j.atherosclerosis.2018.12.008

99. Wood A, Krogan NJ, Dover J, et al. Bre1, an E3 ubiquitin ligase required for recruitment and substrate selection of Rad6 at a promoter. *Mol Cell*. 2003;11(1):267-274. doi:12535539

100. Hwang WW, Venkatasubrahmanyam S, Ianculescu AG, Tong A, Boone C, Madhani HD. A conserved RING finger protein required for histone H2B monoubiquitination and cell size control. *Mol Cell*. 2003;11(1):261-266. http://www.ncbi.nlm.nih.gov/pubmed/12535538.

101. Hibbert RG, Huang A, Boelens R, Sixma TK. E3 ligase Rad18 promotes monoubiquitination rather than ubiquitin chain formation by E2 enzyme Rad6. *Proc Natl Acad Sci U S A*. 2011;108(14):5590-5595. doi:10.1073/pnas.1017516108

102. Sung P, Berleth E, Pickart C, Prakash S, Prakash L. Yeast RAD6 encoded ubiquitin conjugating enzyme mediates protein degradation dependent on the N-end-recognizing E3 enzyme. *EMBO J*. 1991;10(8):2187-2193. http://www.ncbi.nlm.nih.gov/pubmed/2065660.

103. Walter T, Erdmann R. Current Advances in Protein Import into Peroxisomes. *Protein J*. 2019;38(3):351-362. doi:10.1007/s10930-019-09835-6

104. Dove KK, Olszewski JL, Martino L, et al. Structural Studies of HHARI/UbcH7~Ub Reveal Unique E2~Ub Conformational Restriction by RBR RING1. *Structure*. 2017;25(6):890-900.e5. doi:10.1016/j.str.2017.04.013

105. Nakatani Y, Kleffmann T, Linke K, Condon SM, Hinds MG, Day CL. Regulation of ubiquitin transfer by XIAP, a dimeric RING E3 ligase. *Biochem J*. 2013;450(3):629-638. doi:10.1042/BJ20121702

106. Leto DE, Morgens DW, Zhang L, et al. Genome-wide CRISPR Analysis Identifies Substrate-Specific Conjugation Modules in ER-Associated Degradation. *Mol Cell*. 2019;73(2):377-389.e11. doi:10.1016/j.molcel.2018.11.015

107. Klemm EJ, Spooner E, Ploegh HL. Dual Role of Ancient Ubiquitous Protein 1 (AUP1) in Lipid Droplet Accumulation and Endoplasmic Reticulum (ER) Protein Quality Control. *J Biol Chem*. 2011;286(43):37602-37614. doi:10.1074/jbc.M111.284794

108. Schulz J, Avci D, Queisser MA, et al. Conserved cytoplasmic domains promote Hrd1 ubiquitin ligase complex formation for ER-associated degradation (ERAD). *J Cell Sci*. 2017;130(19):3322-3335. doi:10.1242/jcs.206847

109. Burr ML, Cano F, Svobodova S, Boyle LH, Boname JM, Lehner PJ. HRD1 and UBE2J1 target misfolded MHC class I heavy chains for endoplasmic reticulum-associated degradation. *Proc Natl Acad Sci*. 2011;108(5):2034-2039. doi:10.1073/pnas.1016229108

110. Boban M, Ljungdahl PO, Foisner R. Atypical Ubiquitylation in Yeast Targets Lysine-less Asi2 for Proteasomal Degradation. *J Biol Chem*. 2015;290(4):2489-2495. doi:10.1074/jbc.M114.600593

111. Brzovic PS, Keeffe JR, Nishikawa H, et al. Binding and recognition in the assembly of an active BRCA1/BARD1 ubiquitin-ligase complex. *Proc Natl Acad Sci*. 2003;100(10):5646-5651. doi:10.1073/pnas.0836054100

112. Carvalho P, Stanley AM, Rapoport TA. Retrotranslocation of a Misfolded Luminal ER Protein by the Ubiquitin-Ligase Hrd1p. *Cell*. 2010;143(4):579-591. doi:10.1016/j.cell.2010.10.028

113. Ravid T, Hochstrasser M. Diversity of degradation signals in the ubiquitin–proteasome system. *Nat Rev Mol Cell Biol*. 2008;9(9):679-689. doi:10.1038/nrm2468

114. Wu K, Kovacev J, Pan Z-Q. Priming and Extending: A UbcH5/Cdc34 E2 Handoff Mechanism for Polyubiquitination on a SCF Substrate. *Mol Cell*. 2010;37(6):784-796. doi:10.1016/j.molcel.2010.02.025

115. Finley D, Ozkaynak E, Varshavsky A. The yeast polyubiquitin gene is essential for resistance to high temperatures, starvation, and other stresses. *Cell*. 1987;48(6):1035-1046. http://www.ncbi.nlm.nih.gov/pubmed/3030556.

116. Seufert W, Jentsch S. Ubiquitin-conjugating enzymes UBC4 and UBC5 mediate selective degradation of short-lived and abnormal proteins. *EMBO J*. 1990;9(2):543-550. http://www.ncbi.nlm.nih.gov/pubmed/2154373.

117. Rogov V V., Rozenknop A, Rogova NY, et al. A Universal Expression Tag for Structural and Functional Studies of Proteins. *ChemBioChem*. 2012;13(7):959-963. doi:10.1002/cbic.201200045

118. Berndsen CE, Wolberger C. A spectrophotometric assay for conjugation of ubiquitin and ubiquitin-like proteins. *Anal Biochem*. 2011;418(1):102-110. doi:10.1016/j.ab.2011.06.034

119. Bond SR, Naus CC. RF-Cloning.org: an online tool for the design of restriction-free cloning projects. *Nucleic Acids Res*. 2012;40(W1):W209-W213. doi:10.1093/nar/gks396

120. LAEMMLI UK. Cleavage of Structural Proteins during the Assembly of the Head of Bacteriophage T4. *Nature*. 1970;227(5259):680-685. doi:10.1038/227680a0

121. LOWRY OH, ROSEBROUGH NJ, FARR AL, RANDALL RJ. Protein measurement with the Folin phenol reagent. *J Biol Chem*. 1951;193(1):265-275. doi:14907713

5.2 Abbreviations

AAA	ATPase Associated with diverse cellular Activities
APC	anaphase promoting complex
APS	ammonium persulfate
Asi	Amino acid sensor independent
Atg8	Autophagy-related protein 8
ATP	adenosine triphosphate
BIRC7	baculoviral IAP repeat-containing protein 7
BSA	bovine serum albumin
bp	base pair
BARD1	BRCA1-associated RING domain protein 1
BRCA1	Breast Cancer 1
Bre1	Brefeldin-A sensitivity protein 1
CBL	Casitas B-lineage lymphoma
Cdc48	Cell division cycle 48
CHX	cycloheximide
CPY	carboxypeptidase yscY
CSP	chemical shift perturbation
CUE	coupling of ubiquitin conjugation to ER degradation
DBCO	dibenzocyclooctyne
ddH_2O	double deionized water
Der1	Degradation in the endoplasmic reticulum
DNA	deoxyribonucleic acid
dNTPs	deoxynucleotide triphosphates
Doa10	degradation of Matα 10
DTT	dithiothreitol
DUB	deubiquitinating enzyme
E1	ubiquitin activating enzyme
E2	ubiquitin conjugating enzyme
E3	ubiquitin ligase

ECL	Enhanced chemoluminescence
E. coli	*Escherichia coli*
EDTA	ethylenediaminetetraacetic acid
ER	endoplasmic reticulum
ERAD	ER-associated protein degradation
g	gravitational acceleration
GSH	reduced glutathione
GST	glutathione-S-transferase
h	hour(s)
HA	hemagglutinin
HECT	Homologous to the E6AP Carboxy-Terminus
His_6	hexahistidine
Hmg2	3-hydroxy-3-methylglutaryl-coenzyme A reductase
Hrd1	HMG-CoA reductase degradation 1
Hrd3	HMG-CoA reductase degradation 3
HRP	horseradish peroxidase
IgG	immunoglobulin G
IP	immunoprecipitation
IPTG	isopropyl β-D-1-thiogalactopyranoside
ISG15	Interferon-stimulated gene product 15
kB	kilo base pairs
kDa	kilodalton
LB	lysogeny broth
LMNG	lauryl maltose neopentyl glycol
MAT	mating type
MBq	megabecquerel
min	minute(s)
MWCO	molecular weight cut-off
NEDD8	Neural precursor cell expressed, developmentally down-regulated 8

Ni-NTA	nickel-nitrilotriacetic acid
NMR	nuclear magnetic resonance
Npl4	nuclear protein localization 4
OD_{600}	optical density at 600 nm
PAGE	polyacrylamide gel electrophoresis
PBS	phosphate-buffered saline
PCNA	proliferating cell nuclear antigen
PCR	polymerase chain reaction
PDB	Protein Data Bank
PEG	polyethylene glycol
pH	potential of hydrogen
PH	Plekstrin Homology
PMSF	phenylmethylsulfonylfluoride
PQC	protein quality control
PrA	proteinase yscA
PVDF	polyvinylidene fluoride
Rad6	radiation sensitive 6
RBR	RING-in-between-RING
RING	really interesting new gene
RNA	ribonucleic acid
RNase	ribonuclease A
rpm	revolutions per minute
s	seconds
S. cerevisiae	*Saccharomyces cerevisiae*
SCF	Skp1-Cul1-F-box protein
SD	synthetic defined
SDS	sodium dodecyl sulfate
SEC	size exclusion chromatography
Sec61	secretory 61
SEL1L	Suppressor enhancer of Lin12-like

sfGFP	superfolder green fluorescent protein
SOC	super optimal broth with catabolite repression
SPAAC	strain-promoted azide-alkyne cycloaddition
SUMO	Small ubiquitin-like modifier
TAE	Tris-acetate buffer with EDTA
TB	terrific broth
TBT	Tris buffer with Tween
TE	Tris-EDTA buffer
TEMED	Tetramethylethylenediamine
TRIM	tripartite motif
Tris	Tris(hydroxymethyl)aminomethane
U7BR	Ubc7 binding region
Ub	ubiquitin
Ub^{488}	Alexa Fluor™ 488-labeled Ub^{S20C}
Ub_2	di-ubiquitin
Ub_3	tri-ubiquitin
UBA	ubiquitin-associated
UBC	ubiquitin conjugating enzyme catalytic core
UBD	ubiquitin binding domain
Ubx2	ubiquitin regulatory X 2
UBZ	ubiquitin-binding zinc fingers
Ufd1	ubiquitin fusion degradation protein 1
UIM	ubiquitin-interacting motif
Usa1	U1-Snp1 associating
UV	ultraviolet
v/v	volume for volume
w/v	weight per volume
WT	wild type
Yos9	yeast OS-9
YPD	yeast extract peptone dextrose

5.3 Selbständigkeitserklärung

Hiermit erkläre ich, die Dissertation selbständig und nur unter Verwendung der angegebenen Hilfen und Hilfsmittel angefertigt zu haben.

Ich habe mich anderwärts nicht um einen Doktorgrad beworben und besitze keinen entsprechenden Doktorgrad.

Ich erkläre, dass ich die Dissertation oder Teile davon nicht bereits bei einer anderen wissenschaftlichen Einrichtung eingereicht habe und dass sie dort weder angenommen noch abgelehnt wurde.

Ich erkläre die Kenntnisnahme der dem Verfahren zugrunde liegenden Promotionsordnung der Mathematisch-Naturwissenschaftlichen Fakultät I der Humboldt-Universität zu Berlin vom 27. Juni 2012.

Weiterhin erkläre ich, dass keine Zusammenarbeit mit gewerblichen Promotionsberaterinnen/Promotionsberatern stattgefunden hat und dass die Grundsätze der Humboldt-Universität zu Berlin zur Sicherung guter wissenschaftlicher Praxis eingehalten wurden.

Berlin, den 19.07.2019

Christian Lips

5.4 Presentations

2019 Cancer Club Lecture Series of the MDC, **invited speaker**

2018 FASEB SRC, *Ubiquitin & Cellular Regulation*, Snowmass, CO, USA, **invited speaker and poster presentation**

2017 SignGene Symposium, *Ubiquitin in Protein Homeostasis and Autophagy*, Neuruppin, Germany, **invited speaker**

2017 Cold Spring Harbor Meeting, *The Ubiquitin Family Meeting*, Cold Spring Harbor, NY, USA, **invited speaker**

2017 SignGene Symposium, *Frontiers in Cell Signaling and Gene Regulation*, Potsdam, Germany, **poster presentation**

2016 SignGene Winterschool, *High Precision, High Throughput: Biochemistry, Sequencing, and Imaging*, Haifa, Israel, **invited speaker**

2015 SignGene Symposium, *Singles in Biology: Proteins, Cells and Stem Cells*, Neuruppin, Germany, **poster presentation**

5.5 Danksagung

Zuletzt möchte ich mich bei allen bedanken, die mich bei der Anfertigung dieser Arbeit unterstützt haben.

Ich bin überaus dankbar für die einmalige Gelegenheit, meine Arbeit in der Gruppe von Prof. Dr. Thomas Sommer angefertigt zu haben. Vielen Dank für die großartigen Diskussionen, die Unterstützung und den Glauben an mich und meine Fähigkeiten.

Weiterer Dank gilt Dr. Ernst Jarosch für seine wissenschaftliche Unterstützung, die Möglichkeit, jederzeit hilfreichen Input zu erhalten, sowie das Korrekturlesen meiner Dissertation.

Bedanken möchte ich mich auch bei der gesamten Arbeitsgruppe für die unglaubliche Atmosphäre. Die lockere Stimmung im Labor hat den Arbeitsalltag enorm bereichert. Ich werde meine Zeit am MDC euretwegen immer in guter Erinnerung behalten. Ein ganz besonderer Dank gilt Mandy Mustroph und Corinna Volkwein für ihre exzellente technische Unterstützung und die Bereitstellung ihrer magischen Hände. Darüber hinaus danke ich Maximilian von Delbrück und Annika Weber für hilfreiche Diskussionen und die praktische Unterstützung zu Beginn meiner Promotion.

I would like to thank Dr. Tobias Ritterhoff and Prof. Dr. Rachel Klevit for fruitful discussions and the friendly atmosphere during our collaboration.

Mein größter Dank gilt meiner Lebensgefährtin Liane Schuster, meiner Familie und meinen Freunden. Eure Liebe und Unterstützung war meine Motivation. An dieser Stelle möchte ich mich dafür bedanken, dass ihr meine Launen in der finalen Phase dieser Arbeit ausgehalten habt und mich gleichzeitig dafür entschuldigen, dass ihr sie aushalten musstet.